INGENIERÍA TÉCNICA INDUSTRIAL
ESPECIALIDAD MECÁNICA

Universidad
Carlos III de Madrid

DEVELOP A BLADDER ASSISTED RTM TOOL TO MANUFACTURE SEAT POSTS WITH GLASS FIBER & CNT-EPOXY RESIN

BORJA AMORES FERNÁNDEZ

Directores:
Mónica Campos Gómez (UC3M)
Gunnar Rieber (IVW)

Departamento Ciencia e Ing. de Materiales e Ing. Química
Julio, 2015

Declaration of Authorship

Borja Amores Fernández, I declare that wrote my thesis by my own and only used the references that appear at the end of my work.

Madrid 08/07/2015

Acknowledgement

First of all, I would like to express my gratitude to my supervisor Gunnar Rieber for his support, mentoring and dedication to my professional development during the work on this project.

Further, I would like to extend my gratitude and appreciation to Dr.-Ing. Peter Mitschang for giving me the opportunity to perform my work at *Institut für Verbundwerkstoffe GmbH* (IVW).

I'm grateful to the IVW for providing me the opportunity of working in an outstanding environment. I would like to express special appreciation to the whole IVW staff, especially to my colleagues of *Demonstrations und Anwendungszentrum* (D.A.Z.).

Further, I am very thankful to "Faro Global" and Martin Schehl for offering me the opportunity to write my master thesis at the IVW.

I am thankful to Mónica Campos (UC3M) for her help on the redaction of this master thesis.

Last but not least, I would like to give my thanks to my parents Agustín Amores and Manuela Fernández for their emotional and economical support, and my sister Inma and my girlfriend Isabel that support me to finish the thesis.

Madrid, July 2015.

Preface

The present project was done between September 2008 and June 2009 thanks to an internship at the *Institut für Verbundwerkstoffe GmbH* (IVW). The IVW is a nonprofit research organization of Rhineland-Palatinate on the campus of the University of Kaiserslautern. It is engaged in the research and development of new applications of composite materials based on polymer matrix systems. The institute was established in 1990 and expanded in 2002 to a *Demonstrations und Anwendungszentrum* (DAZ). The IVW is one of the strong German and international recognized institutions in the field of composite materials and is also distinguished by its innovative strength.

The tool developed on this project for manufacturing new CNT doped glass fiber reinforced polymer composites were performed at the IVW under to the Inno.CNT-CarboROAD project financially supported by the German Federal Ministry of Education and Research. The CarboROAD project objective is "Development of processes, machines and raw materials to process Carbon Nanotube (CNT) doped resin by liquid composite molding".

The present project took the work done by Alexander Mann on his project "Construction of a transparent tool of PMMA" as basis for the tooling development and supervised by the research associate Dipl.-Sporting. Gunnar Rieber.

Summary

In this project, a bladder-assisted Resin Transfer Moulding tool to manufacture glass fiber bicycle seat posts with epoxy resin charged with carbon nanotubes (CNTs) is developed through the application of a "Systematic Approach to the design of Technical Systems and Products" guideline to provide an optimum solution for the filtering of CNTs during the injection process. The impregnation process is identified as the key characteristic on the tool development.

The bladder assisted-RTM process parameters and manufacturing seat post features are evaluated to define the requirements that fulfill the main task, a homogeneous distribution of CNTs through the fiber glass reinforcement. According to the requirements, the task is divided in function and sub-functions to be fulfilled by the tool development. Interfaces between sub-functions are established in order to re-organize them into realizable modules. This module structure showed a preliminary indication for the breakdown of solution into realizable groups or elements, and together with their interfaces facilitated an efficient distribution of design effort.

Tool constituent elements are designated and multiple principle solutions are provided for every element. Once selected the most adequate individual solution, a tool concept design is presented and begins the layouts development for the individual modules (Housing shape, Cooling system, Front cover with compressed air connection, Rear cover with resin injection port, Rear cover with air-extraction exhaust, closing device, centering of the tool components, gaskets for the tightness and bladder as core design). Detailed drawings and calculations are performed to confirm that the design solution meets the requirements of the general task.

The impregnation concept process using the inflatable bladder designed is explained, showing the collapsible channel operation in order to infuse correctly the braided glass fiber reinforcement using the high viscosity resin due the CNTs addition.

At the end of the project, manufacturing tests are done to select the inflatable bladder with three different elastic materials using a reduced tool. After bladder material selection, a real scale tool is designed and constructed to manufacture a simple inflatable bladder, as first approach to the final bladder manufacturing. For the bladder manufacturing, a real scale bladder dipping mandrel is manufactured using water soluble fugitive core material.

CONTENT

INDEX OF FIGURES

INDEX OF TABLES

LIST OF ABBREVIATIONS

IVW	*Institut für Verbundwerkstoffe*
FRP	Fiber reinforced polymer
FRC	Fiber reinforced composite
OMC	Organic-matrix composite
MMC	Metal-matrix composite
CMC	Ceramic-matrix composite
PMC	Polymer-matrix composites
CNT	Carbon nanotubes
CNF	Carbon nanofibers
SWCNT	Single-wall carbon nanotubes
MWCNT	Multi-wall carbon nanotubes
DWCNT	Double-wall carbon nanotubes
PNC	Polymeric nanocomposite
M-FRC	Multiscale fiber reinforced composite
RTM	Resin Transfer Moulding
VARTM	Vacuum Assisted Resin Transfer Moulding
RLI	Resin Infusion
CTE	Coefficient of thermal expansion
wt%	Percent by mass
Tg	Transition temperature
DGEBA	Diglycidyl ether of bisphenol-A
PMMA	Poly(methyl methacrylate)
PU	Polyurethane

1 Motivation and objective

1.1 Background

Composite materials based in polymeric resins and fiber reinforcements are increasing their use to produce components in sport applications, automotive, aerospace, etc (figure 1.1). The growing demand for these products has developed at high speed systems for production of composite materials developing efficient manufacturing techniques like Resin Transfer Moulding (RTM).

Figure 1.1: Composite materials applications.

As manufacturing techniques are improving, higher requirements are demanded beside the light weight behavior of Fiber Reinforced Polymers (FRPs). From neat polymers it is known that the reinforcing with nanoparticles, nanofibers or carbon nanotubes, so called nanocomposites (figure 1.2), show unique effects like a simultaneous increase of stiffness and toughness, or the ability to get electrical and/or thermal conductivity with particle content less than one percent (<1 wt%). This materials are much lighter than aluminum but also exceptionally strong, that's why they will play a key role in the future for the automotive industry, aeronautic and aerospace sector. They will open the door to technical solutions that are simply not possible today, for example, by enabling weight savings that will result in a reduced energy consumption and lower emissions, but without any sacrifice of safety or comfort.

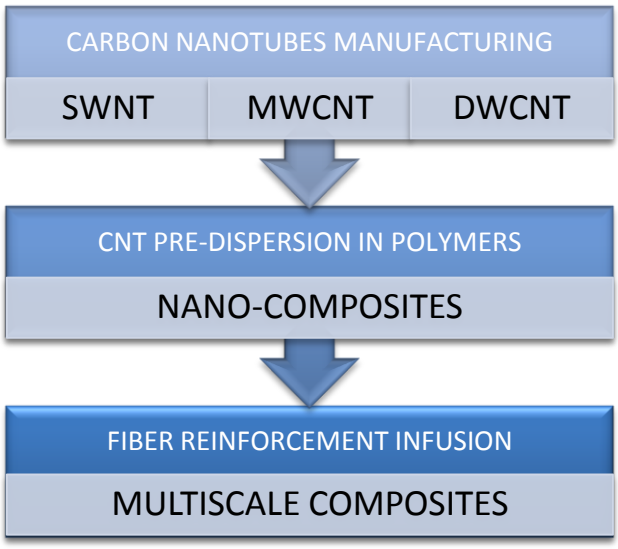

Figure 1.2: Multiscale composites structure.

In recent years, fiber-reinforced polymer composites modified with Carbon Nanotubes (CNTs), known as ‘‘multiscale” composite as they are reinforced with microscale fibers and nanoscale nanotubes (figure 1.2) [1, 2], have drawn significant attention in the field of advanced, high-performance materials. Most of the efforts in multiscale composites research have been focused on improving the matrix-dominated properties by homogeneously dispersing CNTs in the bulk of the matrix, in order to avoid CNT agglomeration (figure 1.3 & 1.4).

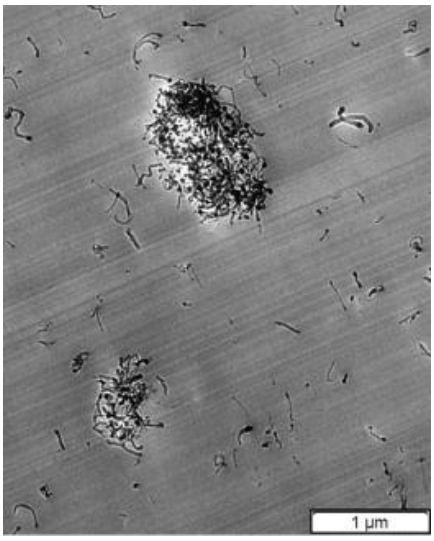

Figure 1.3: Agglomerated CNT-Resin [3].

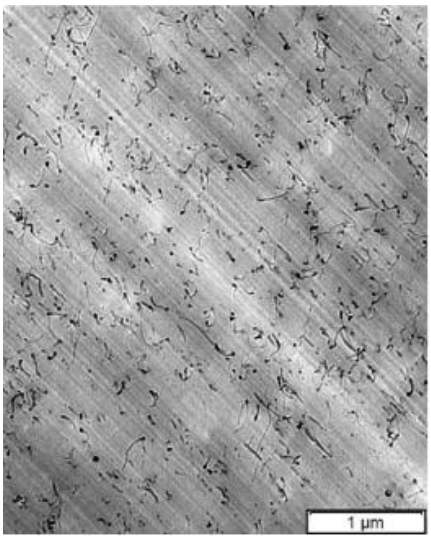

Figure 1.4: Homogeneous CNT-Resin distribution [3].

High-energy sonication has been widely used to ‘‘pre-disperse” CNTs in the resin prior to composite fabrication [4–9]. However, more recently, calendering has gained popularity as a means to disperse CNTs due to its efficiency and scalability, which makes it suitable for high volume, high rate production (figure 1.5) [10–15]. As for integrating resin/CNT mixture and fiber fabric, Resin Transfer Molding (RTM), Vacuum-Assisted Resin Transfer Molding (VARTM) [12, 15, 16] and hand layup [4, 5] are commonly used. Although improvements in mechanical properties of multiscale composites

have been achieved with the addition of CNTs, the transferability of improved matrix properties into continuous-fiber-reinforced composites is a challenging task and limited by many factors [15, 17].

Figure 1.5: Calendering CNT pre-dispersion.

Beside these advantages there are also some disadvantages. One of the major problems to use these resin charged with nano-reinforcements to impregnate fiber structures is the increase of viscosity by some order of magnitudes that difficult their manufacturing process. The highly viscous and CNT-agglomerated resin systems cannot be processed using the conventional composite manufacturing techniques. For example, when fabricating multiscale Fiber Reinforcement Polymers (FRPs) using the VARTM process, nano-reinforcements can become filtered, resulting in an inhomogeneous microstructure of multiscale composites [18, 19, 20, 21]. Filtering is caused by the nano-reinforcements being trapped in inter-tow regions within the fiber preform mesh during fabrication. A comprehensive study [21] revealed a direct correlation between the concentration of Carbon Nanofibers (CNFs) and the processing parameters, such as viscosity and filtering: a CNFs concentration above 1% resulted in a significant filtering effect, leading to the formation of many micro-voids in the composite [22].

To open the door for the use of CNTs in FRP the impregnation technology of the fiber architecture is the key issue. Within this project will be analyzed and developed the RTM technique to manufacture a with glass fiber bicycle seat posts with epoxy resin charged with carbon nanotubes (CNTs).

To provide an optimum solution for the filtering of CNTs during the injection process will be developed an inflatable bladder to improve the fiber impregnation getting a homogeneous distribution of the CNTs through the fiber reinforcement.

To obtain these objective this project proceeds to:

- Analyze the manufacturing process of hollow parts using the RTM technique.

- Development of strategy to impregnate fiber beds.
- Design an inflatable bladder assisted-RTM tool.
- Design and construction of a tool to manufacture a simple inflatable bladder.
- Experimental investigation of bladder material selection.
- Experimental investigation of a bladder dipping mandrel manufacturing.

2 State of the art

On this chapter, it's presented a review of the classification of the composites materials attending to the scale of the reinforcement (figure 2.1).

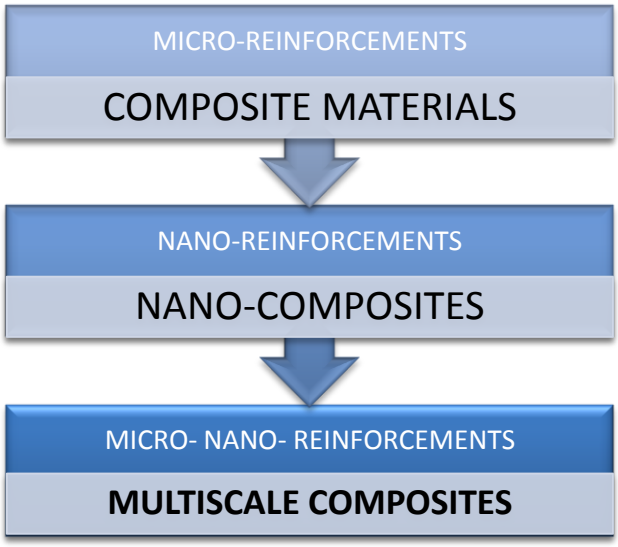

Figure 2.1: Multiscale composites structure.

Once presented the classification of the composite materials, it's done a detailed explanation of the constituent materials (micro-, nano-reinforcement and polymer matrix) and manufacturing techniques for the development of this project.

2.1 Composite materials

Composites

A composite material (or composites) is a macroscopic combination of two or more materials with different physical and chemical properties, having a recognizable interface between them. There are two constituents on a composite material, a continuous phase or matrix that binds together and provides form to an array of a stronger, stiffer reinforcement constituent phase (figure 2.2). The resulting composite material has a balance of structural properties that is superior to either constituent material alone. The improved structural properties generally result from a load-sharing mechanism.

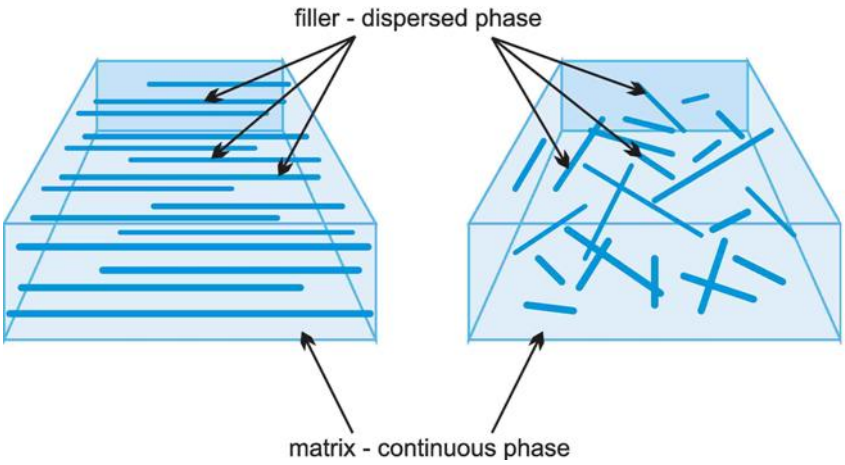

Figure 2.2: Composite material constituents.

Composites are used not only for their structural properties but also for electrical, thermal, tribological and environmental applications. Modern composite materials are usually optimized to achieve a particular balance of properties for a given range of applications.

Thus, composites typically have a reinforcement phase that is stiffer and stronger than the continuous matrix phase. Many types of reinforcements also often have good thermal and electrical conductivity, a coefficient of thermal expansion (CTE) that is less than the matrix, and/or good wear resistance.

Composites are commonly classified at two distinct levels. The first level of classification is usually made with respect to the matrix constituent that is typically a continuous phase throughout the component. The major composite classes include organic-matrix composites (OMCs), metal-matrix composites (MMCs), and ceramic-matrix composites (CMCs). The term "organic-matrix composite" is generally assumed to include two classes of composites: polymer-matrix composites (PMCs) and carbon-matrix composites (commonly referred to as carbon-carbon composites).

The second level of classification refers to the reinforcement form: nano-reinforcements, particulate reinforcements, whisker reinforcements, continuous fiber laminated composites and woven composites, braided and knitted fiber architectures are included in this category. In order to provide a useful increase in properties, there generally must be a substantial volume fraction (~10% or more) of the reinforcement.

Continuous fiber-reinforced composites contain reinforcements having lengths much greater than their cross-sectional dimensions. Such a composite is considered to be a discontinuous fiber or short fiber composite if its properties vary with fiber length. On the other hand, when the length of the fiber is such that any further increase in length does not, for example, further increase the elastic modulus or strength of the composite, the composite is considered to be continuous fiber reinforced. Most

continuous fiber (or continuous filament) composites, in fact, contain fibers that are comparable in length to the overall dimensions of the composite part.

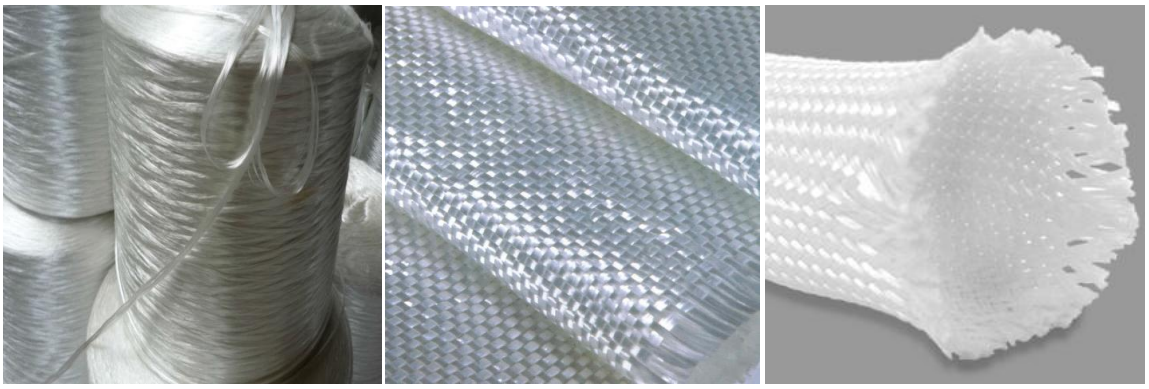

Figure 2.3: Glass fiber architectures.

An important category of fiber architecture (figure 2.3) is that formed by weaving, braiding, or knitting the fiber bundles or "tows" to create interlocking fibers that often have orientations slightly or fully in an orientation orthogonal to the primary structural plane. This approach is taken for a variety of reasons, including the ability to have structural, thermal, or electrical properties in the third or "out-of-plane" dimension. Another often cited reason for using these architectures is that the "unwetted" or dry fiber preforms (fibers before any matrix is added) are easier to handle, lower in cost, and conform to highly curved shapes more readily than the highly aligned, continuous fiber form. These fiber architectures are employed on liquid molding manufacturing technologies like Resin Infusion (RLI), Resin Transfer Molding (RTM), etc [23].

Traditional fiber reinforced composites (FRCs) have shown great promise as high strength structural materials due to their high stiffness to weight ratio and their ease of processing. In addition, FRCs have matured with respect to their material properties. For instance, their in-plane, fiber-dominant properties make them highly desirable compared to metals, but their through-the-thickness or z-axis properties are matrix-dominant and have limited their use. So far, FRCs have found extensive use in aerospace, automotive, construction, and recreational equipment industrial sectors but their previously stated limitations have prohibited them from reaching their full potential [24].

Nano-composites

The transition from micro-reinforcements to nano-reinforcements yields dramatic changes in physical properties. Nanoscale materials have a large surface area for a given volume. In general, nanomaterials provide reinforcing efficiency because of their high aspect ratios (figure 2.4). Since many important chemical and physical interactions are governed by surfaces and surface properties, a nanostructured material can have substantially different properties from a larger-dimensional material

of the same composition. Typical nano-reinforcements currently under investigation include, nanoparticles, carbon nanotubes (CNTs), carbon nanofibers (CNFs), fullerenes, and graphene [25].

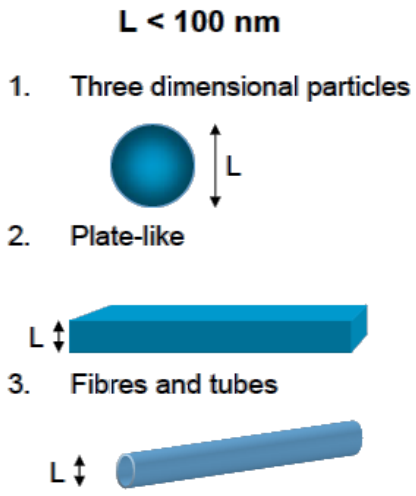

Figure 2.4: Nano-sized reinforcement (L < 100nm) [26].

Research in nanostructured composites or nanocomposites, in which a resin is dispersed with nanoparticles, such CNTs or CNFs, has shown explosive growth in the past decades. Incorporation of nanoscale constituents into composite matrices leads to new or modified property enhancements significantly greater than that attainable using conventional fillers or polymer blends [27]. Researchers using CNFs and CNTs in manufacturing polymeric nanocomposites (PNCs) have reported mechanical, electrical, and thermal property enhancements which result from synergy from the matrix and nanoparticles. Studies have shown that chemically modifying the surfaces of nanoparticles helps them disperse better in polymer matrices and results in improved physical properties [24].

"Multiscale" material

A combination of PNCs with fiber-reinforcement results in a multiscale composite with a hierarchal structure ranging from nanoscale to micron size fibers (figure 2.5). These multiscale composites offer a route by which multifunctionality (enhanced thermal stability, lower coefficient of thermal expansion, high thermal and electrical conductivity) can be imparted to the FRC [27].

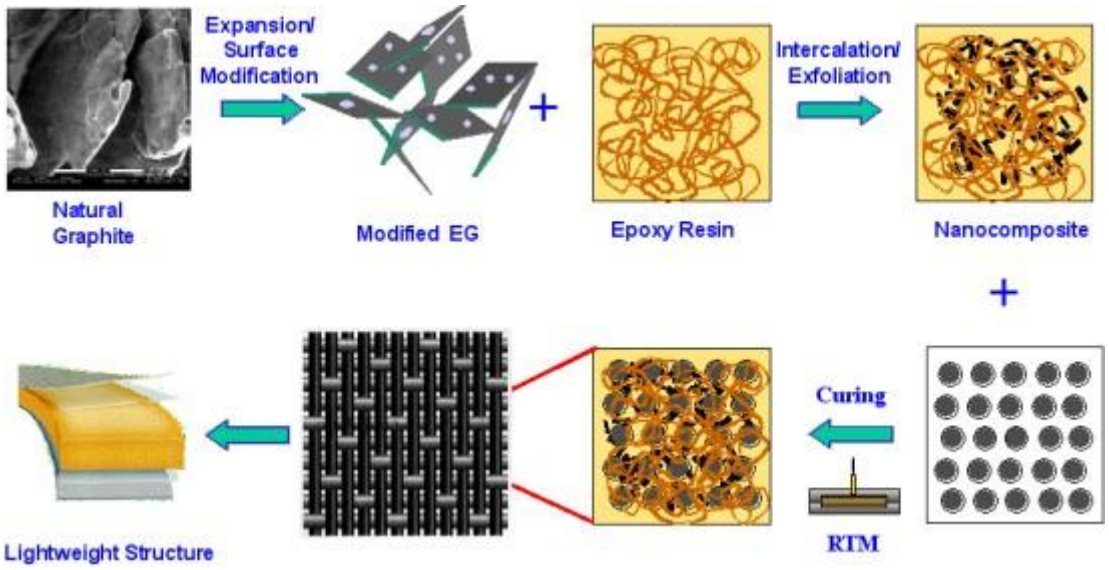

Figure 2.5: Multiscale composite structure [28].

Therefore, enhancing the PNCs matrix properties should lead to property enhancements in the FRCs system and result in a composite with the potential perform in a multifunctional capacity. Modifying the fiber reinforcement constituent within a FRC system by grafting [29] or electrophoretically depositing nanoparticles onto the fiber can serve as a another way to develop multifunctional composites [30-33]. Thus, multiscale fiber reinforced composites (M-FRCs) can be manufactured by either modifying the resin matrix or fiber reinforcement [24]. One route for fabricating M-FRC is to infuse fiber preforms with nanostructured prepolymers, or nanocomposites [27].

2.1.1 Matrix - Thermosetting epoxy resin

The function of the matrix is to bind the reinforcements together by its cohesive and adhesive characteristics, to transfer load to and between reinforcements and to protect the reinforcements from environments and handling. Because the reinforcements are typically stronger and stiffer, the matrix is often the weak link in the composite from a structural view. As a continuous phase, the matrix therefore controls the transverse properties, interlaminar strength, and elevated-temperature strength of the composite. However, the matrix allows the strength of the reinforcements to be used to their full potential by providing effective load transfer from external forces to the reinforcement. The matrix holds reinforcing fibers in the proper orientation and position so that they can carry the intended loads and distributes the loads more or less evenly among the reinforcements (figure 2.6). Further, the matrix provides a vital inelastic response so that stress concentrations are reduced dramatically and internal stresses are redistributed from broken reinforcements. In organic matrix, this inelastic response is often obtained by microcracking. Debonding, often properly considered as an interfacial phenomenon, is an important mechanism that adds to load redistribution and blunting of stress concentrations.

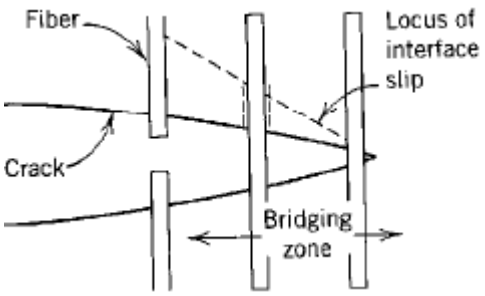

Figure 2.6: Matrix load transfer [23].

One of the most extensively employed organic matrix is the thermosetting epoxy resin. Epoxy resins are a class of thermoset material used in structural and specialty composite applications because they offer a unique combination of properties that are unattainable with other thermoset resins. Available in a wide variety of physical forms from low-viscosity liquid to high-melting solids, it's employed on a wide range of processes and applications. Epoxy resin offer high strength, low shrinkage, excellent adhesion to various substrates, effective electrical insulation, chemical and solvent resistance, low cost and low toxicity. They are easily cured without evolution of volatiles or by-products by a broad range of chemical specie. Epoxy resins are also chemically compatible with most substrates and tend to wet surfaces easily, making them especially well suited to composites applications.

Epoxy resins are routinely used as adhesives, coatings, encapsulates, casting materials, potting compounds, and binders. Some of their most interesting applications are found in the aerospace and recreational industries where resins and fibers are combined to produce complex composite structures. Epoxy technologies satisfy a variety of nonmetallic composite designs in commercial and military aerospace applications, including flooring panels, ducting, vertical and horizontal stabilizers, wings, and even the fuselage. This same chemistry, developed for aerospace applications, is now being used to produce lightweight bicycle frames, golf clubs, snowboards, racing cars, and musical instruments (figure 2.7).

Figure 2.7: Epoxy resin applications [34].

To support these applications, epoxy resins are formulated to generate specific physical and mechanical properties. The designers of these systems must balance the limitations of the raw materials and the chemistry with the practical needs of the part fabricator. While the simplest formulations may combine a single epoxy resin with a curative, more-complex recipes will include multiple epoxy resins, modifiers for toughness or flexibility or flame/smoke suppression, inert fillers for flow control or coloration, and a curative package that drives specific reactions at specified times.

When selecting a thermoset resin, consideration is usually given to tensile strength, modulus and strain, compression strength and modulus, notch sensitivity, impact resistance, heat deflection temperature or glass transition temperature (Tg), flammability, durability in service, material availability, ease of processing, and price. Epoxy resins are of particular interest to structural engineers because they provide a unique balance of chemical and mechanical properties combined with extreme processing versatility. In all cases, thermoset resins may be tailored to some degree to satisfy particular requirements, so formulation and processing information are often maintained as trade secrets.

The three basic elements of an epoxy resin formulation that must be understood when selecting a thermoset system are the base resin, curatives, and the modifiers. When formulating an epoxy resin for a particular use, it is necessary to know what each of these components contributes to the physical and mechanical performance of the part during and after fabrication.

The term “epoxy” describes a broad class of thermosetting polymers in which the primary cross linking occurs through the reaction of an epoxide group. In general, an epoxy resin can be thought of as a molecule containing a three-membered ring, consisting of one oxygen atom and two carbon atoms figure 2.8 [23].

Figure 2.8: Basic chemical structure of epoxy group [23].

While the presence of this functional group defines a molecule as an epoxide, the molecular base to which it is attached can vary widely, yielding various classes of epoxy resins. The commercial success of epoxies is due in part to the diversity of molecular structures that can be produced using similar chemical processes. In combination with judicious selection of a curing agent and appropriate modifiers, epoxy resins can be specifically tailored to fit a broad range of applications.

The first commercial epoxy resin in this class, the diglycidyl ether of bisphenol-A (DGEBA), remains the most widely used today. The structure of pure DGEBA is shown in figure 2.9 [23].

Figure 2.9: Chemical structure of diglycidyl ether of bisphenol-A [23].

Epoxy resins will react with a large number of chemical species called curatives or hardeners. (Other terms often used, sometimes incorrectly, are catalysts and accelerators.) The most commonly used chemical classes of curatives are amines, amine derivatives, and anhydrides.

The third major category of epoxy formulation constituents is modifiers. They are used to provide specific physical and mechanical performance in both the uncured and cured resin. General categories of modifiers include rubbers, thermoplastics, diluents, flame retardants, fillers, and pigments and dyes [23].

2.1.2 Micro-reinforcement - Glass Fiber

The principal purpose of the reinforcement is to provide superior levels of strength and stiffness to the polymer-matrix composites (PMCs). In a continuous fiber-reinforced composite, the fibers provide virtually all of the strength and stiffness. Reinforcing materials may also provide thermal and electrical conductivity, controlled thermal expansion, and wear resistance in addition to structural properties.

The most widely used reinforcement form in high-performance organic-matrix composites OMCs are fiber tows (figure 2.10). These typically consist of thousands of fine filaments arranged in a single bundle. A fiber tow can be handled as a single unit and so can be wrapped or woven using commercial equipment.

Figure 2.10: Glass fiber tow.

Initial scientific and engineering understanding of fiber-reinforced OMCs was based on studies of glass-fiber reinforced composites. Both continuous and discontinuous glass-fiber reinforced composites have found extensive application, ranging from nonstructural, low-performance uses, such as panels in aircraft and appliances, to such high- performance applications as rocket motor cases and pressure vessels. The reasons for the widespread use of glass fibers in composites, both in the past and in the present, include competitive price, availability, good handleability, ease of processing, high strength, and other acceptable properties. Furthermore, the advent of highly efficient silane coupling agents, which are very compatible with either polyester or epoxy matrix, provided a strong and much-needed boost in property translation and in environmental durability.

Glass fiber are among the most versatile industrial materials known today. They are readily produced from raw materials, which are available in virtually unlimited supply [35]. All glass fibers derived from compositions containing silica. They exhibit useful bulk properties such as hardness, transparency, resistance to chemical attack, stability, and inertness, as well as desirable fiber properties such as strength, flexibility, and stiffness [36]. Glass fibers are used in the manufacture of structural composites, printed circuit boards and a wide range of special-purpose products [37].

Glass filaments are highly abrasive to each other [38]. “Size” coatings or binders are therefore applied before the strand is gathered to minimize degradation of filament strength that would otherwise be caused by filament-to-filament abrasion. Binders provide lubrication, protection, and/or coupling. The size may be temporary, as in the form of a starch-oil emulsion that is subsequently removed by heating and replaced with a glass-to-resin coupling agent known as a finish. On the other hand, the size may be a compatible treatment that performs several necessary functions during the subsequent forming operation and which, during impregnation, acts as a coupling agent to the resin being reinforced.

Glass fibers are roughly classified into two categories, low-cost general-purpose fibers and premium special-purpose fibers. Over 90% of all glass fibers are general-purpose products. These fibers are known by the designation E-glass and are subject to ASTM specifications [39]. The remaining glass fibers are premium special-purpose products [23]. On the table 2.1, it's presented a classification of the glass fiber.

Designation	Characteristic
E, electrical	Low electrical conductivity
S, strength	High strength
C, chemical	High chemical durability
M, modulus	High stiffness
A, alkali	High alkali or soda lime glass
D, dielectric	Low dielectric constant

Table 2.1: Fiber glass classification.

The glass fiber most commonly used is known as E-glass, a glass fiber having a useful balance of mechanical, chemical and electrical properties at very moderate cost. Typical strength and stiffness levels for the individual filaments are about 3450 MPa (500 ksi) tensile strength and 75.8 GPa (11×10^6 psi) Young's modulus. Higher-performance, higher-cost S-2 glass fibers have properties of 4830 MPa (700 ksi) tensile strength and a modulus of 96.5 GPa (14×10^6 psi). For specialized applications, such as ablatives, thermal barriers, antenna windows, and radomes, high-silica and quartz fibers are also used [23].

2.1.3 Nano-reinforcement - Carbon Nanotubes CNTs

A carbon nanotube (CNT) can be conceptualized as a tubular microcrystal of graphite and can be considered as a tubular version of fullerene. Therefore, CNTs properties are close to that of an ideal graphite fiber. It consists of one or more cylinders of graphitic shells where trivalent carbon atoms form a hexagonal network [40, 41]. Figures 2.11 & 2.12 show a schematic representation of a graphite layer. Since Ijima's report on CNTs in 1991, scientists have been attracted by CNT's due to their unprecedented geometrical, physical and chemical properties: high aspect ratio, very high specific surface area (up to 1315 m2/g), extremely high strength, lightweight, elasticity, high thermal and air stability (thermal stability up to 2800°C in a vacuum or inert atmosphere), and high electric and thermal conductivity (thermal conductivity twice as high as diamond, and electric-current-carrying capacity 1000 times higher than copper wires) [42, 45]. These properties make nanotubes ideal for many applications as reinforcement in composites improving mechanical, thermal and electrical properties of the bulk product.

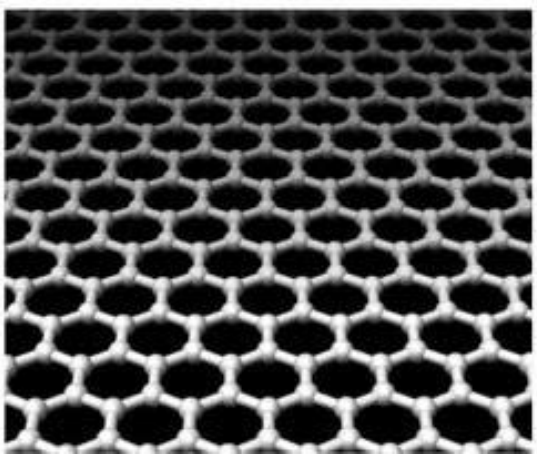

Figure 2.11: Graphitic shell carbon atoms form a hexagonal network [46].

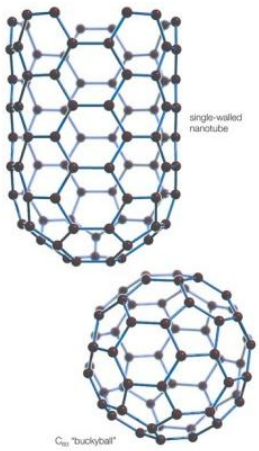

Figure 2.12: CNT as a tubular version of fullerene [47].

Classification of carbon nanotubes according to the number of graphene layers:

- Single-wall carbon nanotubes (SWCNTs): This CNT consists of a single graphene sheet wrapped into a seamless cylindrical tube (figure 2.13). The diameter of SWCNT is around 0.3-10 nm and depends on the corresponding manufacturing method. The length of the SWCNT can reach up to centimeters, therefore yielding an aspect ratio in the range of 105-106 [40, 41, 43, 48].

Figure 2.13: Single-wall carbon nanotube [49].

- Multi-wall carbon nanotubes (MWCNTs): This CNT can be considered as a group of concentric SWCNT (figure 2.14). These concentric layers can be compared to the rings of a tree trunk. The diameter is in the range of 1-200 nm and the constant separation between the layers is 0.339 nm. Hence, by determining the number of nested SWCNT, the MWCNT wall thickness can be calculated [40, 41, 43, 48].

Figure 2.14: Multi-wall carbon nanotube [49].

- Double-wall carbon nanotubes (DWCNTs): This CNT are a special case of MWCNT with two concentric graphene layers (figure 2.15). They combine very similar morphology and properties as SWCNT, and at the same time they have the possibility of functionalizing the outer wall, which will ensure the connections with the matrix, when they are used as reinforcement fillers in composites. In addition, this second wall will improve significantly their resistance to chemicals,

which are usually used in the functionalization of the CNTs in order to add them new properties [50].

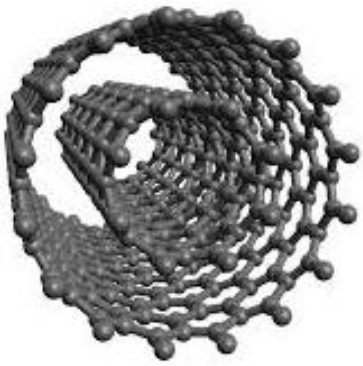

Figure 2.15: Double-wall carbon nanotube [51].

A further and more useful distinction between CNTs can be made when the carbon atom arrangement is taken into account. As it has been explained, CNTs are formed when a graphene layer is wrapped into a seamless cylindrical tube. The graphene layer is formed with carbon atoms which are connected forming carbon hexagons. When the lattice is curved to form a tube, the edges of the lattice, which carry unoccupied bonding sites, need to pair with the available sites. There are many ways in which the edges can pair up; therefore, there are many possible crystallographic orientations of the surface hexagons. The helicity of the tube refers to a crystallographic parameter [52]. In this respect by rolling a graphene sheet in different directions typical nanotubes can be obtained (figure 2.16 & 2.17).

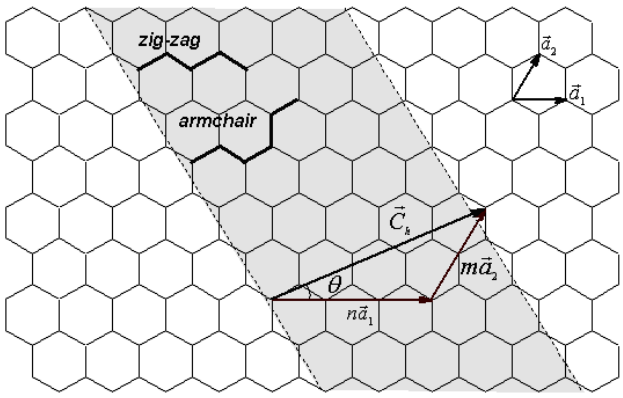

Figure 2.16: Schematic representation of rolling graphene layer to create CNT [53].

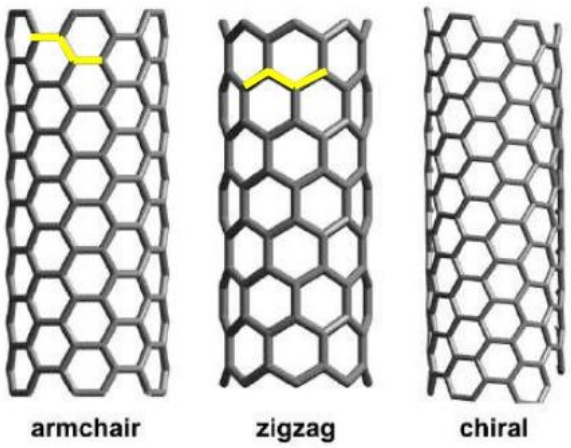

Figure 2.17: Armchair, Zigzag & Chiral Nanotubes [54].

The chirality is an important characteristic in nanotubes. It has a great relevance in the physical properties that depend on the tube diameter. It has been verified that all the armchair tubes are metallic, whereas the zigzag and chiral tubes are either metallic or semiconducting [55].

The production method has an important influence on the properties of the CNTs. The ideal method would be a low cost process which produces large amounts of high purity and uniform CNTs. However, nowadays there is not a method which fulfills all these requirements. Depending on the manufacturing procedure, diameter, length, purity and defects of the CNTs might vary significantly. Arc-discharge, laser vaporization/ablation, chemical vapor deposition and high pressure conversion of carbon monoxide are some methods [40, 41].

Numerous investigators have reported remarkable physical and mechanical properties of CNTs.

- Electrical Properties: The unique electrical properties of CNTs are mainly derived from their 1-D character and the special electronic structure of graphite [56]. Depending on the chirality, CNTs can be conducting (metallic) or semiconducting. They are metallic if the integers of Equation 1.1 are: n=m (armchair) or n-m=3i (where is an integer). All other structures are predicted to be semiconducting [57].

  Resistance occurs when an electron collides with a defect in the crystal structure of the material through which it is passing. These collisions deflect the electron from its path. But in CNTs due to their one-dimensional nature (aspect ratio up to millions), charge carriers can travel through nanotubes without scattering resulting in ballistic transport (it refers to conduction where Ohm's law does not apply and the resistance doesn't depend on the CNT's length). The absence of scattering means that Joule heating is minimized, so that nanotubes can carry very large current densities of up to $1x10^9$A/cm2, 1000 times higher than copper wires (copper wires burn at about $1x10^6$ A/cm2) [45, 48, 58].

  MWCNTs have metallic properties (electrical conductivity > 10^3 S/cm) .They are considered as a collection of concentric SWCNTs with various electrical properties, where electronic coupling takes place between shells. [43, 44, 59].

- Mechanical Properties: CNTs possess high stiffness and axial strength [52]. The tensile strength of CNTs is much higher than high strength steel (1-2GPa) [48].

  It can be seen that MWCNTs are weaker than SWCNTs. This occurs because the individual cylinders, which built MWCNTs, slide with respect to each other. It can also be noted, that tensile strength decreases as nanotube diameter increases [40, 60].

  Due to their hollow cores, CNTs are very stiff in axial direction but very flexible in all other directions, with reversible bending up to angles of 110° for both SWCNTs and MWCNTs [43]. Therefore, they are considered as being very resilient. In addition, they show a high capability to

sustain strain in tension (20-40 %) without brittleness, plastic deformation, or bond rupture [55, 56].

The density of CNTs is about 1.33-1.40 g/cm3, which is just a half of aluminum. Thus, they have an excellent specific strength. Because of all these properties, CNTs are considered as perfect composites‘ nanofillers with many applications, such as, aerospace nanocomposites [43, 48].

- Thermal Properties: CNTs are also very conductive for phonons; the thermal conductivity of SWCNTs is theoretically predicted to be around 6600 W/mK at room temperature; which is nearly the double of diamond of 3320 W/mK [21]. This high conductivity takes place in the CNT axial direction, on the other hand, in the radial direction thermal conductivity is very small. Moreover, SWCNTs are stable up to 2800 ºC in vacuum and 750 ºC in air, whereas metal wires in microchips melt at 600-1000 ºC [43, 48, 56, 61].

2.2 Manufacturing technologies of multiscale composites

Composite materials reinforced by nanoparticles (or nanocomposites) are a prominent topic of recent and ongoing composites research. The improvement of material properties that can be obtained from relatively small quantities of nanoparticles has been a strong motivation for further exploration, leading to optimistic predictions of greatly enhanced mechanical properties across the board for such materials.

Various studies involving nanoparticle enhancement have shown specific increases in static strength [62–66], fracture toughness [65,67–71], and fatigue life [72–76], among other properties, confirming the notion that nanoparticles can have impressive benefits at low concentrations. The resulting enhancements can vary widely depending on the type of property under investigation, the choice of materials, nanoparticle type, concentration and dispersion, and processing methods.

The use of exceptional properties of CNTs in a composite depends strongly on how the CNTs are integrated into the three-phase multiscale composites. The incorporation of nanoscale CNTs with conventional microscale fiber reinforcements in a common polymer matrix can be achieved by modifying either the matrix resin or the fiber reinforcement using the CNTs.

Modifying the matrix resin by dispersing CNTs in the polymer offers the most conventional, facile and industrially compatible route. A number of different techniques have been developed for CNT dispersion into a polymer matrix, which includes shear mixing, calendaring, extrusion, ultrasonication and ball milling [33] (figure 2.18). Many of the recent studies are often based on the use of a combination of aforementioned techniques, such as ultrasonication plus ball milling [78], and ultrasonication plus extrusion [79, 80].

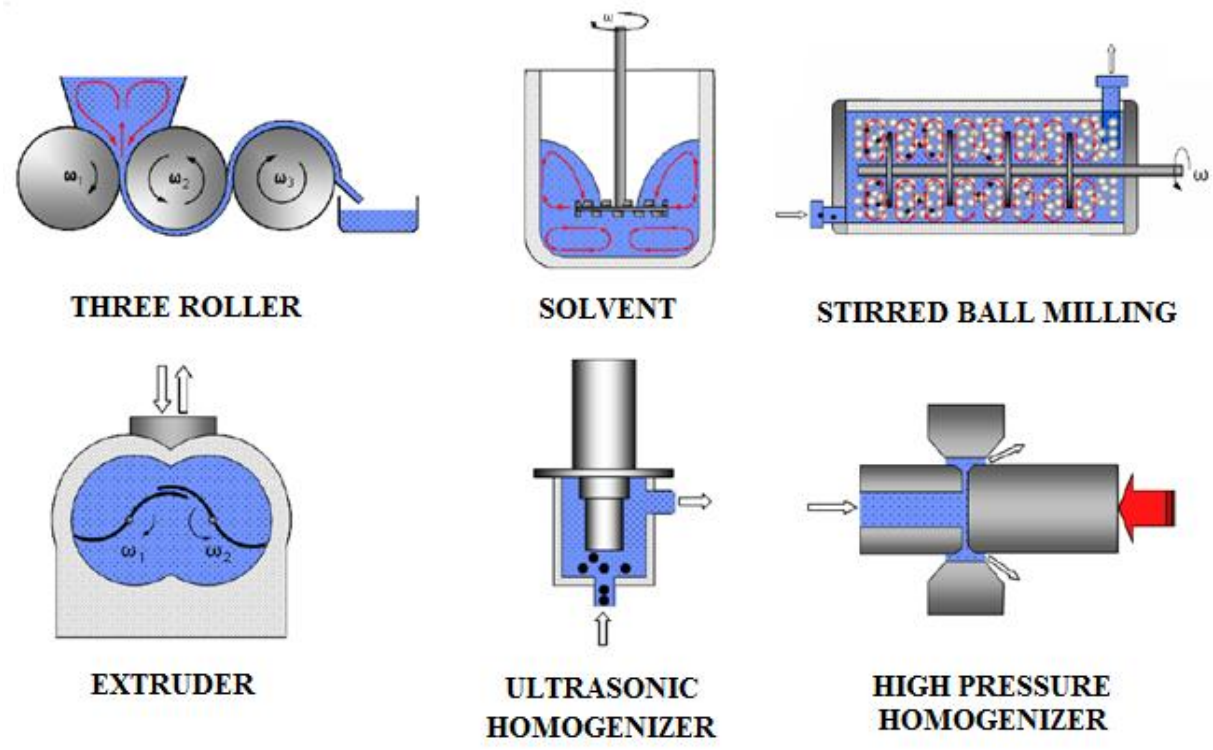

Figure 2.18: Modifying CNT-Resin techniques [81].

Fabrication of multiscale FRCs using modified resins has some limitations that difficult their development and widespread applications. One of the main problems in this approach is that the viscosity of a CNT-modified matrix increases dramatically with increasing CNT content, even with a very small content below 1 wt%, leading to severe agglomeration of CNTs in the bulk of the composite. The highly viscous and CNT-agglomerated resin systems cannot be processed using the conventional composite manufacturing techniques. For example, when fabricating multiscale FRPs using the vacuum assisted resin transfer molding (VARTM) process, nanofillers can become filtered, resulting in an inhomogeneous microstructure of multiscale composites [82-85]. Filtering is caused by the nanofillers being trapped in inter-tow regions within the fiber preform mesh during fabrication. A comprehensive study [85] revealed a direct correlation between the concentration of CNFs and the processing parameters, such as viscosity and filtering: a CNF concentration above 1% resulted in a significant filtering effect, leading to the formation of many microvoids in the composite.

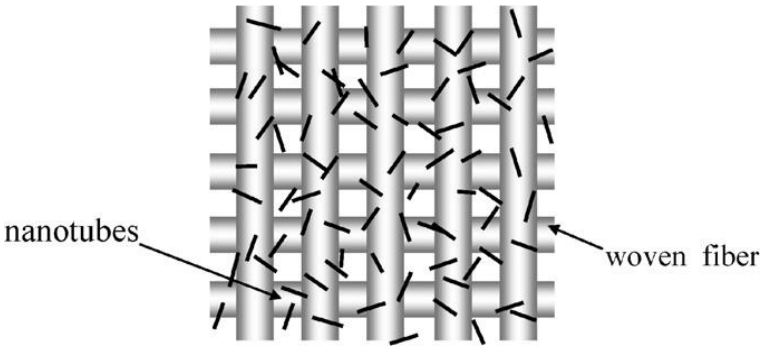

Figure 2.19: Overcoating method for distributing nanotubes onto woven fiber prior to VARTM processing [72].

Apart from the above conventional techniques of mixing CNTs with a polymer resin before incorporation with fiber reinforcements, more systematic approaches have been developed to fabricate advanced FRPs, including i) attachment, grafting or growth of CNTs on the reinforcing fibers or fabrics (figure 2.19), ii) interleaving Bucky papers made from CNTs at certain laminar interfaces, iii) manual spreading or spraying of CNTs on prepregs. The key advantages of direct attachment of CNTs on the fibers/fabrics or interleaving technique are the ability to incorporate CNTs at high concentrations and incorporate the CNTs selectively at the locations of interest within a composite. The effects of growth conditions on CNT morphology have been evaluated [86-90]. Grafting of aligned CNTs or CNFs on to the conventional fiber surface resulted in a 3D hierarchical composite (figure 2.20) with enhanced mechanical and multifunctional properties [91-93].

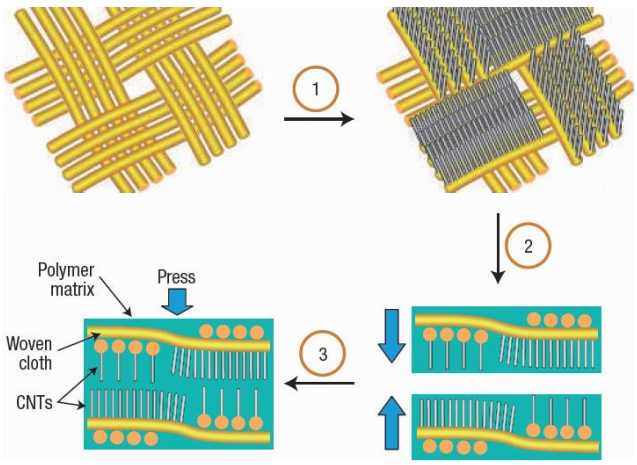

Figure 2.20: 3D Hierarchical composite [91].

Introducing aligned CNTs to CFRPs was accomplished by growing a vertically-aligned CNT forest at a high temperature, and then transfer-printing the CNTs to prepregs at room temperature [94]. The prepreg was attached to a cylindrical drum that was rolling under pressure across the substrate containing the CNT forest to transfer the CNTs to prepregs, taking advantage of the tack of the prepregs to separate the CNT forest from the growth substrate (figure 2.21). Electrophoretic deposition (EPD) is another technique that has been widely applied to selectively deposit CNTs on fabrics. CNTs were uniformly deposited on the surface of carbon fabrics using the EPD technique where both as-received and oxidized CNTs were deposited onto the carbon fiber electrodes under an applied electric field [95]. EPD is a simple and versatile technique that can be readily automated and scaled up for mass production.

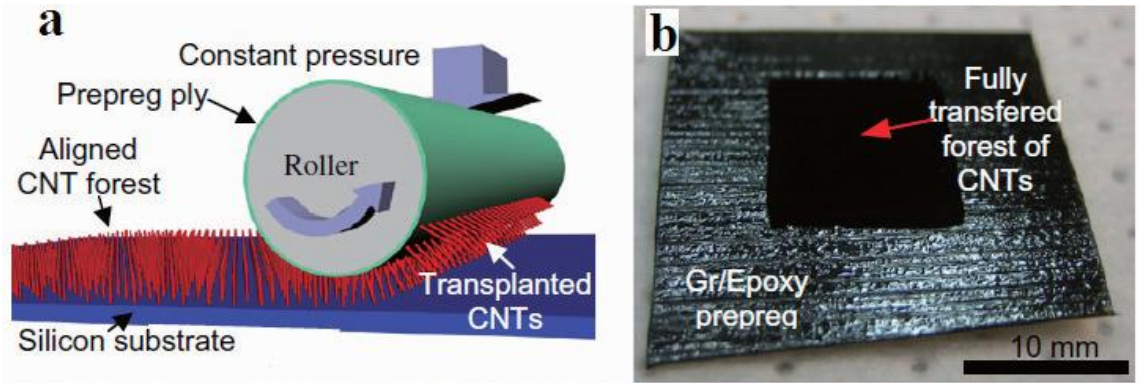

Figure 2.21: CNTs transfer-printing to prepregs [94].

A technique known as 'powder method' was devised to add CNTs onto the ply surface [96]. The method is schematically described in figure 2.22 where the powder of vapor grown carbon fibers (VGCFs) are manually spread at the mid-plane of CFRP laminates using a sifter with a mesh size about 70 μm. A VGCF interlayer is automatically formed during melting and curing of resin at a high temperature and pressure in the autoclave. A CNT-solvent paste, e.g. CNF-ethanol past, was also applied manually on a CFRP prepreg using a metal roller [97]. After evaporating the solvent on the prepreg sheets, the two parts of prepregs were bonded together and cured. A CNF interlayer of 50-200 μm in thickness was naturally formed by the fusion of CNFs and epoxy resin during curing. A thin layer of CNTs was also dispersed onto the surface of woven fabric using a spray-up process [60]. This process involved coating of a pre-dispersed CNT-solvent solution on the fabric using a spray gun, and deposition of CNTs at the prescribed weight percentage on the fabric after evaporation of the solvent. Composites were then produced through a RTM process. CNTs were also integrated into FRPs by adding CNTs in the fiber sizing formulation through which the continuous fibers were drawn [99].

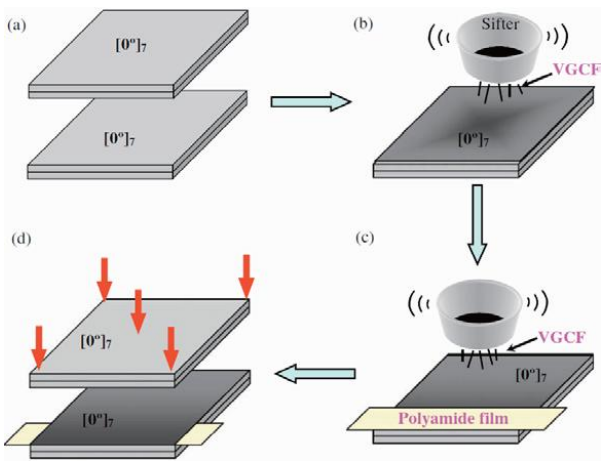

Figure 2.22: Powder of vapor grown carbon fibers [96].

Interleaves containing well-dispersed CNTs in a β-stage epoxy thin film were developed to insert between plies in a laminate composite, which was subsequently co-cured with the infused epoxy resin based on a VARTM process [100]. The interleaving thin films were produced by dispersing CNTs in

epoxy after sonication and casting on a release paper using a thin film coater. This technique is limited to low CNT contents because the films are produced by dispersing CNTs in a resin using a conventional method. However, the CNT contents in the interleaves can be drastically increased if CNT Bucky papers are employed. Composite thin films have recently been produced using partially cured epoxy-CNF Bucky papers of high CNF contents for use as interleaves in CFRPs [101], where the CNF Bucky paper was impregnated with an epoxy resin by vacuum infiltration. The partially cured composite thin film was placed between CFRP prepregs before curing to improve the interlaminar fracture resistance of the bulk composites. This approach allowed the incorporation of high CNT contents in FRPs, avoiding the difficulties associated with high viscosity arising from the high nanofiller contents.

The choice and application of the aforementioned techniques for integration of CNTs and CNFs in FRPs depend on many factors, including the availability of required tools or equipment, CNT contents and the final composite properties being sought [22].

2.3 Resin Transfer Molding

In the RTM process, the dry fiber-reinforcement preform is first placed in an open matched mold. The mold is closed and reactive liquid resin is injected at low pressure into ports in the mold to obtain thermoset polymer composites (figure 2.23), excess air is forced out other vents in the mold.

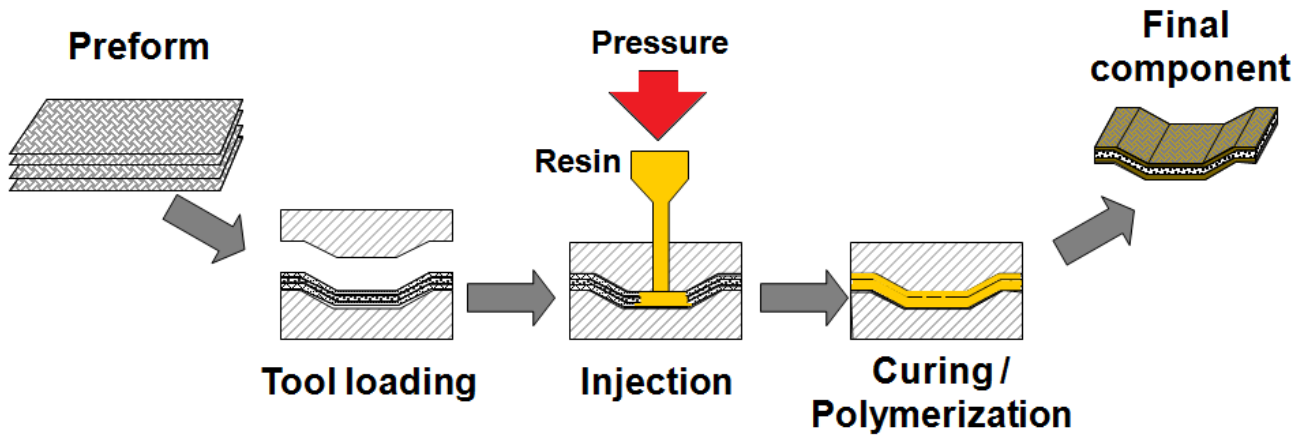

Figure 2.23: RTM process [103].

In vacuum-assisted resin transfer molding, vacuum can be applied to the vent ports to assist in drawing the resin into the fiber preform and removing any trapped air. There are many variations of the resin infusion process. For example, for cost reduction, molds can contain a single-sided hard tool side, where the opposite side of the tool can just be a simple, flexible vacuum bag. Other variations contain an air gap or high permeability layers over the platform surface of the part, to allow the liquid resin to flow quickly over and "above" the surface (figure 2.23), before the slower process of diffusing

through the preform (hence, using this method, the liquid has only to diffuse through the preform thickness, not across the part width direction as in RTM). In one variation of this process, Liquid Compression Molding, once the resin has flowed through the air gap over the preform, the tool can be further closed creating additional pressure to force the resin into the preform [23] (figure 2.24).

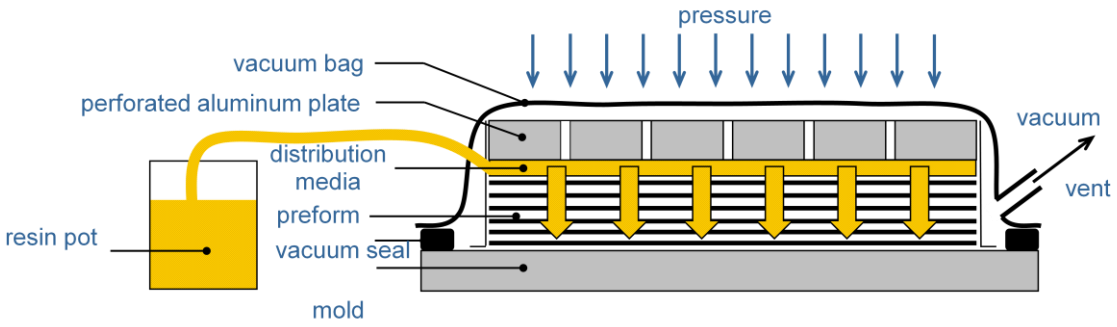

Figure 2.24: Liquid compression molding [109].

Resin injection through a fibrous reinforcement is modeled as a flow through a porous medium and obeys Darcy's law (figure 2.25), which states that the resin flow rate through a unit area of material is proportional to the pressure gradient in the mold [102]. The coefficient of proportionality is the permeability of the porous medium (measured by appropriate experiments) divided by the viscosity of the resin (which varies in time with temperature and degree of cure). Permeability becomes lower when the fiber volume content of the composite increases, whereas viscosity decreases with temperature.

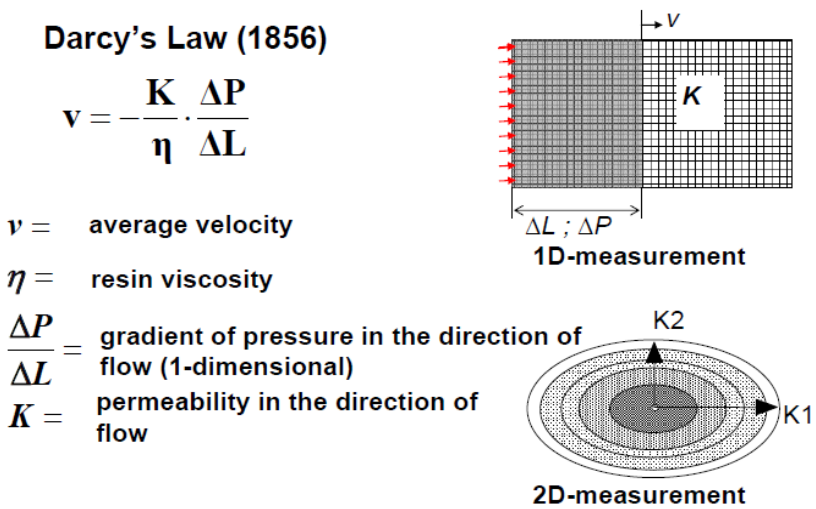

Figure 2.25: Darcy's law [103].

The pressure field in the mold may also be displayed. A correct knowledge of mold filling allows adequate positioning of the injection ports and vents. There are three ways to facilitate the resin flow in the mold: decrease the fiber volume content (for example, by lifting slightly the mold cover during

injection), increase the injection pressure, or heat the mold and/or the resin to reduce viscosity. Using the appropriate simulation software, these three parameters can be studied and tuned adequately. A RTM simulation software should contain the following four critical features [104]:

- It must satisfy the exact conservation of resin mass during injection.
- It must be able to simulate race tracking, that is, the much faster resin flows that occur in specific areas of the mold, such as the edges.
- It must solve the heat transfer problem during resin injection (i.e., calculate the temperature field in the mold and in the part).
- Finally, it must simulate curing of the part.

Linking the RTM finite-element software to the composite engineering software through a RTM interface provides a more accurate description of the resin injection process by incorporating in the RTM model local variations due to the composite material draping process. Draping may generate local changes in ply thickness and directional variations in porosity and permeability due to material scissoring [23].

Resin transfer molding has the potential to overcome the disadvantages of traditional hand lay-up by being less labor intensive and having the ability to form complex shapes and hollow parts. RTM has some advantages over prepreg construction: Prepreg is stiff and difficult to form into shapes, RTM does not require secondary bonding and has better surface finish because it has hard tooling on all sides. The main disadvantages of RTM are associated with tooling. Resin flow is difficult to control, making mold design and temperature critical. Tool tolerances are important. This technique combines to make tooling costs high, and there are additional costs for pumps and a press [105].

2.3.1 Hollow parts manufacturing

Hollow structures offer a significant weight and cost saving compared with sandwich panels, but require more imagination to produce by RTM, figure 2.26 [106]. A common technique here is to use an elastomeric bladder, which may be filled with particulates. The bladder is filled, loaded into the mold, and evacuated to rigidize the core. The preform skins are added and the matrix resin is injected. Following resin cure, the core can be removed after releasing the vacuum. In a further variant, a positive pressure is applied to the bladder after the end of injection and prior to resin cure in order to consolidate the laminate. One potential advantage here is that the core may be formed with indentations in the surface that provide a runner system to aid resin distribution. These channels are destroyed when positive pressure is applied to the bladder, and the excess resin is bled out through the

laminate. If particulates are used to stabilize the bladder, these can be extracted after venting. The bladder itself may be sacrificial or reusable [23].

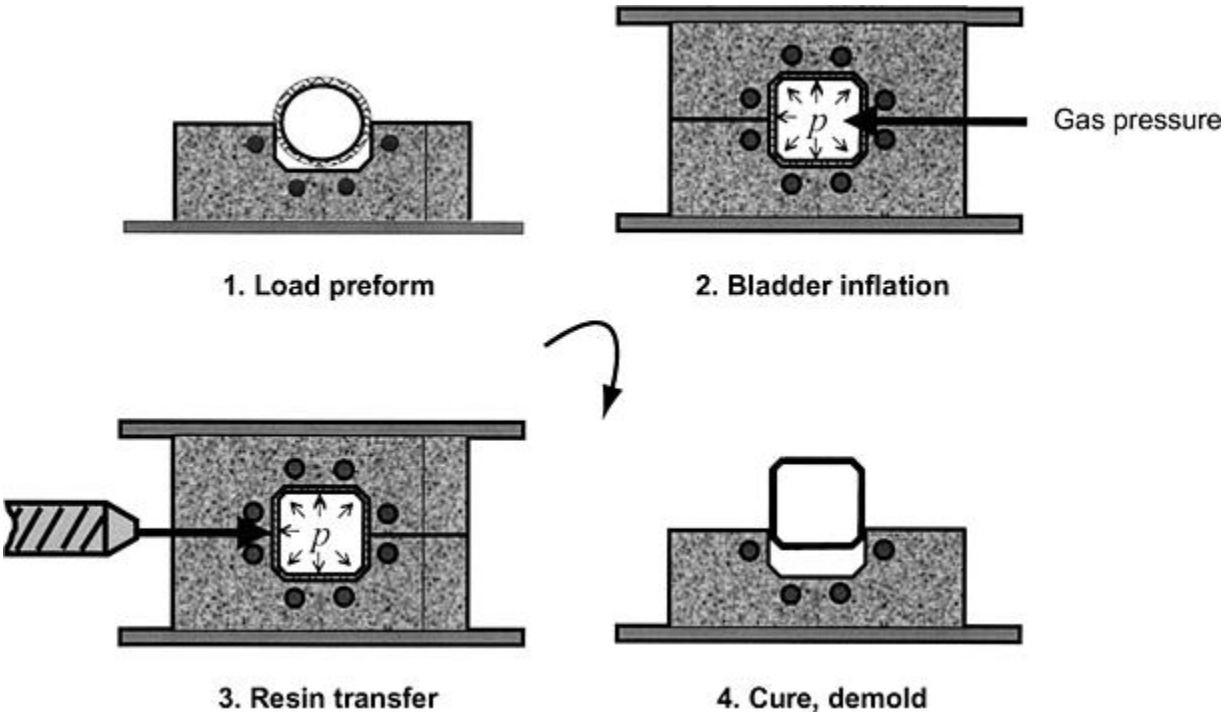

Figure 2.26: Bladder inflation molding for hollow RTM structures [106].

3 Manufacturing process development

3.1 Part description

A bicycle seat post is a tube that extends upwards from the bicycle frame to the saddle, support the weight of the rider and resists mechanical stress of pedaling. Figure 3.1, shows the location of the seat post in a bicycle.

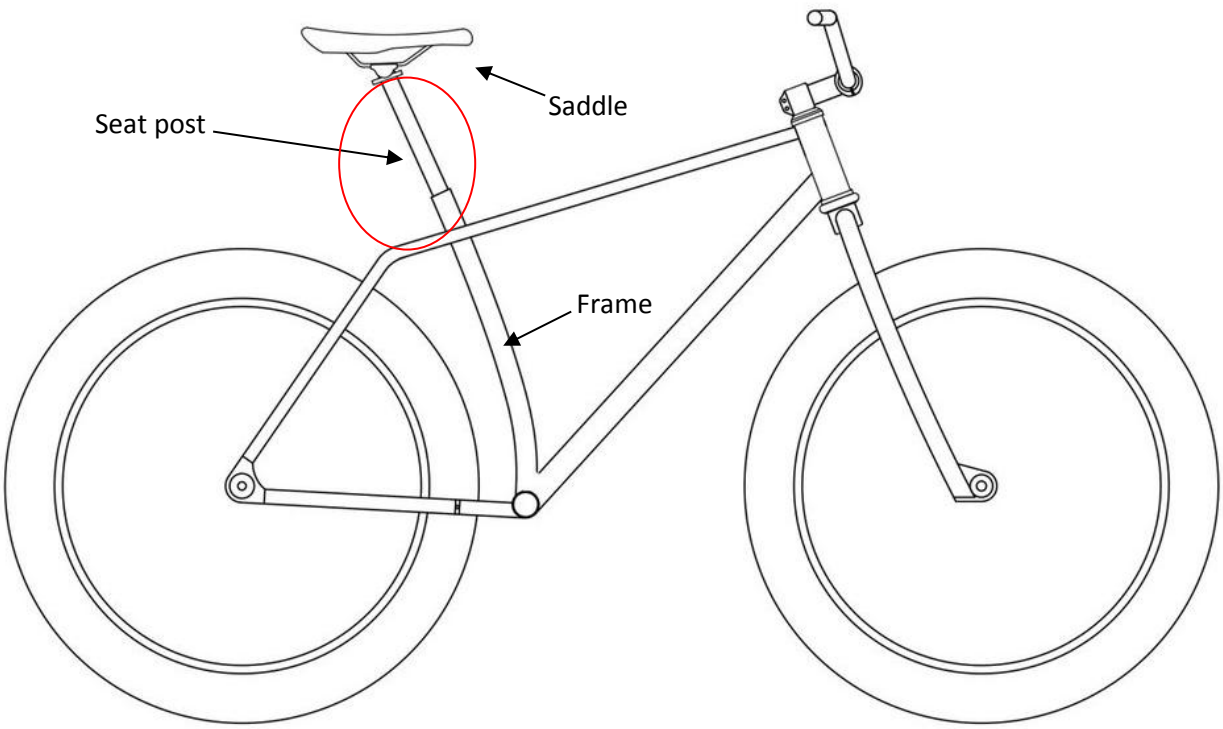

Figure 3.1: Bicycle seat post location (by moonmenbikes).

A plain bicycle seat post consists on a tube with clamp at the top to attach the saddle. One bolt tightens the clamp and the saddle rails at the same time. On this project, the target is seat post made with glass fiber and resin modified with carbon nanotubes in which the manufacturing process is focused. Figure 3.2, shows the basic design of a plain the seat post.

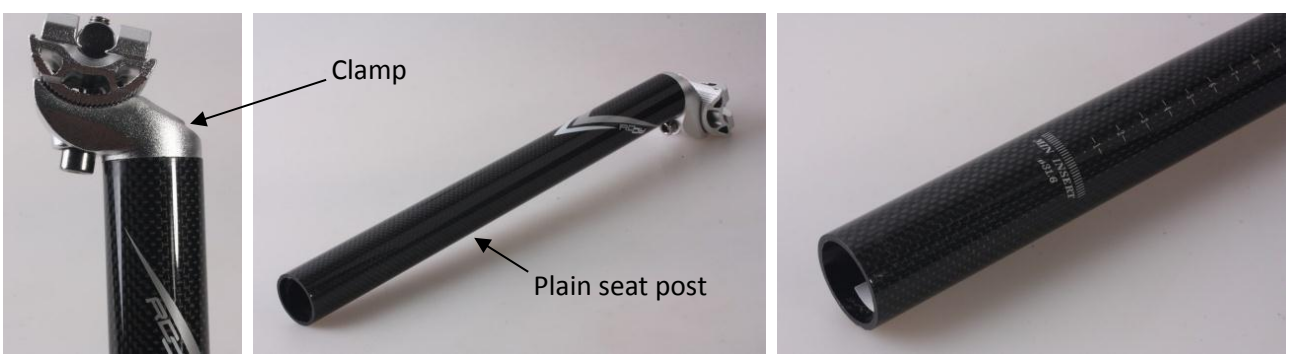

Figure 3.2: Plain seat post.

The specifications of the seat post have been set in the project in order to have standard dimensions. Standard outside diameter is necessary because it accommodate standard parts like lugs, clamps, etc. The dimensions of the seat post object of this project are standard for high quality bicycles. Table 3.1 and figure 3.3 collect all the dimensions necessaries for the tooling development.

Variable	Acronym	Value
Outer diameter	D_o	27,2 mm.
Thickness	t	2 mm.
Inner diameter	D_i	23,2 mm.
Length	L	300 mm.
Weight	P	< 185 gr.

Table 3.1: Seat post dimensions.

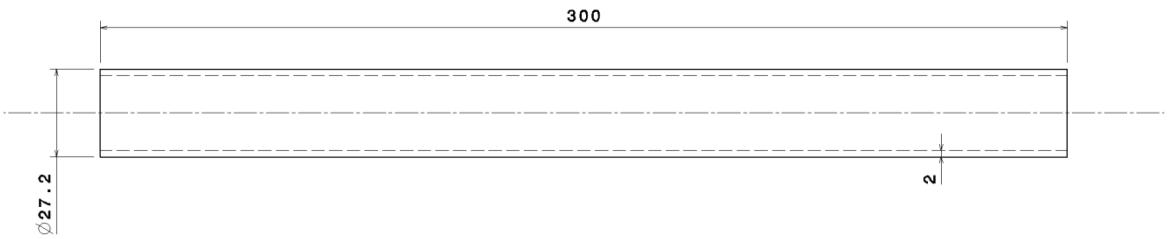

Figure 3.3: Seat post dimensions.

An aesthetically attractive CAD model (figure 3.4) has been obtained with the required dimensions for the seat post object of the following tooling development (section 4.2, 4.3, 4.4).

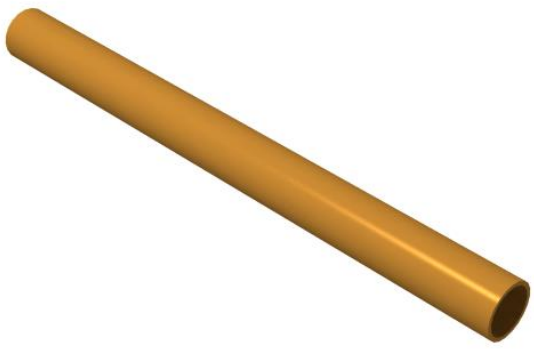

Figure 3.4: Seat post 3D CAD model.

3.2 Developing a RTM technique to manufacture seat posts with CNTs

The present project focuses on the development of a bladder assisted-RTM tool to manufacture seat post tubes made of multiscale composites based on glass fiber-epoxy resin modified with carbon nanotubes. The target is to take advantage of the bladder assisted-RTM process characteristics to get a homogeneous distribution of CNTs within the glass fiber reinforcement. This development project include the design of an innovative inflatable bladder key to the impregnation process. On the figure below (figure 3.5), it's shown a preliminary concept of the impregnation process.

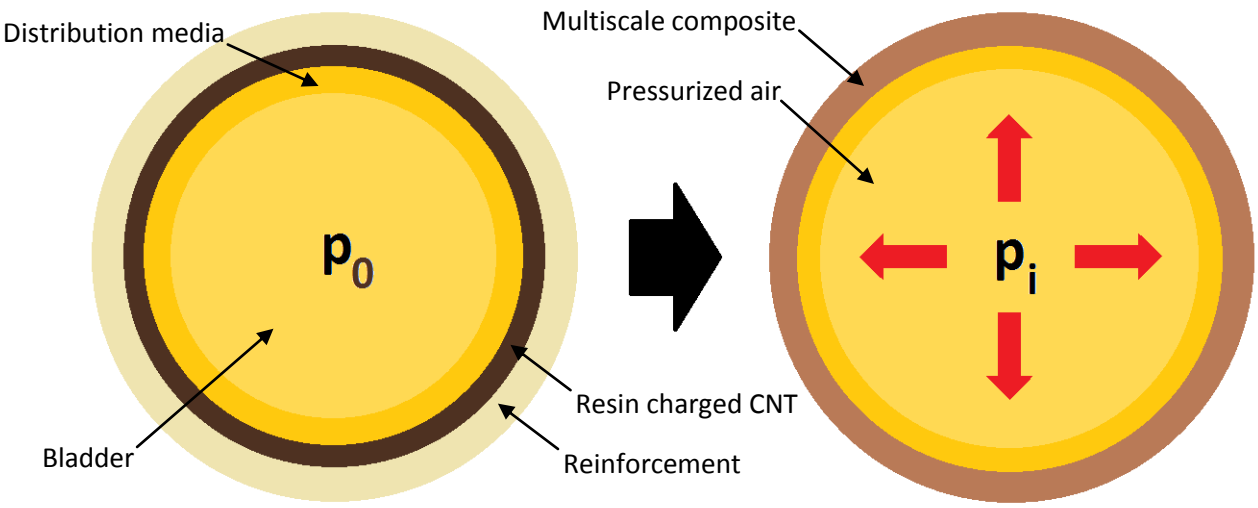

Figure 3.5: Preliminary bladder assisted-RTM concept.

The inflatable bladder must provide a resin distribution media on its external surface that facilitates the impregnation of its high viscosity resin due the CNT addition. Before resin injection, the CNTs must be homogeneously dispersed on the resin matrix.

The application of positive pressure inside the bladder will elastically deform it and the external surface will force the resin matrix to flow through the laminate thickness. Thus, the CNTs filtration is reduced through the laminate thickness.

3.3 Tooling design

The development of the bladder assisted-RTM tooling have been done following the stages of the VDI (*Verein Deutscher Ingenieure*) Society for product Development, Design and Marketing published Guideline VDI 2221, "Systematic Approach to the design of Technical Systems and Products" in 1987. That guideline examined the most important fundamental principles for a systematic approach to design (see figure 3.6) [107].

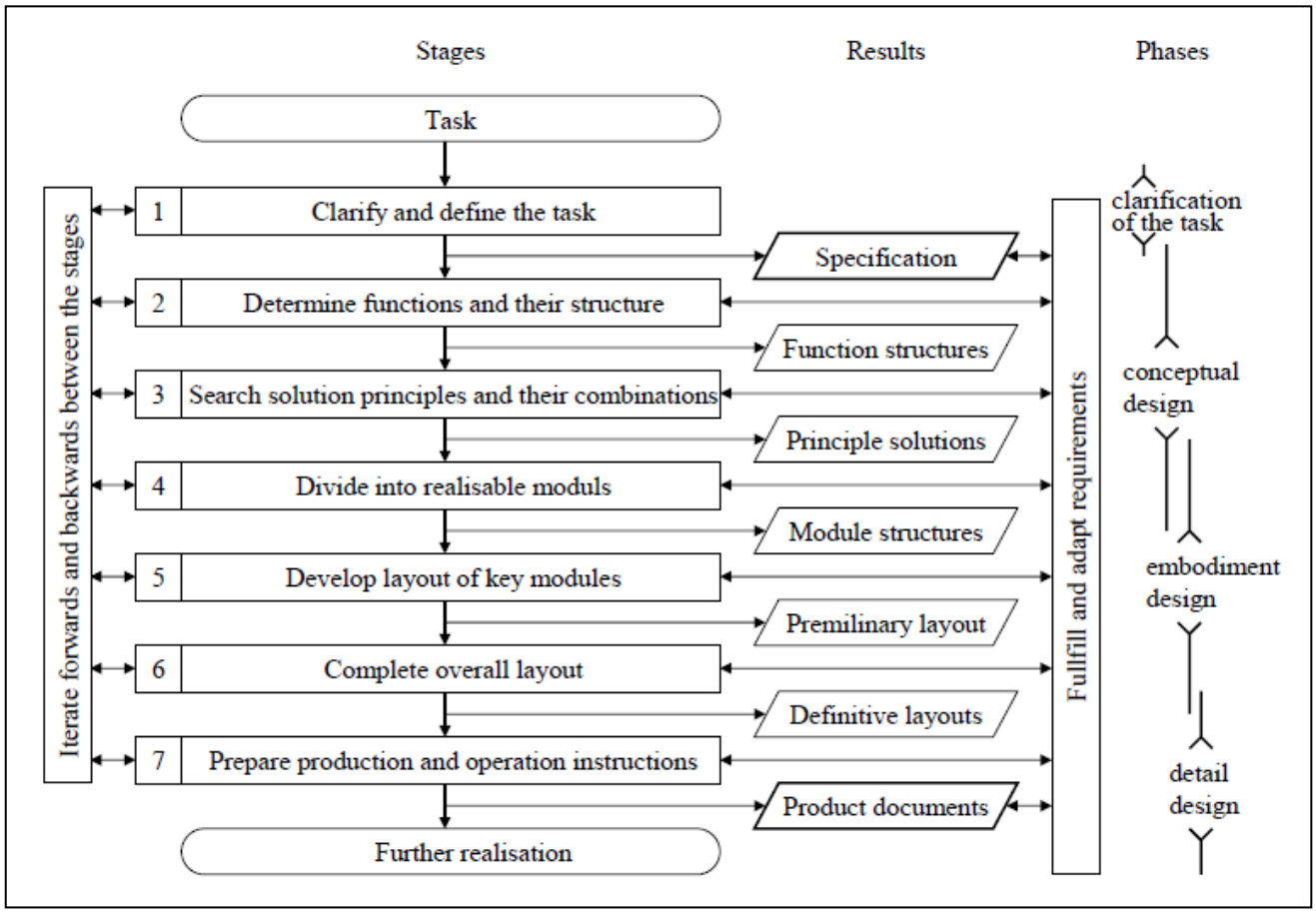

Figure 3.6: General approach to design [103].

This is the model used in this project to provide a solution to the problem by providing a clear structure that is easy to understand and follow.

4 Bladder assisted RTM tool development

4.1 Analysis stage

In the first stage of the design, the task and the boundary conditions of the bladder assisted-RTM tool are preliminary defined. This definition is done according to the investigation lines open on the project *CarboRoad* and based on the literature review done in the field of multiscale composite manufacturing. This phase of the project is also called "phase information".

Boundary conditions are defined by an external mould and a core tool that provides the shape and surface finish of the seat post. Different zones identified on the sketch model (figure 4.1), for the manufacturing of hollow parts with RTM, will serve to organize the functions into realizable modules during the design process. Figure 4.1 presents the boundary conditions.

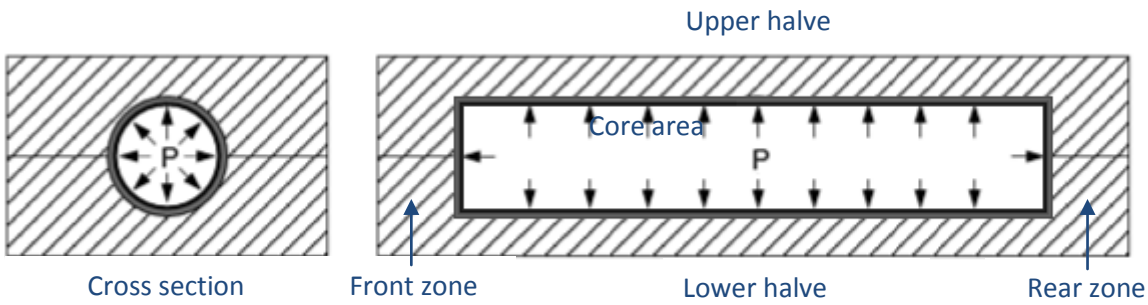

Figure 4.1: Boundary conditions.

In order to clarify and define the task of the project, the information of the process is collected in a checklist and then entered into a request list, which determine whether there is a demand, a wish or a recommendation for individual requirements. The result of the analysis done to define the task is presented on the request lists (see table 4.1), which include all the requirements for the tooling development. This work was started by Alex Mann on his work [108], and updated for this project.

Nr.	RTM mould tool requirement	Demand	Request	Recommendation
1	Transparent tooling to check the impregnation behavior	X		
2	External part diameter; D_o = 27,2mm.	X		
3	External part length; L = 300mm.	X		
4	Part thickness; t = 2mm.	X		
5	Vacuum connection (max. 0,5 bar)	X		
6	Tool surface finish (external & internal part surfaces)		X	
7	Compressed air connection	X		
8	Port connection for resin injection	X		
9	Support internal pressure of 2.5 bar	X		
10	Modular tooling	X		
11	Easy to clean (maintenance)		X	
12	Easy de-molding		X	
13	Heating/cooling system		X	
14	Tightness (avoid resin leakage)	X		
15	Mechanical closing device		X	
16	Elastic core tool	X		
17	Stiff core to support the fiber preform		X	
18	Resin distribution media	X		
19	Thermal resistance (~ 100ºC)		X	
20	Reusable	X		
21	Prevent oxidation		X	
22	Lightweight and handy			X

Table 4.1: Requirements list for bladder assisted-RTM tool.

4.2 Conceptual design

In this second phase is developed a functional structure from the listed requirements on table 4.1. The functions of the bladder assisted-RTM tooling are determined, first the overall function and then the most important sub-functions to be fulfilled by the development. This function structure is presented in an organizational chart on the figure below (figure 4.2).

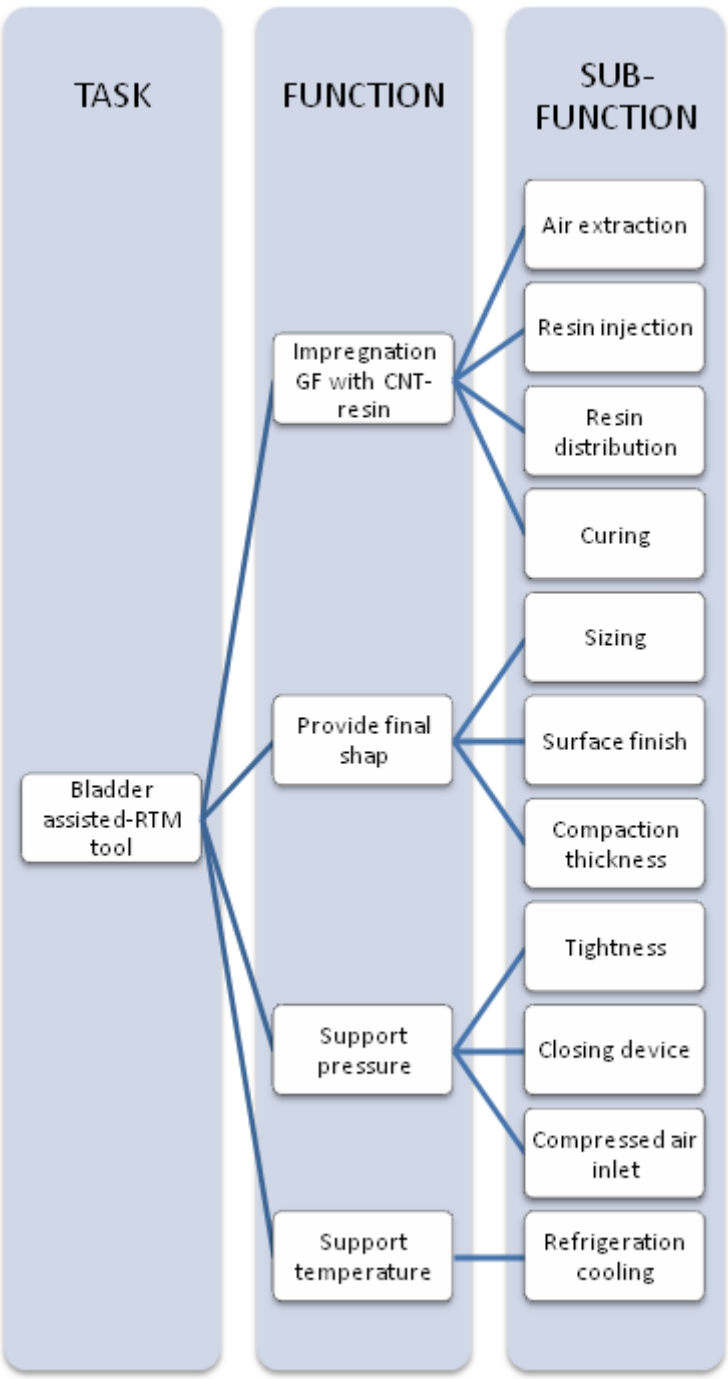

Figure 4.2: Function structure chart.

In this organizational chart, that arises from the analysis done on the list of requirements, the overall target functions are broken down into sub-functions based on operational considerations.

The classification and combination of these sub-functions into structures forms a basis for the search of solutions for the overall product. At this point of the project, the sub-functions are organized into realizable modules, before starting the complex and time-consuming process of defining these modules in more concrete terms. The interfaces between sub-functions are established roughly and classified in the following organizational chart, according to the future location of the function on the bladder assisted-RTM tool. The chart in figure 4.3 serves for a better understanding of the next design steps.

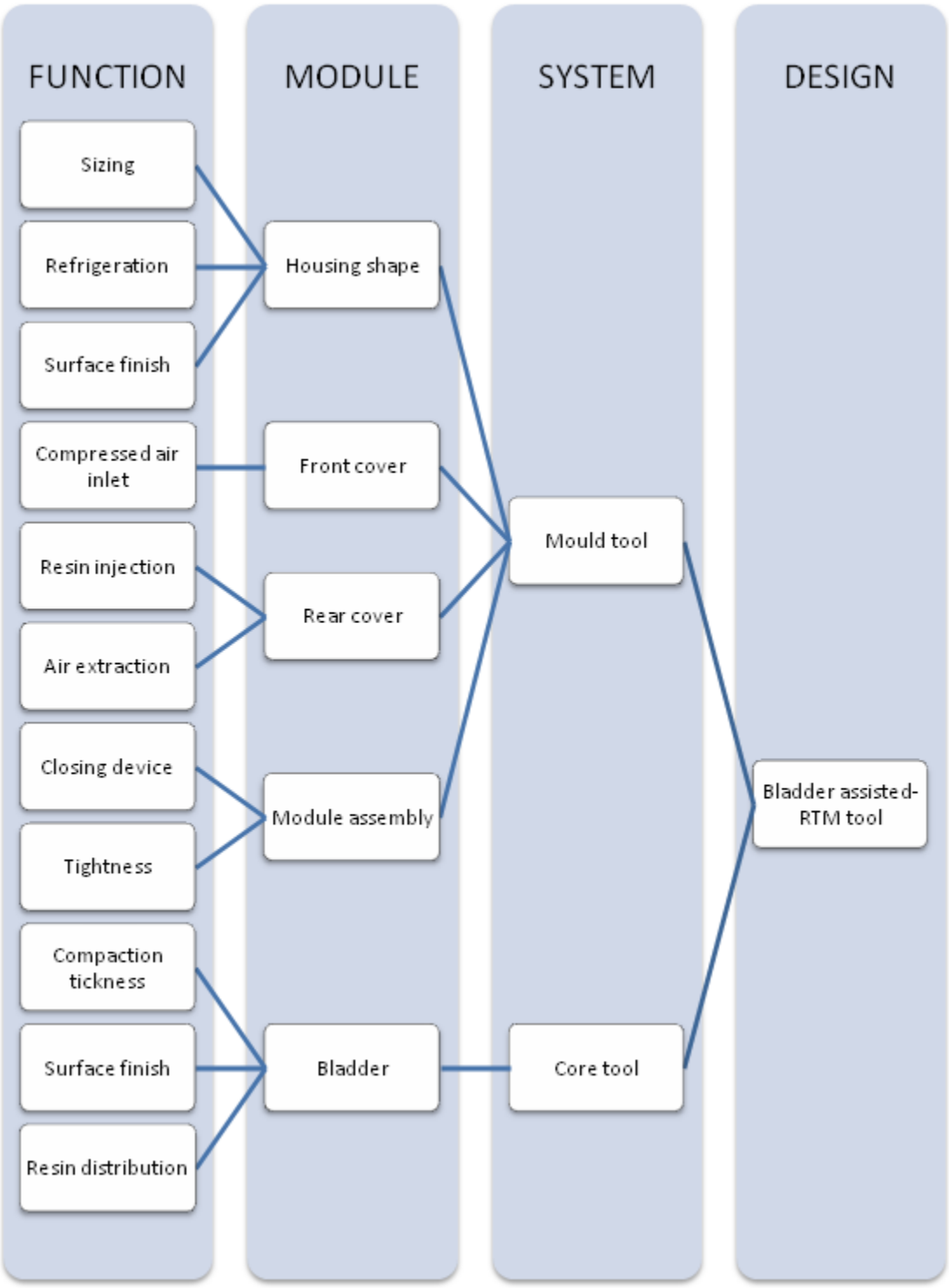

Figure 4.3: Module structures chart for the bladder assisted-RTM tool.

In contrast to the function structure, a module structure provides a preliminary indication for the breakdown of solution into the realizable groups and elements, which together with their interfaces are essential for its implementation. A module structure facilitates the efficient distribution of design effort and helps with the identification and solution of embodiment design problems.

Following the modules structure chart are provided possible solutions for every module in order to obtain an optimal solution for the project task. The result of this work is presented in a morphological box made with individual solutions proposed for the different modules (table 4.2 & 4.3). It is a useful scheme, in which each principle solution will be followed. The individual principle solutions are made with the help of a brainstorming session after researching the literature. Each solution provide its advantages and disadvantages, and it is discussed on next steps in order to find the best solution.

Module		Housing shape		Front cover	Rear cover	
Function		Sizing	Cooling system	Air-extraction	Resin Injection	Compressed Air-inlet
Principle Solution	1	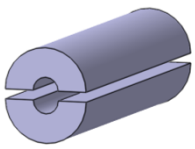 Round	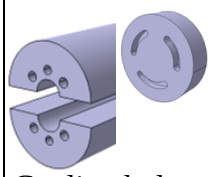 Cooling holes	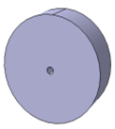 Centered	 Simple	 Simple
	2	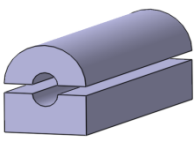 Half round	External system	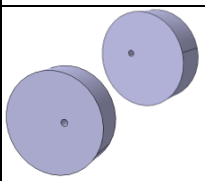 Offset	 Offset	 Offset
	3	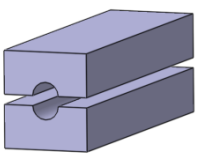 Rectangular		 Distributed		
	4	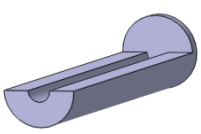 Half-open				
	5	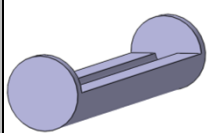 With ends				
	6	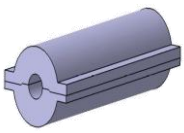 Round-Flange				

Table 4.2: Sub-functions principle solutions for the RTM tool.

Module		Module Assembly			Bladder	
Function		Closing device	Centering	Tightness	Surface finish Resin distribution	Path design
Principle Solution	1	 Screw	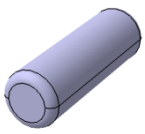 Pins	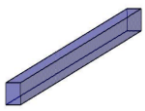 Longitudinal	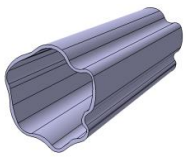 standard	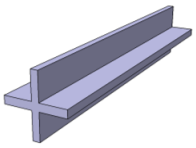 Without holes
	2	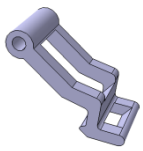 Clips	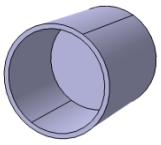 Cylinder	 Circular	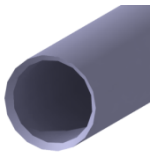 Circular	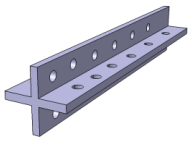 With holes
	3	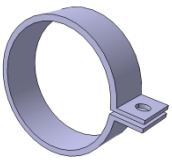 Ring	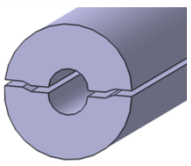 Slope (angle)	Without Surface-Surface	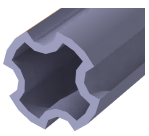 4 channels	Without
	4	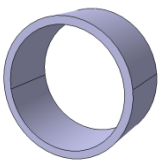 Hollow cylinder	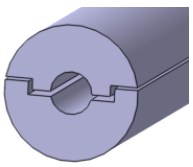 Edge		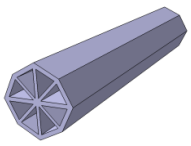 Reinforced	
	5		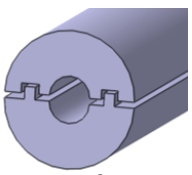 Profile		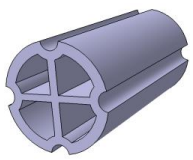 4 Channel cross	
	6				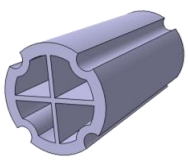 4 channels	
	7				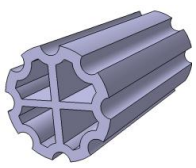 8 channels	

Table 4.3: Sub-functions principle solutions for the RTM tool.

After analyze all principle solutions for every module, it have been selected the most adequate solution to ensure the task of the tooling development. Selected principle solutions are presented on the table below (table 4.4), with some explanations for its selection.

Nr.	Sub-function	Principle Solution	Why is selected?
1	**- Body mould - Housing shape**	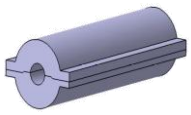 Round	• Symmetry of the part. • Easy handling. • Provide area for mechanical closing. • Facilitate de-moulding process.
2	**Cooling system**	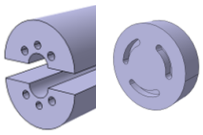 Cooling holes	• Symmetry of the seat post. • Low temperature reaction. • Low investment (water).
3	**- Front cover - Air-extraction**	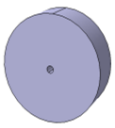 Centered	• Symmetry of the seat post.
4	**- Rear cover - Resin Injection**	 Offset	• Direct injection on the fibre reinforcement.
5	**- Rear cover - Compressed air connection**	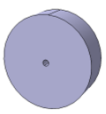 Simple	• Symmetry of the seat post.
6	**Closing device**	 Screw	• Avoid complex hidraulic systems. • Ensure mould closing during all the RTM process.
7	**Centering of the items (parts)**	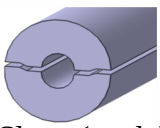 Slope (angle)	• Easy assembly.
8	**- Gaskets - Tightness**	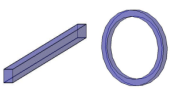 Longitudinal Circular Gaskets	• Avoid resin leakage. • Mix of resin and water. • Vacuum drop.
9	**- Bladder - Core design**	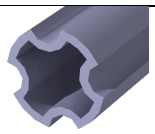 4 channels	• Facilitate CNT-resin distribution a long the laminate. • Facilitate the bladder manufacturing.

Table 4.4: Principle solutions selected.

The assembly of all the principle solutions already selected define the concept design for the bladder assisted-RTM tool for the manufacturing of multiscale composites. At this step the concept design is finish and the functional-logical solution to the problem is defined (figure 4.4 & 4.5).

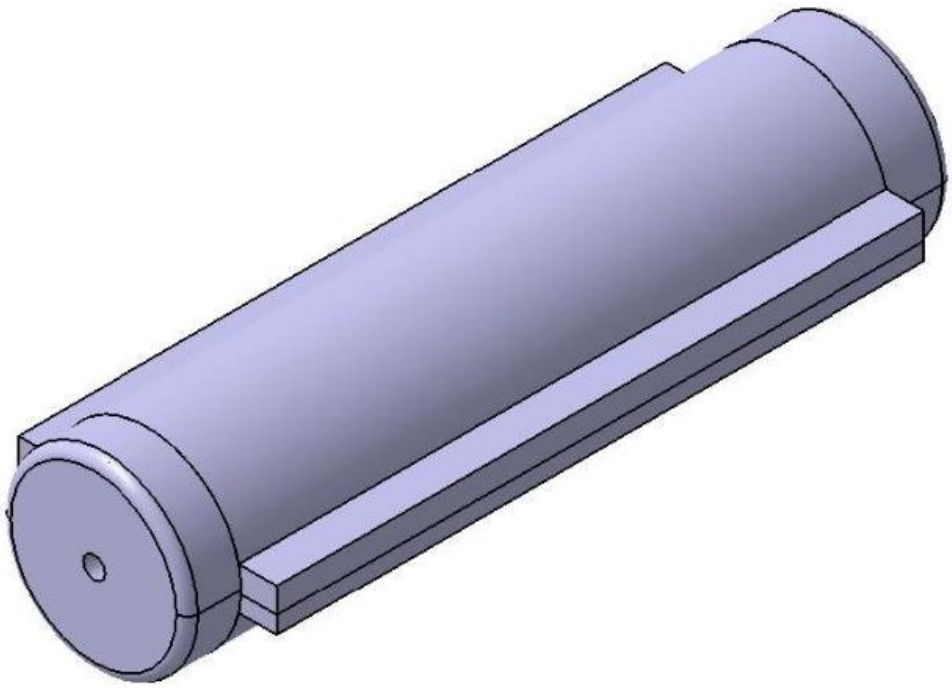

Figure 4.4: Concept mould design.

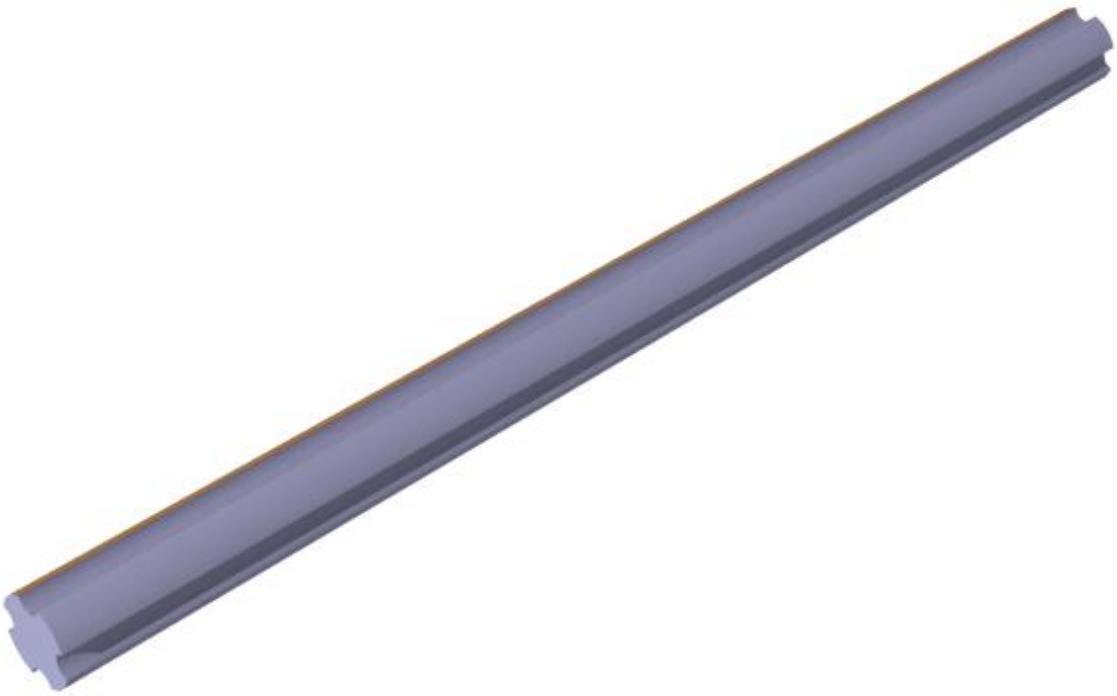

Figure 4.5: Concept core tool / bladder design.

4.3 Design stage

The design phase consists on developing the layouts of the individual modules. The selected solutions for the individual modules are detail designed and calculated to confirm that the solution meets the requirements of the overall function. The level of refinement of the geometry, materials and other details should only be pursued as far as to allow the optimum design to be selected.

The result of the design phase is a set of layouts for the individual modules (table 4.5), see appendix C.

Component	Parts quantity	Drawing
Upper mould	1	1/8
Lower mould	1	2/8
Front cover	1	3/8
Rear cover	1	4/8
Inflatable bladder	1	5/8
Longitudinal sealing gasket	2	6/8
Circular sealing gasket	4	7/8
Screw	12	8/8

Table 4.5: Module layouts.

At the end of this section, all the individual solutions are combined to form the overall design and it must be ensured that the solution meets the requirements of the bladder assisted-RTM tool.

4.3.1 Upper mould

The upper mould has the task of shaping and surface finish to the outer side of the seat post. It assembles mechanically with the lower mould to form the body mould. It accommodates channels for the cooling phase after the curing process and support the internal pressure.

The material selected for the manufacturing is PMMA because of his optical attribute of being transparent that allow to follow the resin flow during the injection process. PMMA has also an optimal weather and scratch resistance, compared with other similar materials like polycarbonate or polystyrene, that provide a reduced maintenance and extends the life of the tool. The low density of the PMMA material gives light weight to the tool assembly in comparison with metallic materials.

General characteristics of the upper mould:

- Made of PMMA.
- General measurements 300 x 120 x 43,6 R [mm].
- Stages on the flanges for mould assembly.
- Holes location on flanges and ends of the mould for mechanical closure.
- Longitudinal channels in the body for cooling system.

On the following figure 4.6 is detailed the design of the upper mould.

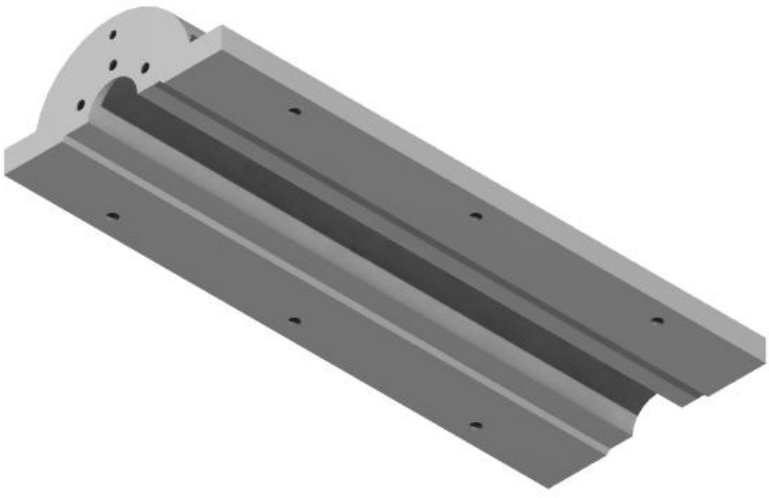

Figure 4.6: Upper mould CAD model.

See attached drawing in appendix C for detailed measurements and the calculation of the PMMA tool in appendix B.

4.3.2 Lower mould

The lower and upper moulds have the task of shaping and surface finish to the outer side of the seat post. It assembles mechanically with the upper mould to form the body mould a The internal diameter formed by the assembly of both halves are 27,2mm., that will correspond to the external diameter of the future seat post.

General characteristics of the lower mould:

- Made of PMMA.
- Measurements 300 x 120 x 43,6 R [mm].
- Stages on the flanges for mould assembly.
- Holes location on flanges and ends of the mould for mechanical closure.
- Longitudinal channels in the body for cooling system.
- Longitudinal accommodations for sealing gaskets.

On the following figure 4.7 is detailed the design of the lower mould.

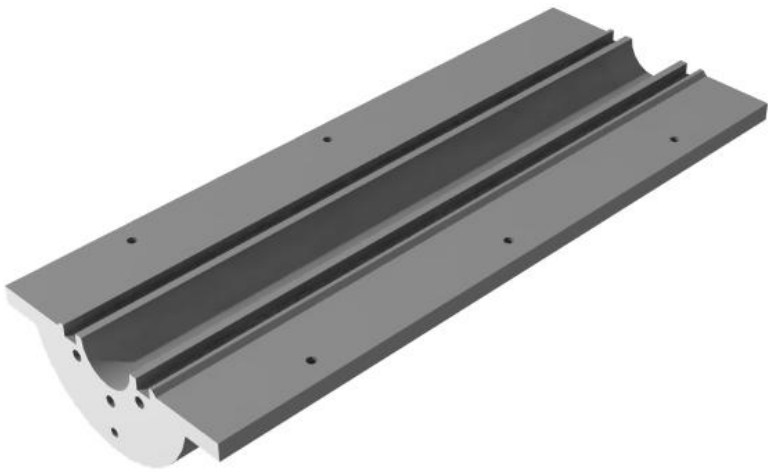

Figure 4.7: Lower mould CAD model.

See attached drawing in appendix C for detailed measurements and the calculation of the PMMA tool in appendix B.

4.3.3 Front cover

The front cover has a central hole to accommodate the connection for vacuum the application. One side of the cover contains grooves that connect the cooling channels of the upper and lower mould and create the cooling system. To prevent the leakage of the refrigeration liquid (water) and avoid the mixture of resin and water during the seat post manufacturing process, there are two accommodations for sealing gaskets.

General characteristics of the front cover:

- Made of PMMA.
- Measurements 30 x 87,2 ϕ [mm].
- Central hole for vacuum connection (air extraction).
- Holes located close to the contour for mechanical closure.
- Circular grooves for cooling system.
- Circular accommodations for sealing gaskets.

On the following figure 4.8 is detailed the design of the front cover.

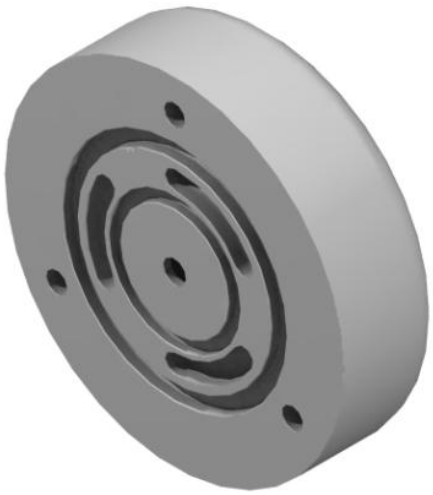

Figure 4.8: Front cover CAD model.

See attached drawing in appendix C for detailed measurements and the calculation of the PMMA tool in appendix B.

4.3.4 Rear cover

Three different connections located on the rear cover confer to that module a relevant importance. The rear cover accommodate the resin injection port that its located at the height of the fiber reinforcement. This resin intake is in a 30º plane from the cross section which facilitates the resin distribution during the seat post manufacturing process. There is a circular groove concentrically placed to the fiber reinforcement to help the initial distribution of the resin. The bladder channels are connected during the injection process with this groove.

The rear cover also contains grooves that connect the cooling channels of the upper and lower mould, and together with the front cover close the cooling system circuit. Two holes correspond to the inlet-exhaust for the refrigeration liquid in the cooling system and the hole in the center accommodate the nozzle of the inflatable bladder for pressure application.

General characteristics of the rear cover:

- Made of PMMA.
- Measurements 30 x 87,2 ϕ [mm].
- Central hole for inflatable bladder nozzle.
- Hole for resin injection.
- Circular groove for resin distribution.
- Holes located close to the contour for mechanical closure.
- Circular grooves for cooling system.
- Holes for refrigeration liquid re-circulation (inlet-exhaust).
- Circular accommodations for sealing gaskets.

On the following figure 4.9 is detailed the design of the rear cover.

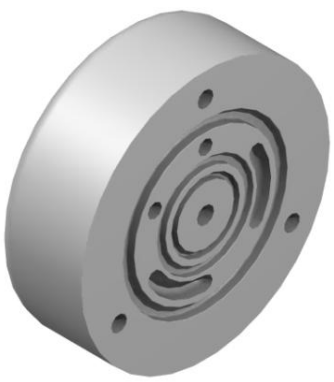

Figure 4.9: Rear cover CAD model.

See attached drawing in appendix C for detailed measurements and the calculation of the PMMA tool in appendix B.

4.3.5 Inflatable bladder

The inflatable bladder has the tasks of shaping the inner side of the seat post and serve as a distribution media during the resin injection process. The bladder design developed accommodates 4 channels for the CNT-resin distribution. The bladder supports the internal pressure applied to compact the fiber reinforcement.

The material selected for the manufacturing is Polyurethane because of his elastic deformation allow the pressure inflates the bladder and compact the composite during the seat post manufacturing process. The stiffness of the Polyurethane allow to place the fiber reinforcement on the bladder without pressure inside.

General characteristics of the inflatable bladder:

- Made of Polyurethane.
- General measurements 297 x 19 ϕ [mm].
- Bladder thickness 1,5 [mm].
- Nozzle at the end for pressure connection (Radius 3mm.).
- 4 longitudinal channels in the body for resin distribution.
- Channels radius: 3 [mm].

On the following figure 4.10 is detailed the design of the inflatable bladder.

Figure 4.10. Inflatable bladder CAD model.

See attached drawing in appendix C for detailed measurements and the calculation of the Inflatable bladder in appendix A.

4.3.6 Longitudinal sealing gasket

The longitudinal gaskets have the task to seal the mould between the upper and lower halves in the assembly and avoid resin leakage during the manufacturing process. It permits the application of high pressure inside for material compaction and air extraction.

The material selected for the manufacturing is Silicone because of his sealing properties and flexible deformation.

General characteristics of the longitudinal sealing gasket:

- Made of Silicone.
- Measurements 300 x 7 x 5 [mm].
- Rectangular and constant cross section.
- Quantity: 2 units.

On the following figure 4.11 is detailed the design of the longitudinal sealing gasket.

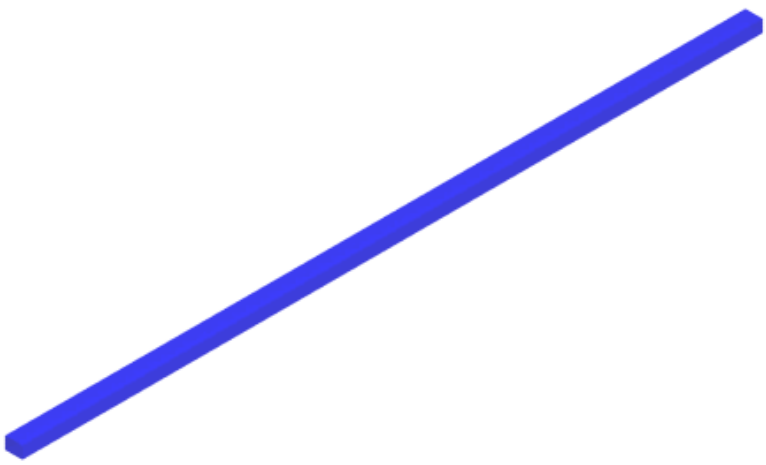

Figure 4.11: Longitudinal sealing gasket CAD model.

See attached drawing in appendix C for detailed measurements.

4.3.7 Circular sealing gasket

The circular gaskets have the task to seal the mould between the covers and the housing in the assembly. Its prevent resin and refrigeration liquid leakage, and avoid the mixture of resin and water during the seat post manufacturing process. These gaskets permit the application of high pressure inside for material compaction and air extraction.

The material selected for the manufacturing is Silicone because of his sealing properties and flexible deformation.

General characteristics of the circular sealing gasket:

- Made of Silicone.
- Circular shape and constant cross section.
- Quantity: 4 units (2 inner & 2 outer gaskets).
- Measurements outer gaskets: 14 $\phi_{in.}$ x 16,9 ϕ_{out} [mm], height 2,2 [mm].
- Measurements inner gaskets: 25 $\phi_{in.}$ x 28,8 ϕ_{out} [mm], height 2,95 [mm].

On the following figure 4.12 is detailed the design of the circular sealing gasket.

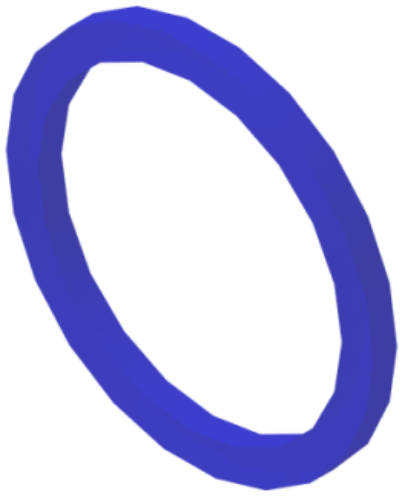

Figure 4.12: Circular sealing gasket CAD model.

See attached drawing in appendix C for detailed measurements.

4.3.8 Screw

The screw have the task to fix the parts of the tool during the assembly and support the pressure inside.

The material selected for the manufacturing is Stainless steel because of his mechanical and non-degradation properties.

General characteristics of the circular screws:

- Made of Stainless steel.
- Measurements 4,25 ϕ x 25 [mm].
- Standards parts: DIN 912 ALLEN HEAD SCREW.
- Quantity: 12 units.

On the following figure 4.13 is detailed the design of the screw.

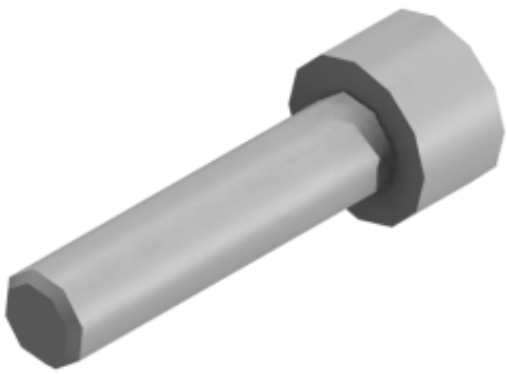

Figure 4.13: Screw CAD model.

See attached drawing in appendix C for detailed measurements.

4.3.9 Assembly

Once all the components have been designed, it can be proceed the combination of all components or assembly process. The tool is mainly composed of 4 parts. The assembly of 2 of them (upper & lower mould) forms the body of the tool with cylindrical shape. The assembly of the covers (front & rears) to the body close the tool resulting a close volume for the seat post manufacturing. The main task of the tool is to provide a sealed chamber for the process. On the covers are located the connections for the air-pressure inlet, vacuum exhaust and resin injection. Together with the tool, the inflatable bladder allows the manufacturing of complex hollow parts using high viscosity resin. On the table 4.6 is sequentially presented the assembly process.

Step 1: Mould gaskets assembly.	Step 2: Body assembly.
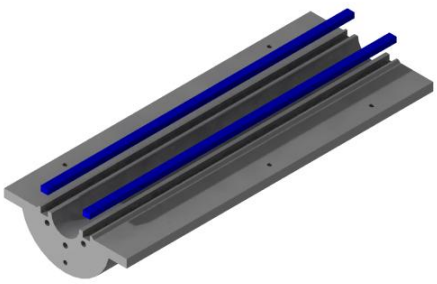	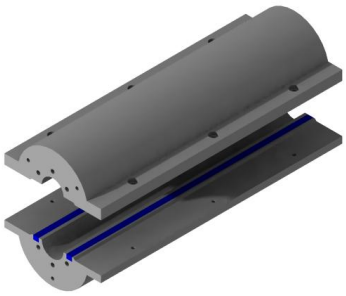
Step 3: Cover gaskets assembly.	Step 4: Bladder installation.
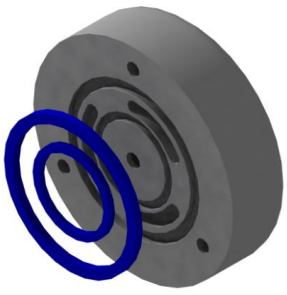	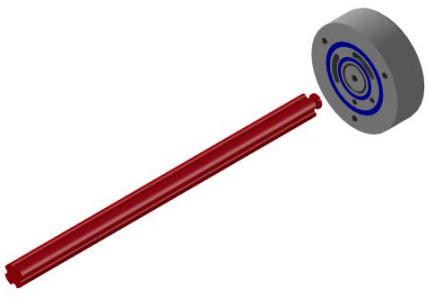
Step 5: Front cover & body assembly.	Step 6: Mould closing.
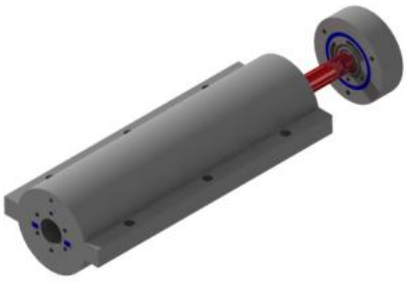	

Table 4.6: Assembly process.

On the following figures (figure 4.14 & 4.15), its presented the final assembly tool:

Figure 4.14: Tool assembly front isometric view (front).

Figure 4.15: Tool assembly rear isometric view (rear).

The real assembly tool is presented on the figure 4.16, where it can be observed the transparency of the PMMA material for the resin impregnation follow up.

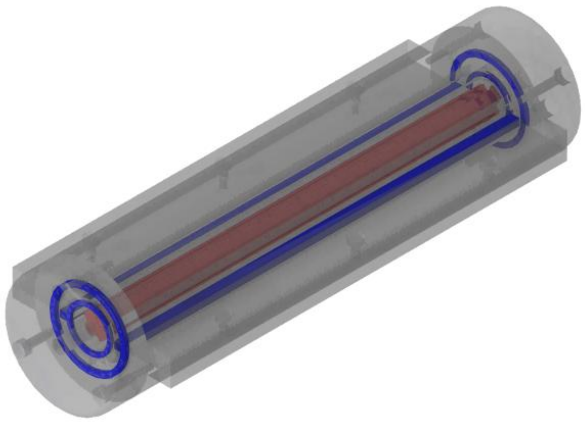

Figure 4.16: PMMA tool assembly rear isometric view.

4.4 Inflatable bladder development process

On this section, it's explained the impregnation process of glass fiber using resin charged with carbon nanotubes. The figure 4.17, shows the impregnation process flow chart as introduction.

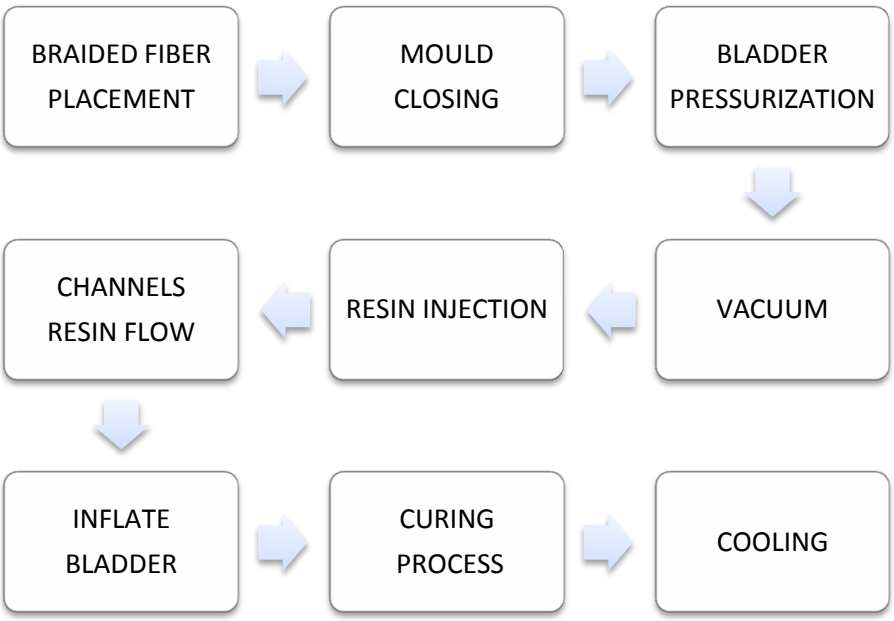

Figure 4.17. Impregnation process flow chart.

The fiber is placed around the inflatable bladder following the seat post configuration (figure 4.18). On this project, it's selected a continuous braided fiber glass. This type of reinforcement provide hollow parts without any seams or discontinuities and improves the performance of the laminate. It also facilitates the lay-up process as the bladder is simply inserted inside a tubular pre-form instead of having to wrap it.

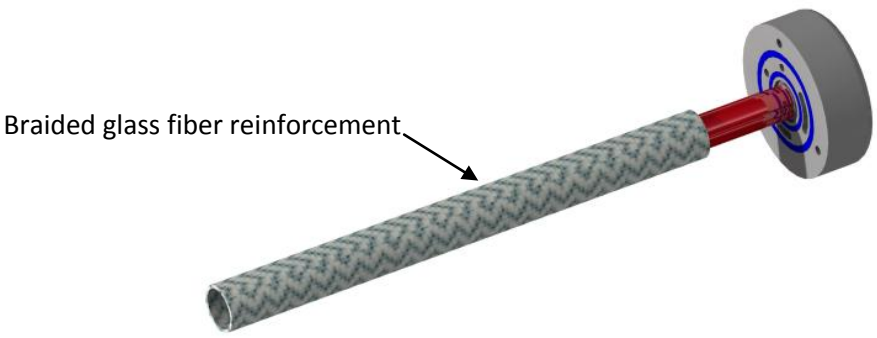

Figure 4.18: Braided fiber glass placement.

With the reinforcement located on the bladder, the RTM tool is mechanically closed and all the connections plugged in (vacuum, air pressure, resin injection and cooling system).

Now the bladder is pressurized to compact the fiber reinforcement against the external body mould. The channels of the bladder are designed to support this first stage of pressure applied (figure 4.19).

Prior to the resin injection, it is applied vacuum pressure into the mould, which combined with the injection pressure will permit the resin flow. Once started the resin injection, the longitudinal channels on the bladder will be quickly filled by the CNT-resin as they have been designed to keep their shape with pressure (first stage) and vacuum, and therefore to operate as a resin distribution media. When the CNT-resin reach the end of the channels, then the pressure inside the bladder is increased. This high pressure inflates the bladder and collapse distribution channels forcing the resin to flow through the laminate thickness. This impregnation process homogenized the CNT's distribution throughout the part and avoid the filter effect characteristic on the standard RTM processes. This concept is the most important contribution done on this project to the bladder assisted RTM technique.

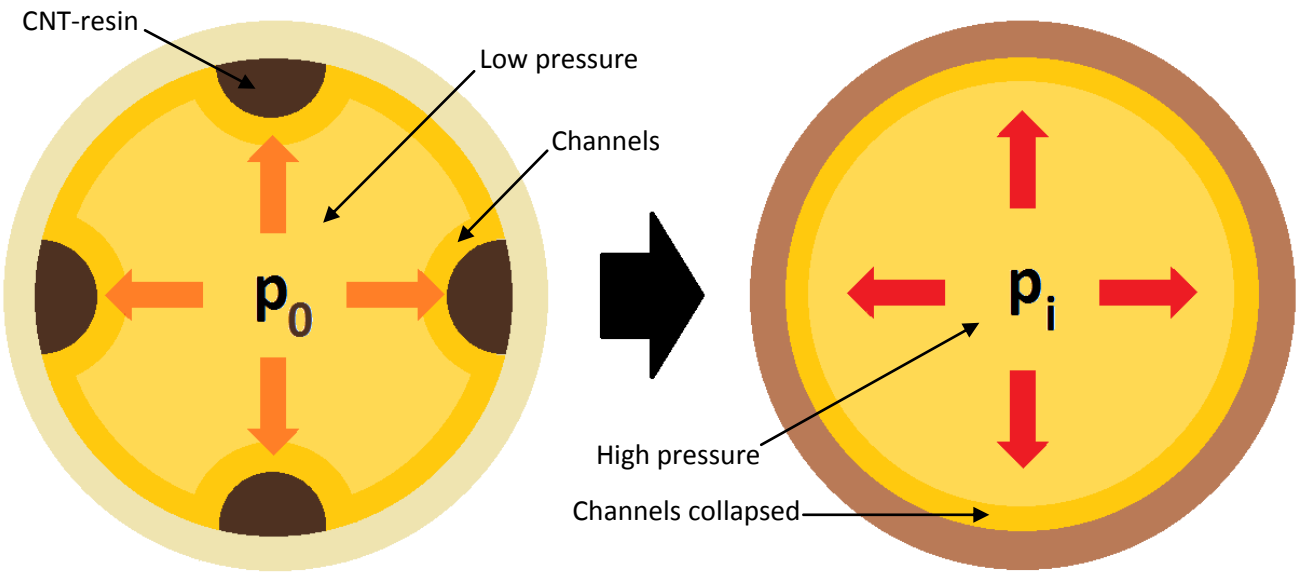

Figure 4.19. Inflatable bladder assisted impregnation process.

When the CNT-resin has fully impregnated the fiber reinforcement and cured, the mold is cooled maintaining bladder pressure in order to consolidate the final seat post dimensions.

4.5 Tool manufacturing

A RTM-prototype for impregnation tests was manufactured on the IVW by Alex Mann during the development of this project and the material selected for this prototype was also PMMA (see figure 4.20). The bladder assisted RTM-tool developed on this project was not manufactured until the prototype performance validation.

Figure 4.20: RTM-Prototype.

On this project the most innovative module designed is the inflatable bladder which create the hollow shape of the seat post and facilitate the laminate impregnation with resin charged CNTs.

As a starting point for the inflatable bladder manufacturing, the blabber configuration selected has a circular section without external channels to make a first and simple approach to the bladder manufacturing complexity (figures 4.21 & 4.22).

Figure 4.21: Circular section bladder CAD model.

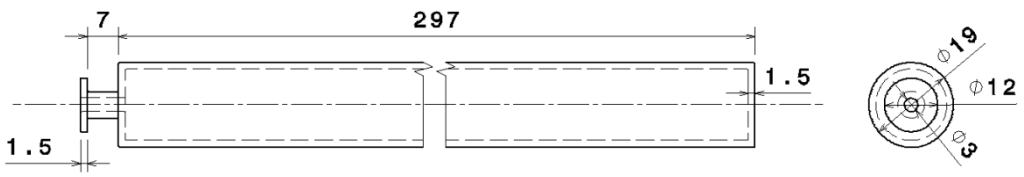

Figure 4.22: Bladder dimensions.

Before manufacture a specific tool to manufacture the real scale bladder, several tests have been done using material existing on the IVW facilities. These tests have been performed to develop a real scale tool and also to select the bladder material. The test procedure consists on dipping a round rod stainless steel in a Teflon cavity filled with different solutions. The tool used had reduced dimensions in order to optimize costs (figure 4.23 & 4.24).

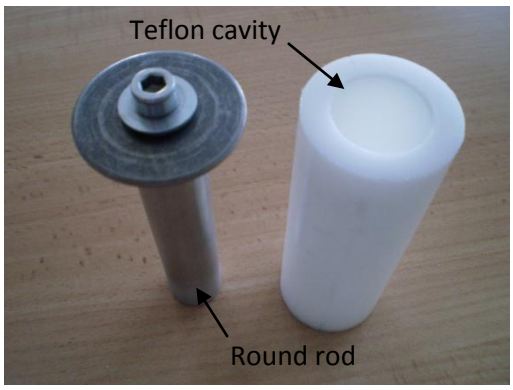

Figure 4.23: Tools for dipping tests.

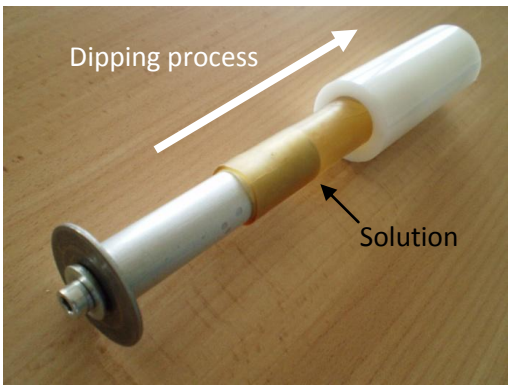

Figure 4.24: Dipping tests.

Following table 4.7 brings a summary of the tests performed for the bladder material selection:

Test	Material reference	Result
1	ELASTOSIL® RT 607 Wacker (Silicone rubber)	
2	Airtech (Elastomeric rubber)	
3	Biresin® U1404 SIKA (Polyurethane)	

Table 4.7: Bladder material selection tests.

4.6 Final discussions

The bladders were made with approximately one millimeter-thickness, to make sure that they would be resistant enough to be de-moulded from this experimental tool. Two of the scale bladders manufactured were broken during the de-moulding process, showing low elastic properties. The material selected was the Biresin® U1404 because of his elastic properties compared with the other materials available. This Biresin® U1404 material is two component polyurethane (PUR) system, that is insensitive to moisture, very soft, high elongation at break, good tensile strength and elasticity, and has very low shrinkage. These properties makes the material adequate for the manufacture of elastic, flexible mouldings and components like inflatable bladders.

Once the bladder material is selected and the dipping process has been tested, it proceeds to the real scale bladder manufacture. For the manufacturing of the bladder, a specific tool has been designed and constructed using the excess material from the PMMA prototype (figure 4.20). This tool consist in a two halves mould with two cavities, one for the bladder mandrel manufacturing and the other for the bladder dipping mandrel in the polyurethane solution selected that will provide the final inflatable bladder (figure 4.25 & 4.26).

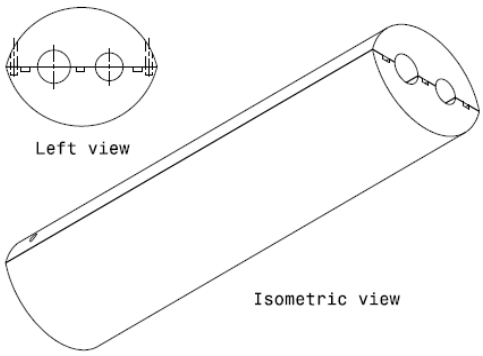

Figure 4.25: Mould design for the bladder manufacturing.

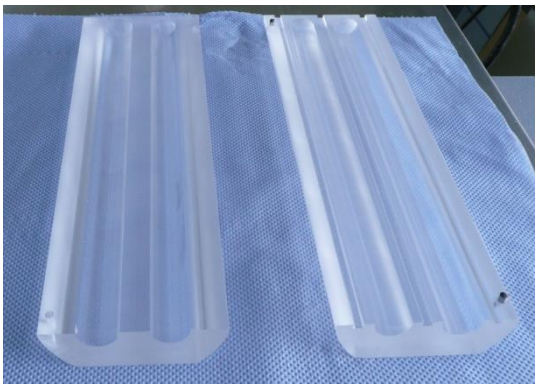

Figure 4.26: Mould for the bladder manufacturing.

A water soluble fugitive core material called Aquacore^{TM} (by AeroConsultants) was used for the bladder mandrel manufacturing. A stainless steel screw was inserted at the end of the mandrel to create the bladder nozzle. The cavity of the tool with diameter 16 mm was used for the mandrel manufacturing. The figures 4.27 & 4.28 show the result of the mandrels manufactured.

Figure 4.27. Bladder mandrel.

Figure 4.28: Bladder mandrel.

Once selected the bladder material and successfully manufactured the mandrel should follow the bladder dipping mandrel process in the polyurethane solution employing the second cavity of the tool to obtain the final inflatable bladder. Due the conclusion of the internship at IVW, this process step was not carried being object of future works on the *CarboRoad* project frame.

5 Conclusions and outlook

A Resin Transfer Moulding tool to manufacture seat posts with prolonged fatigue life has been designed in this project. The challenge on this development is homogeneously distribute the CNTs in the reinforcement textile, as the CNTs are filtered when conventional infusion processes are used.

An innovative injection molding process to prevents filtering has been developed, which consists of a resin distribution media formed by collapsible flow channels located on the external surface of the inflatable bladder. These channels create a preference lane for the resin flow along the laminate without resistance before increase the pressure inside the bladder that collapse the channels forcing the resin to flow through the laminate thickness. The technique developed in this project reduces the filtering of CNTs during the injection process and allows the use of higher viscosity resins in the multiscale composite manufacturing. Avoiding the filtering also will increase the content of CNT in the resin (>1 wt%) and therefore the mechanical properties. Because of the process is based on pre-dispersion of CNTs in a epoxy matrix prior to impregnation of fiber reinforcements is a scalable technique for mass production.

Once the bladder assisted-RTM tool were developed, bladder dipping mandrel test to select the material were performed using a water soluble material that permits to retire the mandrel after the bladder dipping and curing process without any bladder damage taking to account the reduced nozzle dimensions. The material selected for the inflatable bladder was a polyurethane formulation due their good elastic properties in comparison with the other materials tested on the IVW facilities. The tests performed at the workshop to develop the bladder manufacturing process gave to the project practical knowledge which resulted in a tool designed and constructed to get a simple inflatable bladder.

The experimental work of this project finished with a real size bladder dipping mandrel manufactured in the specific tool constructed. Due the lack of time and the conclusion of the internship during which this project was done, the inflatable bladder was not manufactured. The work done in the present project had its continuity and at the finalization of the CarboRoad project a collapsible channels bladder were manufactured (figure 5.1), result of the work begun here.

Figure 5.1: CarboRoad bladder (by IVW).

No additional information has been found about the success of the bladder assisted-RTM tool developed but future works must be focused on the tool set-up process, after its construction. All the RTM process parameters are very important to be controlled and adjusted because strongly influence the fiber impregnation and they can decrease the behavior of the innovative bladder developed on this project. For example, temperature and pressure injection of the resin could improve the CNTs distribution, also the moment of pressure application inside the bladder.

Experimental investigation viscosity in relation to CNTs content must be performed during this tool set-up to check if it's possible to distribute contents of CNTs >1% wt., using this inflatable bladder process concept. An important contribution to the multiscale composites manufacturing could be done if this bladder assisted-RTM tool concept is transformed and implemented to another architecture fibers and shapes. It could open the door for a multiscale composites mass production in multiple applications (transport, sport gear, energy, etc).

6 References

[1] Thostenson EST, Li WZ, Wang DZ, Ren ZF, Chou TW. *Carbon nanotube/carbon fiber hybrid multiscale composites*. J. Appl. Phys 2002;91(9):6034–7.

[2] Bekyarova E, Thostenson ET, Yu A, Kim H, Gao J, Tang J, et al. *Multiscale carbon nanotube-carbon fiber reinforcement for advanced epoxy composite*s. Langmuir 2007;23:3970–4.

[3] Sven Pegel, Petra Potschke, Gudrun Petzold , Ingo Alig , Sergej M. Dudkin b, Dirk Lellinger. *Dispersion, agglomeration, and network formation of multiwalled carbon nanotubes in polycarbonate melts*. Polymer 49 (2008) 974 - 984.

[4] Iwahori Y, Ishiwata S, Sumizawa T, Ishikawa T. Mechanical properties improvements in two-phase and three-phase composites using carbon nanofiber dispersed resin. Compos Part A 2005;36:1430–9.

[5] Liao YH, Liang Z, Park YB, Wang B, Zhang C. Fabrication and characterization of carbon nanotube/glass fiber-reinforced multiscale composites. In: 47th AIAA/ ASME/ASCE/AHS/ASC Structures, Structural Dynamics, and Materials Conference, Newport, RI, 2006.

[6] Zhou Y, Pervin F, Lewis L, Jeelani S. Fabrication and characterization of carbon/epoxy composites mixed with multi-walled carbon nanotubes. Mater Sci Eng A 2007;452–453:657–64.

[7] Puglia D, Valentini L, Kenny JM. Analysis of the cure reaction of carbon nanotubes/epoxy resin composites through thermal analysis and Raman spectroscopy. J Appl Polym Sci 2003;88:452–8.

[8] Kim B, Lee J, Yu I. Electrical properties of single-wall carbon nanotube and epoxy composites. J Appl Phys 2003;94(10):6724–8.

[9] Liao YH, Marietta-Tondin O, Liang Z, Zhang C, Wang B. Investigation of the dispersion process of SWNTs/SC-15 epoxy resin nanocomposites. Mater Sci Eng A 2004;385:175–81.

[10] Gojny FH, Wichmann MHC, Köpke U, Fiedler B, Schulte K. Carbon nanotubereinforced epoxy-composites: enhanced stiffness and fracture toughness at low nanotube content. Compos Sci Technol 2004;64:2363–71.

[11] Thostenson ET, Chou TW. Processing-structure-multi-functional property relationship in carbon nanotube/epoxy composites. Carbon 2006;44:3022–9.

[12] Gojny FH, Wichmann MHG, Fiedler B, Bauhofer W, Schulte K. Influence of nano-modification on the mechanical and electrical properties of conventional fibre-reinforced composites. Compos Part A 2005;36:1525–35.

[13] Gojny FH, Wichmann MHG, Fiedler B, Schulte K. *Influence of different carbon nanotubes on the mechanical properties of epoxy matrix composites – a comparative study*. Compos Sci Technol 2005;65(15–16):2300–13.

[14] Gojny FH, Wichmann MHG, Fiedler B, Kinloch I, Bauhofer W, Windle AH. Evaluation and identification of electrical and thermal conduction mechanisms in carbon nanotube/epoxy composites. Polymer 2006;47:2036–45.

[15] Wichmann MHG, Sumfleth J, Gojny FH, Quaresimin M, Fiedler B, Schulte K. Glass-fibre-reinforced composites with enhanced mechanical and electrical properties – benefits and limitations of a nanoparticle modified matrix. Eng Fract Mech 2006;73:2346–59.

[16] Thostenson ET, Chou TW. Carbon nanotube network: sensing of distributed strain and damage for life prediction and self healing. Adv Mater 2006;18:2837–41.

[17] Myungsoo Kim, Young-Bin Park *, Okenwa I. Okoli, Chuck Zhang. *Processing, characterization, and modeling of carbon nanotube-reinforced multiscale composites*, Composites Science and Technology 69 (2009) 335–342.

[18] Fan, Z. and Advani, S. G. (2005). Characterization of orientation state of carbon nanotubes in shear flow. Polymer, 46, 5232-5240.

[19] Green, K. J., Dean, D. R., Vaidya, U. K., and Nyairo, E. (2009). Multiscale fiber reinforced composites based on a carbon nanofiber/epoxy nanophased polymer matrix: Synthesis, mechanical, and thermomechanical behavior. Composites Part A: Applied Science and Manufacturing, 40, 1470-1475.

[20] Qiu, J., Zhang, C., Wang, B., and Liang, R. (2007). Carbon nanotube integrated multifunctional multiscale composites. Nanotechnology, 18, 275708.

[21] Sadeghian, R., Gangireddy, S., Minaie, B., and Hsiao, K. T. (2006). Manufacturing carbon nanofibers toughened polyester/glass fiber composites using vacuum assisted resin transfer molding for enhancing the mode-I delamination resistance. Composites Part A: Applied Science and Manufacturing, 37, 1787-1795.

[22] Shafi Ullah KHAN, Jang-Kyo Kim. *Impact and Delamination Failure of Multiscale Carbon Nanotube-Fiber Reinforced Polymer Composites: A Review.* Int'l J. of Aeronautical & Space Sci. 12(2), 115–133 (2011).

[23] *Composites*, ASM Handbook - Volume 21, (2001).

[24] Derrick Dean a,*, Apollo M. Obore b, Sylvester Richmond b, Elijah Nyairo. *Multiscale fiber reinforced composites based on a carbon nanofiber/epoxy nanophased polymer matrix: Synthesis, mechanical, and thermomechanical behavior.* Composites: Part A 40 (2009): 1470–1475.

[25] Farzana Hussain, Mehdi Hojjati, Masami Okamoto and Russell E. Gorga. *Review article: Polymer-matrix Nanocomposites, Processing, Manufacturing, and Application: An Overview*. Journal of Composite Materials (2006); 40 : 1511.

[26] Dr. Klaus Edelmann, Bernd Räckers, Dr. Benjamin L. Farmer. *Airbus Nanocomposites for Future*. Airbus Airframes Wissenschaftstag.

[27] Derrick Dean, Apollo M. Obore, Sylvester Richmond, Elijah Nyairo. M*ultiscale fiber-reinforced nanocomposites: Synthesis, processing and properties.* Composites Science and Technology 66 (2006): 2135–2142.

[28] http://www.composites.northwestern.edu/research/nanomulticomp/

[29] He X, Zhang F, Wang R, Liu W. *Preparation of a carbon nanotube/carbon fiber multi-scale reinforcement by grafting multi-walled carbon nanotubes onto the fibers*. Carbon 2007; 45 (13): 2559–63.

[30] Bekyarova E, Thostenson ET, Yu A, Kim H, Gao J, Tang J, et al. *Multiscale carbon nanotube-carbon fiber reinforcement for advanced epoxy composites*. Langmuir 2007; 23 (7): 3970–4.

[31] Mathur RB, Chatterjee S, Singh BP. *Growth of carbon nanotubes on carbon fibre substrates to produce hybrid/phenolic composites with improved mechanical properties*. Compos Sci Technol 2008; 68 (7–8): 1608–15.

[32] Park JK, Do I-H, Askeland P, Drzal LT. *Electrodeposition of exfoliated graphite nanoplatelets onto carbon fibers and properties of their epoxy composites*. Compos Sci Technol 2008; 68 (7–8): 1734–41.

[33] Boccaccini AR, Cho J, Roether JA, Thomas BJC, Jane Minay E, Shaffer MSP. *Electrophoretic deposition of carbon nanotubes*. Carbon 2006; 44 (15): 3149–60.

[34] InChem Corporation.

[35] K.L. Loewenstein, *The Manufacturing Technology of Continuous Glass Fibers*, 3rd revised ed., Elsevier, 1993

[36] F.T. Wallenberger, Structural Silicate and Silica Glass Fibers, in *Advanced Inorganic Fibers Processes, Structures, Properties, Applications,* F.T. Wallenberger, Ed., Kluwer Academic Publishers, 1999, p 129–168

[37] F.T. Wallenberger, Melt Viscosity and Modulus of Bulk Glasses and Fibers: Challenges for the Next Decade, in *Present State and Future Prospects of Glass Science and Technology*, Proc. of the Norbert Kreidl Symposium (Triesenberg, Liechtenstein), 1994, p 63–78

[38] D.M. Miller, Glass Fibers, *Composites*, Vol 1, *Engineered Materials Handbook*, ASM International, 1987, p 45–48

[39] "Standard Specification for Glass Fiber Strands", D 578-98, Annual Book of ASTM Standards, ASTM.

[40] Ahir, S.V.; Terentjev, E.M.: Polymers containing carbon nanotubes: active composite materials In Nalwa H.S.: Polymeric Nanostructures and Their Applications. Vol 1, American Scientific Publishers, (2006), p. 1-48.

[41] Ajayan, P.M.; Zhou, O.Z.: Applications of Carbon Nanotubes. Topics Appl. Phys. 80, (2001), p. 391-425.

[42] Wichmann, M.H. G.; Sumfleth, J.; Fiedler, B.; F. Gojny, H.; Schulte, K.: Multiwall carbon nanotube/epoxy composites produced by a masterbach process. Mechanics of Composite Materials, Vol. 42, No. 5, (2006) p. 395-406.

[43] Maciej, O.: Carbon Nanotube Composites - Mechanical, Electrical and Optical properties. Dissertation zur Erlandung des Doktorgrades (Dr. rer. Nat.) der Mathematisch-Naturwissenschaftlichen Fakultät der Rheinischem Friedrich-Wilhelms-Universitäat Bonn. Bonn (2006).

[44] Coleman, J.N.; Khan, U.; Blau, W. J.; Gun´ko, Y. K.: Small but strong: A review of the mechanical properties of carbon nanotube-polymer composites. Carbon 44. Elsevier Ltd., (2006), p. 1624-1652.

[45] Du, J.H.; Bai, J.; Cheng, H-M.: The present status and key problems of carbon nanotube based polymer composites. eXPRESS Polymer letters Vol.1, No.5, (2007), p. 253-273.

[46] http://boomeria.org/chemlectures/organic/organic2.html

[47] http://www.allposters.co.jp/-sp/Two-Fullerene-Structures-an-Elongated-Carbon-Nanotube-and-Spherical-Buckminsterfulleren-Posters_i13056690_.htm

[48] Thostenson, E. T.; Li, C.; Chou, T.-W.: Nanocomposites in context. Composites Science and Technology 65. Elsevier Ltd, (2004), p. 491-516.

[49] http://itech.dickinson.edu/chemistry/wp-content/uploads/2008/04/swnt_mwnt.jpg

[50] Flahaut, E.; Bacsa, R.; Peigney, A.; Laurent, C.: Gram-scale CCVD synthesis of double-walled carbon nanotubes. Chem. Commun., (2003), p. 1442–1443.

[51] http://nanotechweb.org/cws/article/lab/60669

[52] Alcca Quispe, F.: Estructura y Síntesis de Nanotubos de Carbono. (2005) http://sisbib.unmsm.edu.pe/bibvirtualdata/tesis/Basic/alcca_qf/alcca_qf.pdf(14.09.2008)

[53] https://sites.google.com/site/cntcomposites/structure-of-cnts

[54] http://faculty.ycp.edu/~jforesma/swcnts.html

[55] Antonucci, V.; Hsiao, K.-T.; Advani, S. G.: Review of Polymer Composites with Carbon Nanotubes. Advanced Polymeric Materials. Structure Property Relationships.CRC Press LLC (2003).

[56] Rupesh, K.; Suryasarathi, B.: Carbon Nanotube Based Composites. Journal of Miderals & Materials Characterization & Engineering, Vol. 4, No1, (2005), p. 31-46.

[57] Bernholc, J.; Brenner, D.; Buongiorno Nardelli, M.; Meunier, V.; Roland, C.: Mechanical and Electrical Properties of Nanotubes. Annu. Rev. Mater. Res. Vol. 32, (2002), p. 347–75.

[58] Lee, Y.-S.; Buongiorno Nardelli, M.; Marzari, N.: Ballistic Transport in Carbon Nanotubes from First-Principles Molecular Dynamics Simulations (2004).

[59] Kaneto, K.; Tsuruta, M.; Sakai, G.; Cho, W. Y.; Ando, Y.: Electrical conductivities of multi-wall carbon nano tubes. Elsevier Science. Vol. 103, No 1-3, (1999), p. 2543-2546.

[60] Daenen, M.; Fouw, R.D.; Hamers, B.; Hamers, B.; Schouteden, K.; M.A.J. Veld: The Wondrous World of Carbon Nanotubes. Eindhoven University of technology, (2003).

[61] Begtrup, G. E.; Ray, K. G.; Kessler, B. M.; Yuzvinsky, T. D.; Garcia, H.; Zettl A.: Extreme thermal stability of carbon nanotubes. Phys. Stat. Sol. (b) 244, No. 11, (2007), p.3960–3963.

[62] Iwahori Y, Ishiwata S, Sumizawa T, Ishikawa T. Mechanical properties improvements in two-phase and three-phase composites using carbon nanofiber dispersed resin. Composites Part A 2005;36(10):1430–9.

[63] Bekyarova E, Thostenson ET, Yu A, Kim H, Gao J, Tang J, et al. Multiscale carbon nanotube-carbon fiber reinforcement for advanced epoxy composites. Langmuir 2007;23. 3970-04.

[64] Daniel IM, Cho JM. Multiscale hybrid nano/microcomposites-processing, characterization, and analysis, chapter 12. In: Gilat R, Banks-Sills L, editors. Advances in Mathematical Modeling and Experimental Methods for Materials and Structures. Springer; 2010. p. 161–72.

[65] Inam F, Wong DY, Kuwata M, Peijs T. Multiscale hybrid micro–nanocomposites based on carbon nanotubes and carbon fibers. J Nanomater 2010;1(1).

[66] Rodriguez AJ, Guzman ME, Lim CS, Minaie B. Mechanical properties of carbon nanofiber/fiber-reinforced hierarchical polymer composites manufactured with multiscale-reinforcement fabrics. Carbon 011;49(3):937–48.

[67] Gojny FH, Wichman MHG, Fiedler B, Bauhofer W, Schulte K. Influence of nanomodification on the mechanical and electrical properties of conventional fibrereinforced composites. Composites Part A 2005;36(11):1525–35.

[68] Gojny FH, Wichmann MHG, Fiedler B, Schulte K. Influence of different carbon nanotubes on the mechanical properties of epoxy matrix composites – A comparative study. Compos Sci Technol 2005;65(15–16):2300–13.

[69] Sun L, Gibson RF, Gordaninejad F, Suhr J. Energy absorption capability of nanocomposites: a review. Compos Sci Technol 2009;69:2392–409.

[70] Davis DC, Whelan BD. An experimental study of interlaminar shear fracture toughness of a nanotube reinforced composite. Compos Part B-Eng 2011;42(1):105–16.

[71] Khan SU, Iqbal K, Munir A, Kim JK. Quasi-static and impact fracture behaviors of CFRPs with nanoclay-filled epoxy matrix. Composites Part A 2011;42(3):253–64.

[72] Zhang W, Picu RC, Koratkar N. Suppression of fatigue crack growth in carbon nanotube composites. Appl Phys Lett 2007;91(19).

[73] Grimmer CS, Dharan CKH. High-cycle fatigue of hybrid carbon nanotube/glass fiber/polymer composites. J Mater Sci 2008;43(13):4487–92.

[74] Boger L, Sumfleth J, Hedemann H, Schulte K. Improvement of fatigue life by incorporation of nanoparticles in glass fibre reinforced epoxy. Composites Part A 2010;41(10):1419–24.

[75] Manjunatha CM, Sprenger S, Taylor AC, Kinloch AJ. The tensile fatigue behavior of a glass-fiber reinforced plastic composite using a hybrid-toughened epoxy matrix. J Compos Mater 2010;44(17):2095–109.

[76] Manjunatha CM, Jagannathan N, Padmalatha K, Kinloch AJ, Taylor AC. Improved variable-amplitude fatigue behavior of a glass-fiber-reinforced hybrid-toughened epoxy composite. J Reinf Plast Comp 2011;30(21): 1783–93.

[77] Ma, P. C., Siddiqui, N. A., Marom, G., and Kim, J. K. (2010). Dispersion and functionalization of carbon nanotubes for polymer-based nanocomposites: a review. Composites Part A: Applied Science and Manufacturing, 41, 1345-1367.

[78] Ma, P. C., Wang, S. Q., Kim, J. K., and Tang, B. Z. (2009). In-situ amino functionalization of carbon nanotubes using ball milling. Journal of Nanoscience and Nanotechnology, 9, 749-753.

[79] Isayev, A. I., Kumar, R., and Lewis, T. M. (2009). Ultrasound assisted twin screw extrusion of polymer-nanocomposites containing carbon nanotubes. Polymer, 50, 250-260.

[80] Moniruzzaman, M., Du, F., Romero, N., and Winey, K. I. (2006). Increased flexural modulus and strength in SWNT/ epoxy composites by a new fabrication method. Polymer, 47, 293-298.

[81] Prof. Dr.-Ing. Arno Kwade. Partikeltechnik für Faserverbunde. Institut für Partikeltechnik TU Braunschweig

[82] Fan, Z. and Advani, S. G. (2005). Characterization of orientation state of carbon nanotubes in shear flow. Polymer, 46, 5232-5240.

[83] Green, K. J., Dean, D. R., Vaidya, U. K., and Nyairo, E. (2009). Multiscale fiber reinforced composites based on a carbon nanofiber/epoxy nanophased polymer matrix: Synthesis, mechanical, and thermomechanical behavior. Composites Part A: Applied Science and Manufacturing, 40, 1470-1475.

[84] Qiu, J., Zhang, C., Wang, B., and Liang, R. (2007). Carbon nanotube integrated multifunctional multiscale composites. Nanotechnology, 18, 275708.

[85] Sadeghian, R., Gangireddy, S., Minaie, B., and Hsiao, K. T. (2006). Manufacturing carbon nanofibers toughened polyester/glass fiber composites using vacuum assisted resin transfer molding

for enhancing the mode-I delamination resistance. Composites Part A: Applied Science and Manufacturing, 37, 1787-1795.

[86] Thostenson, E. T., Li, W. Z., Wang, D. Z., Ren, Z. F., and Chou, T. W. (2002). Carbon nanotube/carbon fiber hybrid multiscale composites. Journal of Applied Physics, 91, 6034-6037.

[87] Cesano, F., Bertarione, S., Scarano, D., and Zecchina, A. (2005). Connecting carbon fibers by means of catalytically grown nanofilaments: formation of carbon-carbon composites. Chemistry of Materials, 17, 5119-5123.

[88] Hung, K. H., Tzeng, S. S., Kuo, W. S., Wei, B., and Ko, T. H. (2008). Growth of carbon nanofibers on carbon fabric with Ni nanocatalyst prepared using pulse electrodeposition. Nanotechnology, 19, 295602.

[89] Yamamoto, N., John Hart, A., Garcia, E. J., Wicks, S. S., Duong, H. M., Slocum, A. H., and Wardle, B. L. (2009). High-yield growth and morphology control of aligned carbon nanotubes on ceramic fibers for multifunctional enhancement of structural composites. Carbon, 47, 551- 560.

[90] Zhu, S., Su, C. H., Lehoczky, S. L., Muntele, I., and Ila, D. (2003). Carbon nanotube growth on carbon fibers. Diamond and Related Materials, 12, 1825-1828.

[91] Veedu, V. P., Cao, A., Li, X., Ma, K., Soldano, C., Kar, S., Ajayan, P. M., and Ghasemi-Nejhad, M. N. (2006). Multifunctional composites using reinforced laminate with carbon-nanotube forests. Nature Materials, 5, 457-462.

[92] Downs, W. B. and Baker, R. T. K. (1995). Modification of the surface properties of carbon fibers via the catalytic growth of carbon nanofibers. Journal of Materials Research, 10, 625-633.

[93] Donnet, J. B., Wang, T. K., Peng, J. C. M., and Rebouillat, S. (1998). Carbon Fibers. 3rd ed. New York: Marcel Dekker.

[94] Garcia, E. J., Wardle, B. L., and John Hart, A. (2008a). Joining prepreg composite interfaces with aligned carbon nanotubes. Composites Part A: Applied Science and Manufacturing, 39, 1065-1070.

[95] Bekyarova, E., Thostenson, E. T., Yu, A., Kim, H., Gao, J., Tang, J., Hahn, H. T., Chou, T. W., Itkis, M. E., and Haddon, R. C. (2007). Multiscale carbon nanotube-carbon fiber reinforcement for advanced epoxy composites. Langmuir, 23, 3970-3974.

[96] Li, Y., Hori, N., Arai, M., Hu, N., Liu, Y., and Fukunaga, H. (2009). Improvement of interlaminar mechanical properties of CFRP laminates using VGCF. Composites Part A: Applied Science and Manufacturing, 40, 2004-2012.

[97] Arai, M., Noro, Y., Sugimoto, K. i., and Endo, M. (2008). Mode I and mode II interlaminar fracture toughness of CFRP laminates toughened by carbon nanofiber interlayer. Composites Science and Technology, 68, 516-525.

[98] Zhu, J., Imam, A., Crane, R., Lozano, K., Khabashesku, V. N., and Barrera, E. V. (2007). Processing a glass fiber reinforced vinyl ester composite with nanotube enhancement of interlaminar shear strength. Composites Science and Technology, 67, 1509-1517.

[99] Warrier, A., Godara, A., Rochez, O., Mezzo, L., Luizi, F., Gorbatikh, L., Lomov, S. V., VanVuure, A. W., and Verpoest, I. (2010). The effect of adding carbon nanotubes to glass/epoxy composites in the fibre sizing and/or the matrix. Composites Part A: Applied Science and Manufacturing, 41, 532-538.

[100] Sun, L., Warren, G. L., and Sue, H. J. (2010). Partially cured epoxy/SWCNT thin films for the reinforcement of vacuum assisted resin-transfer-molded composites. Carbon, 48, 2364-2367.

[101] Khan, S. U. and Kim, J. K. (2011). Interlaminar shear properties of CFRP composites with CNF-bucky paper interleaves. The 18th International Conference on Composite Materials, Jeju, Korea.

[102] R. Gauvin and M. Chibani, The Modelling of Mold Filling in Resin Transfer Molding, Int. Poly. Process., Vol 1 (No. 1), 1986, p 42–46

[103] G. Rieber. The 2D-COMP - A high level permeability measurement technique. IVW-Alumnitreffen, Kaiserslautern den 5. Oktober 2007

[104] F. Trochu, R. Gauvin, and D.M. Gao, Numerical Analysis of the Resin Transfer Molding Process by the Finite Element Method, Adv. in Polym. Technol., Vol 12 (No. 4), 1993, p 329–342

[105] Cynthia Cole. *Guide for Low Cost Design and Manufacturing of Composite General Aviation Aircraft*. AGATE-WP3.1-031200-130-Design Guideline. National Institute for Aviation Research Wichita State University (2001) 30-31.

[106] U. Lehmann and W. Michaeli, Automated Production of Hollow Composite Parts with Complex Geometry in RTM, Proc. Int. Conf. Automated Composites (ICAC 97) (Glasgow, U.K.), 4–5 Sept 1997, Institute of Materials, London, U.K., p 43–58.

[107] VDI Society for product Development, Design and Marketing published Guideline. *Verein Deutscher Ingenieure* (VDI 2221) 1987.

[108] Alexander Mann. *Konstruktion eines transparenten Werkzeuges*. University of Kaiserslautern (2009).

[109] Pierre Celle, Sylvain Drapier, Jean-Michel Bergheau. Numerical Model for Fluid Infusion during Infusion-Based Processes. FPCM9 July 2008, Poly Montreal (Canada).

Appendix A. Calculation of the Inflatable bladder

On this appendix are detailed the calculation performed for the bladder design:

1. Resin quantity

First of all, it's necessary to calculate the quantity of resin required to impregnate the glass fiber reinforcement and then use this value for sizing the resin distribution channels.

Calculation of the seat-post volume:

$$V = A \cdot L = \pi \cdot r^2 \cdot L \Rightarrow \text{Cylinder volume equation.}$$

$$V_{\text{seat post}} = A_o \cdot L - A_i \cdot L = (A_o - A_i) \cdot L = (r_o^2 - r_i^2) \cdot \pi \cdot L$$

Where:

$V_{\text{seat post}}$ = Volume of the seat-post.

A_o = Area of the cylinder with outer diameter of the seat-post.

A_i = Area of the cylinder with inner diameter of the seat-post.

L = Lenght of the seat-post.

r_o = Outer radio of the seat-post.

r_i = Inner radio of the seat-post.

The table A.1 shows the values defined for the design process.

Dimension	Acronym	Value	Unit
Length of the seat-post	L	300	mm
Outer radio of the seat-post	r_o	27,2	mm
Inner radio of the seat-post	r_i	23,2	mm

Table A.1: Dimensions of the seat-post.

Result of seat-post volume:

$$V_{\text{seat post}} = \left(\left(\frac{27{,}2 \text{ mm}}{2}\right)^2 - \left(\frac{23{,}2 \text{ mm}}{2}\right)^2\right) \cdot \pi \cdot 300 \text{ mm} = 47500{,}88 \text{ mm}^3 = 47{,}50 \text{ cm}^3$$

On the table A.2 are presented the design variables predetermined for the calculation of the fiber volume content (V_f):

Dimension	Acronym	Value	Unit
Seat-post thickness	t	2	mm
Number of fiber glass layers	n	5	Layers
Fiber reinforcement surface density	A_w	621	$\frac{g}{cm^2}$
Fiber glass density	ρ_f	2,60	$\frac{g}{cm^3}$

Table A.2. Design variables.

As the number of fiber plies and laminate thickness are defined, we can calculate the fiber volume fraction following the formula below:

$$V_f = \frac{n \cdot A_w}{t \cdot \rho_f} = \frac{5 \cdot 621 \ \frac{g}{cm^2}}{2 \cdot 1000 \cdot 2{,}60 \ \frac{g}{cm^3}} = 0{,}5971 = 59{,}71\%$$

The fiber volume fraction is inversely proportional to laminate thickness.

With the $V_{seatpost}$ and the V_f determined, then it's possible to calculate the resin volume needed for the fiber glass reinforcement impregnation according to:

$$V_{resin} = V_{seatpost} \cdot (1 - V_f) = 47{,}50 \ cm^3 \cdot (1 - 0{,}5971) = 19{,}14 \ cm^3$$

2. Inflatable bladder channels radio

The radio of the bladder channels is obtained by:

$$V_{channel} = \frac{1}{2} \cdot \pi \cdot r_{channel}^2 \cdot L_{channel}$$

$$V_{resin} = N \cdot V_{channel} = n \cdot \frac{1}{2} \cdot \pi \cdot r_{channel}^2 \cdot L_{channel} \Rightarrow \text{Where } N = 4 \text{ channels.}$$

$$r_{channel} = \sqrt{\frac{2 \cdot V_{resin}}{N \cdot \pi \cdot L_{channel}}} = \sqrt{\frac{2 \cdot 19{,}14 \ cm^3 \cdot 1000}{4 \cdot \pi \cdot 297 \ mm}} = 3{,}20 \ mm \approx 3 \ mm$$

For the design of the channels, the radio is adjusted to 3 mm for measurement standardization.

3. Inflatable bladder general dimensions

For the design, it's considered an elongation coefficient for the bladder of 1. It's means that the channels and the bladder arcs maintain their length. The pressure applied inside the bladder deform the channels forcing the resin to impregnate the fiber reinforcement (figure A.1).

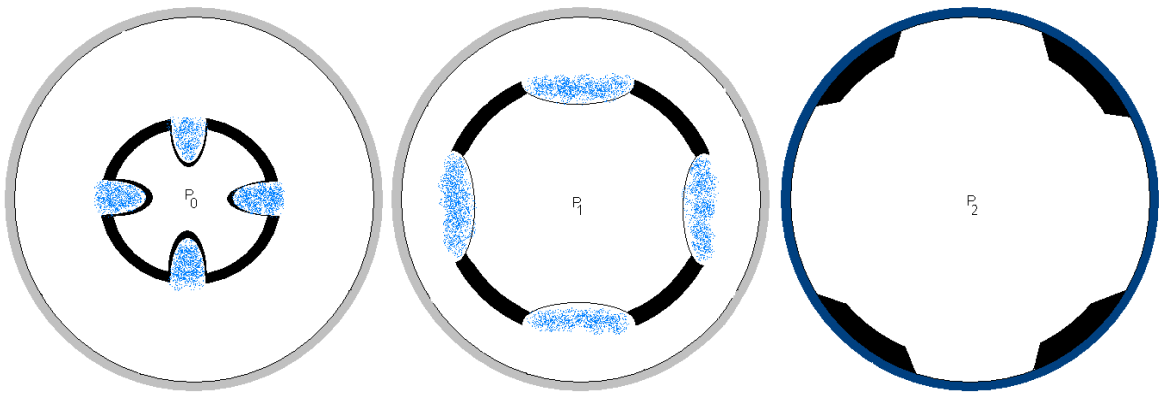

Figure A.1: Inflatable bladder process concept.

Calculation the channel and bladder arc lengths:

$$P_{i\,seatpost} = \pi \cdot D_i = \pi \cdot 23{,}2\ mm = 72{,}88\ mm$$

$$P_{channel} = \pi \cdot r_{channel} = \pi \cdot 3\ mm = 9{,}42\ mm$$

Where:

$P_{i\,seatpost}$ = Inner perimeter of the seat post.

$P_{channel}$ = Perimeter of the channel.

P_{arc} = Perimeter of the bladder arc.

$r_{channel}$ = Radio of the bladder channels.

D_i = Inner diameter of the seat-post.

$$P_{arc} = \frac{P_{i\,seatpost} - N \cdot P_{channel}}{N} = \frac{72{,}88\ mm - 4 \cdot 9{,}42\ mm}{4} = 8{,}80\ mm$$

With these values, the external diameter of the bladder is obtained from the CAD program and the result is an external diameter of 19 mm.

4. Seat-post mass

To finish this appendix, a theoretical calculation of the seat post weight is obtained according to:

$$M_f = \rho_f \cdot V_f = \rho_f \cdot V_{seatpost} \cdot V_f = 2{,}6\ \frac{g}{cm^3} \cdot 47{,}50\ cm^3 \cdot 0{,}5971 = 73{,}74\ g$$

$$M_r = \rho_r \cdot V_r = \rho_r \cdot V_{seatpost} \cdot (1 - V_f) = 2{,}6\ \frac{g}{cm^3} \cdot 47{,}50\ cm^3 \cdot (1 - 0{,}5971) = 21{,}28\ g$$

$$M_{seatpost} = M_f + M_r = 95{,}05\ g$$

Where:

$M_{seatpost}$ = Mass of the seat-post.

M_f = Mass of the glass fiber reinforcement.

M_r = Mass of the resin.

ρ_f = Density of the fiber.

ρ_r = Density of the resin.

$V_{seatpost}$ = Seat-post volume.

V_f = Fiber volume fraction.

Appendix B. Calculation of the PMMA tool

On the table B.1 are presented the principal properties of the PMMA material selected for the RTM tool construction:

Property	Acronym	Value	Unit
Density	ρ	1,19	$\frac{g}{cm^3}$
Coef. of thermal expansion	$\propto$	$8 \cdot 10^{-5}$	$\frac{1}{K}$
Tensile modulus	E	3300	$\frac{N}{mm^2}$
Tensile strength	σ_t	77	$\frac{N}{mm^2}$
Max. operating temperature	ϑ	90	°C

Table B.1: PMMA 8N PLEXIGLAS bibliography data (EVONIK Industries).

The table B.2 presents a summary of the main dimensions predetermined for the RTM body tool and the internal pressure during the process:

Dimensions	Values
Internal pressure	p = 2,5 bar.
Inner diameter of the tool	d_i = 27,2 mm.
Wall thickness of the tool	S = 30 mm.
Tool length	L = 300 mm.

Table B.2: RTM body tool main dimensions.

1. Wall thickness requirement: $S > S_{min.}$

To check that the wall thickness selected for the body mould withstand the internal pressure with the strength of the PMMA material is employed the Barlow's formula for hoop stress in pipe:

$$S_{min} = \frac{p \cdot d_i}{2 \cdot \sigma_{zul}} = \frac{250000 \frac{N}{m^2} \cdot 0{,}0272\ m}{2 \cdot 77000000 \frac{N}{m^2}} = 0{,}0000416\ m = 0{,}0416\ mm$$

Where:

p = Pressure.

σ_{zul} = Allowable stress.

S_{min} = Minimum wall thickness.

d_i = Inner diameter.

Wall thickness selected satisfy the requirement:

$$S > S_{min} \Rightarrow 30\ mm > 0{,}0416\ mm$$

This calculation is only valid for circular body shapes, which are connected at their periphery a long their entire length. The resulting RTM tool consists on this project of a lower and an upper half that are mechanically connected by bolts. The oversizing of the wall thickness allows the location of the refrigeration channels.

2. Stress in the tool.

To calculate the stress inside the RTM mould due the internal pressure applied, it is also employed the Barlow's formula for hoop stress in pipe:

$$\sigma = \frac{p \cdot d_i}{2 \cdot s} = \frac{250000 \frac{N}{m^2} \cdot 0{,}0272\ m}{2 \cdot 0{,}03\ m} = 113333{,}33 \frac{N}{m^2} = 0{,}136 \frac{N}{mm^2}$$

Where:

p = Pressure.

σ_{zul} = Allowable stress.

S_{min} = Minimum wall thickness.

d_i = Inner diameter.

3. Length and volume expansion.

To calculate the length expansion of the RTM mould due the temperature reached due the chemical reaction of the resin matrix, it is employed the following equation:

$$\Delta l = \propto \cdot L \cdot \Delta T$$

Where:
Δl = Difference in length.
$\propto$ = Coefficient of thermal expansion.
L = Initial length.
ΔT = Temperature gradient.

The assumption for the length expansion calculation is that the RTM tool at the beginning of the manufacturing process has 20ºC and the maximum temperature reached during the polymerization reaction is 90ºC.

3.1. Length in the body mould length direction

$$\Delta l_1 = \propto \cdot l \cdot \Delta T = 7 \cdot 10^{-5} \frac{1}{K} \cdot 300\ mm \cdot 70\ K = 1{,}47\ mm$$

3.2. Length in the mould thickness direction

$$\Delta l_2 = \propto \cdot s \cdot \Delta T = 7 \cdot 10^{-5} \frac{1}{K} \cdot 30\ mm \cdot 70\ K = 0{,}147\ mm$$

3.3. Volume expansion

To calculate the volume expansion of the RTM mould due the temperature reached due the chemical reaction of the resin matrix, it is employed the following equation:

$$\Delta V = V_0 \cdot 3 \cdot \propto \cdot \Delta T$$

Where:

ΔV = Difference in volume.
$\propto$ = Coefficient of thermal expansion.
V_0 = Initial volume.
ΔT = Temperature gradient.

$$A = \frac{\pi \cdot d^2}{4} - \frac{\pi \cdot d_i^2}{4} = \frac{\pi \cdot (87{,}2)^2}{4} - \frac{\pi \cdot (27{,}2)^2}{4} = 5390{,}973\ mm^2$$

$$V_0 = A \cdot L = 5390{,}973\ mm^2 \cdot 300\ mm = 1617291{,}898\ mm^3$$

$$\Delta V = 1617291{,}898 mm^3 \cdot 3 \cdot 7 \cdot 10^{-5} \frac{1}{K} \cdot 70K = 23774{,}1909\ mm^3 = 23{,}774 \cdot 10^{-3}\ dm^3$$

4. Temperature inside the tool

In the case of a defective tool core is calculated the temperature reached inside the RTM tool in order to check if the PMMA material withstand this temperature:

- Ambient conditions:

$$p_{amb}(\vartheta_0 = 0°C) = 1{,}013 bar; \quad \vartheta_{amb} = 20°C; \quad T_{amb} = 293{,}15 K$$

- Atmospheric air magnitudes:

$$C_p = 1{,}005 \frac{kJ}{kg \cdot K}; \quad C_v = 0{,}716 \frac{kJ}{kg \cdot K}; \quad \kappa = \frac{c_p}{c_v} = \frac{1{,}005 \frac{kJ}{kg \cdot K}}{0{,}716 \frac{kJ}{kg \cdot K}} = 1{,}404; \quad \beta = \frac{1}{273} \frac{1}{K}$$

- Calculation:

$$V_1 = V_0 \cdot (1 + \beta \cdot \Delta T) = V_0 \cdot \left(1 + \frac{1}{273} \frac{1}{K} \cdot 20\ K\right) = V_0 \cdot 1{,}07326 \leftarrow \text{Ratio}$$

$$\frac{p_{amb} \cdot V_0}{T_0} = \frac{p_1 \cdot V_1}{T_{amb}}$$

$$p_1 = \frac{p_{amb} \cdot V_0 \cdot T_{amb}}{T_0 \cdot V_1} = \frac{1{,}013\ bar \cdot 1\ l \cdot 293{,}15\ K}{273{,}15\ K \cdot 1{,}07326\ l} = 1{,}013\ bar$$

$$\frac{T_{amb}}{T_{inside}} = \left(\frac{p_{amb}}{p_{inside}}\right)^{\frac{\kappa-1}{\kappa}}$$

$$T_{inside} = T_{amb} \cdot \left(\frac{p_{inside}}{p_1}\right)^{\frac{\kappa-1}{\kappa}} = 293{,}15\ K \cdot \left(\frac{2{,}5\ bar}{1{,}013\ bar}\right)^{\frac{1{,}404-1}{1{,}404}} = 380{,}175\ K = 107{,}025\ °C$$

The temperature reached inside the tool is high than the temperature of deflection on the material data sheet $103°C < 107{,}25°C$ considering different strengths (see table B.3). It must be controlled the refrigeration of the tool in order to reduce the temperature of the PMMA material.

Thermal properties	Load	Temperature
Temperature of deflection under Load (Data sheet)	0,45 MPa	103 °C
Temperature of deflection under Load (Real)	0,25 MPa	107,025 °C

Table B.3: Thermal properties vs strength.

5. Screws selection for tooling cohesion

For this project, screws with grade A2-50 have been selected.

The tensile strength of the screws is: $R_e = 210 \frac{\mathrm{N}}{\mathrm{mm^2}}$

Using the following equation is calculated the maximum force that must withstand mechanically the screws:

$$F = p \cdot D_i \cdot L = 250000 \frac{\mathrm{N}}{\mathrm{m^2}} \cdot 0{,}0272\ \mathrm{m} \cdot 0{,}3\ \mathrm{m} = 2040\ \mathrm{N}$$

Where:

F = Maximum strength.

p = Pressure inside the RTM tool.

D_i = Inner diameter.

L = Initial length.

The formula below provides the section of the screws needed to support the pressure of the RTM process:

$$A_{erf} = \frac{\mathrm{F}}{\mathrm{R_e}} = \frac{2040\ \mathrm{N}}{210\ \frac{\mathrm{N}}{\mathrm{mm^2}}} = 9{,}714\ \mathrm{mm^2}$$

Where:

A_{erf} = Section of the screws needed.

F = Maximum strength.

$\mathrm{R_e}$ = Screw tensile strength.

To withstand the forces its need a screw size M5. For the tool several M5 screws are used, which offer a great safety and risk avoidance.

Appendix C. Scale drawings

The result is a set of product documents detailed on the table C.1:

Component	Parts quantity	Drawing
Seat Post	1	1/1
Upper mould	1	1/8
Lower mould	1	2/8
Front cover	1	3/8
Rear cover	1	4/8
Inflatable bladder	1	5/8
Longitudinal sealing gasket	2	6/8
Circular sealing gasket	4	7/8
Screw	12	8/8
Simple Inflatable Bladder	1	1/1

Table C.1. Detailed drawings.

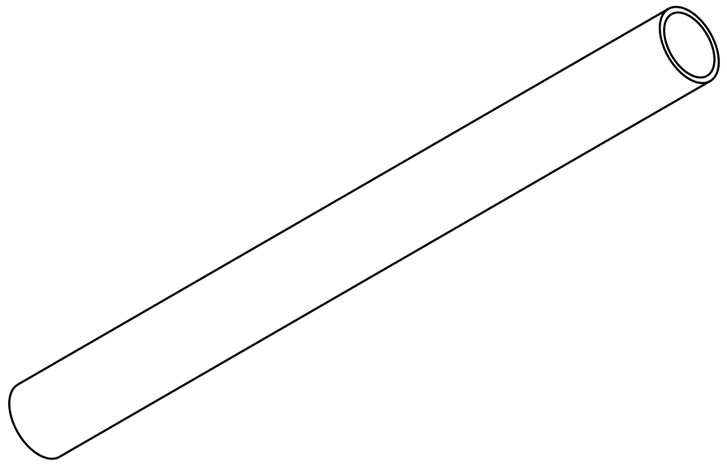

Isometric view
Scale: 1:2

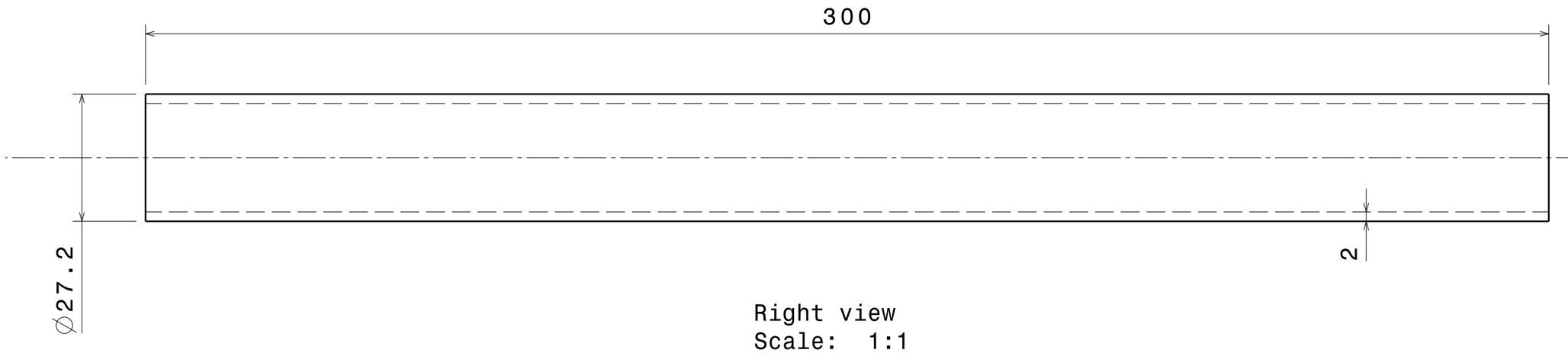

Right view
Scale: 1:1

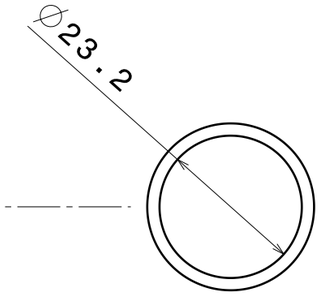

Front view
Scale: 1:1

PAGE	TECHNICAL REFERENCE	MADE BY	VALIDATED BY	SCALE
		BORJA AMORES		1:1

Institut für Verbundwerkstoffe

DOCUMENT	STATUS
TITTLE: SEAT POST	DIN ISO 2768-mK

OTHER	DATE	Spr.	SHEET
	30/04/2015		1/1

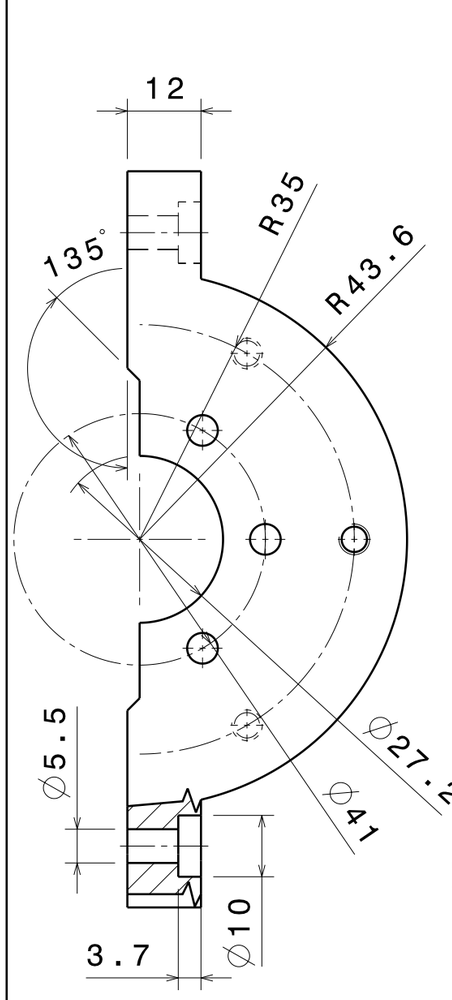

Scale: 1:1

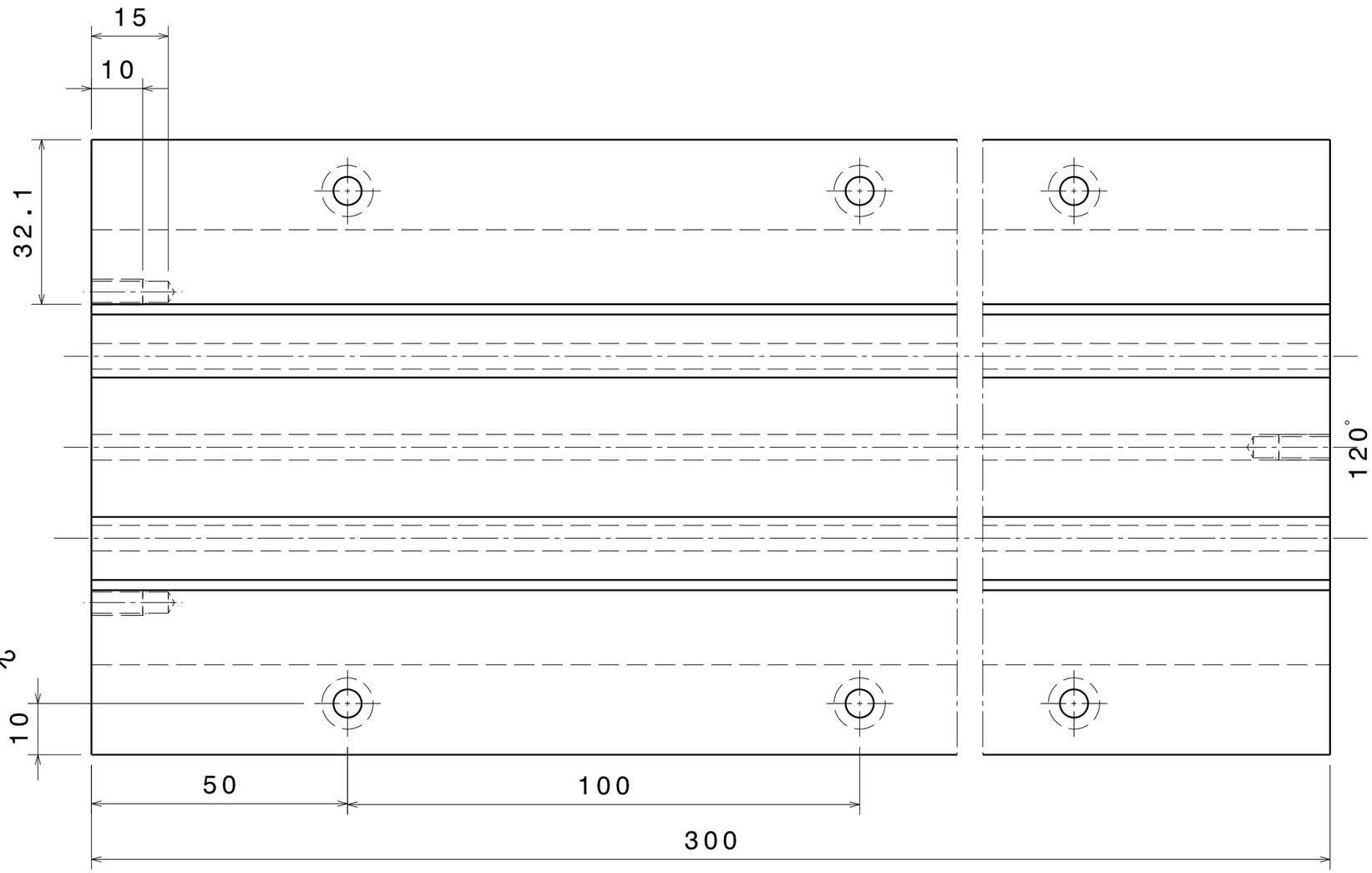

Scale: 1:1

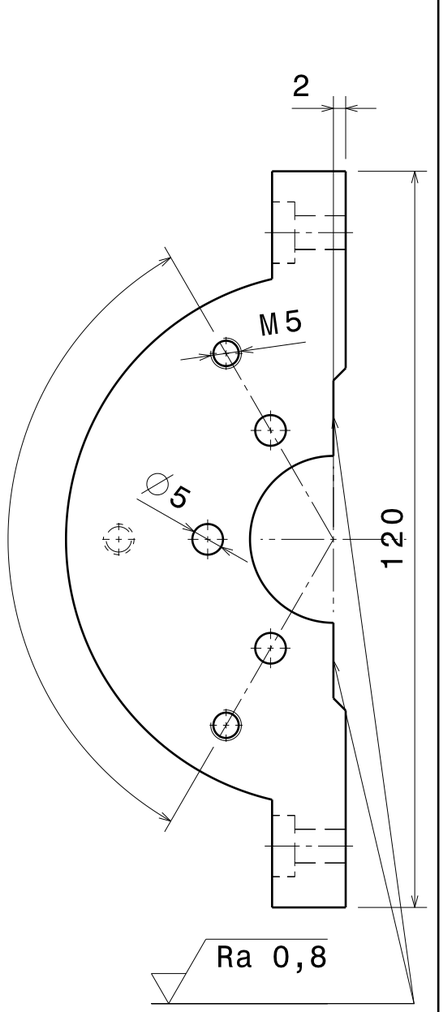

Scale: 1:1

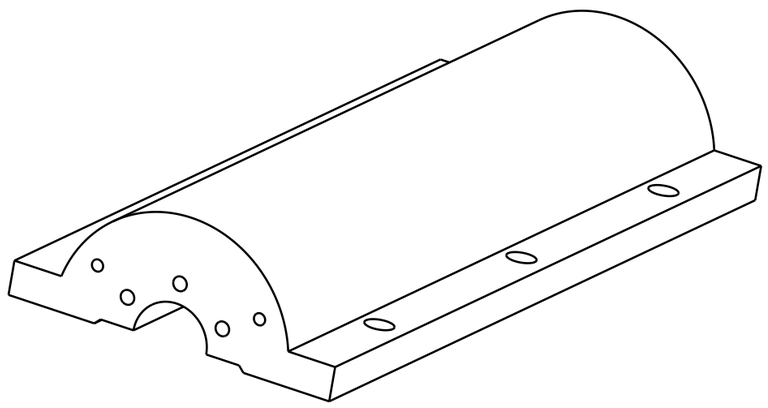

Scale: 1:2

Ra 0,8

PAGE	TECHNICAL REFERENCE	MADE BY	VALIDATED BY	SCALE
		BORJA AMORES		1:1

Institut für Verbundwerkstoffe

DOCUMENT	STATUS
TITTLE: UPPER MOULD	DIN ISO 2768-mK

OTHER	DATE	Spr.	SHEET
	30/04/2015		1/8

0,05

300

Ra 0,8

Ra 0,8

A

B

M5

120

8

2

25.9

∅5

R43.6

M5

∅27.2

17.1

45°

R20.5

R35

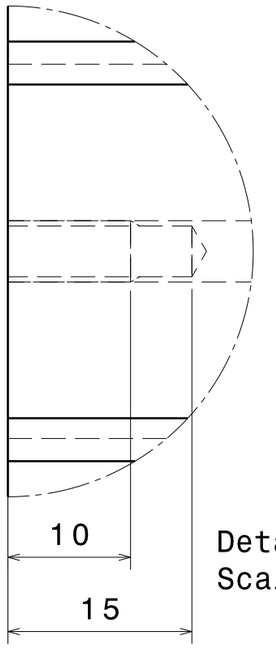

Detail A
Scale: 2:1

Sealing accomodation
Longitudinal gasket

Ra 0,8

Detail B
Scale: 2:1

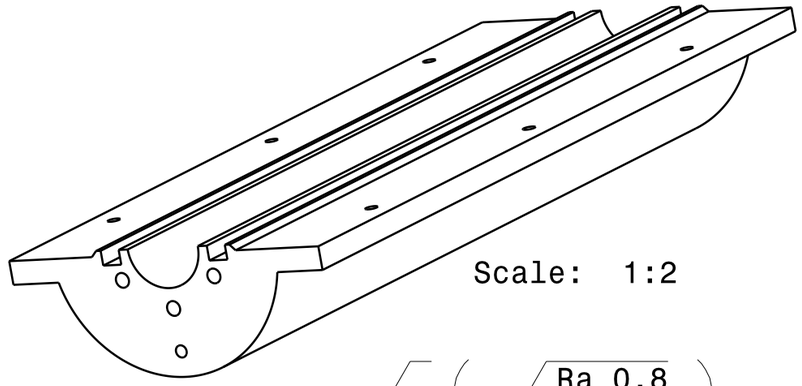

Scale: 1:2

Ra 0,8

PAGE	TECHNICAL REFERENCE	MADE BY	VALIDATED BY	SCALE
		BORJA AMORES		1:1

Institut für Verbundwerkstoffe

DOCUMENT	STATUS		
TITTLE: LOWER MOULD	DIN ISO 2768-mK		
	OTHER	DATE: 30/04/2015	Spr.	SHEET: 2/8

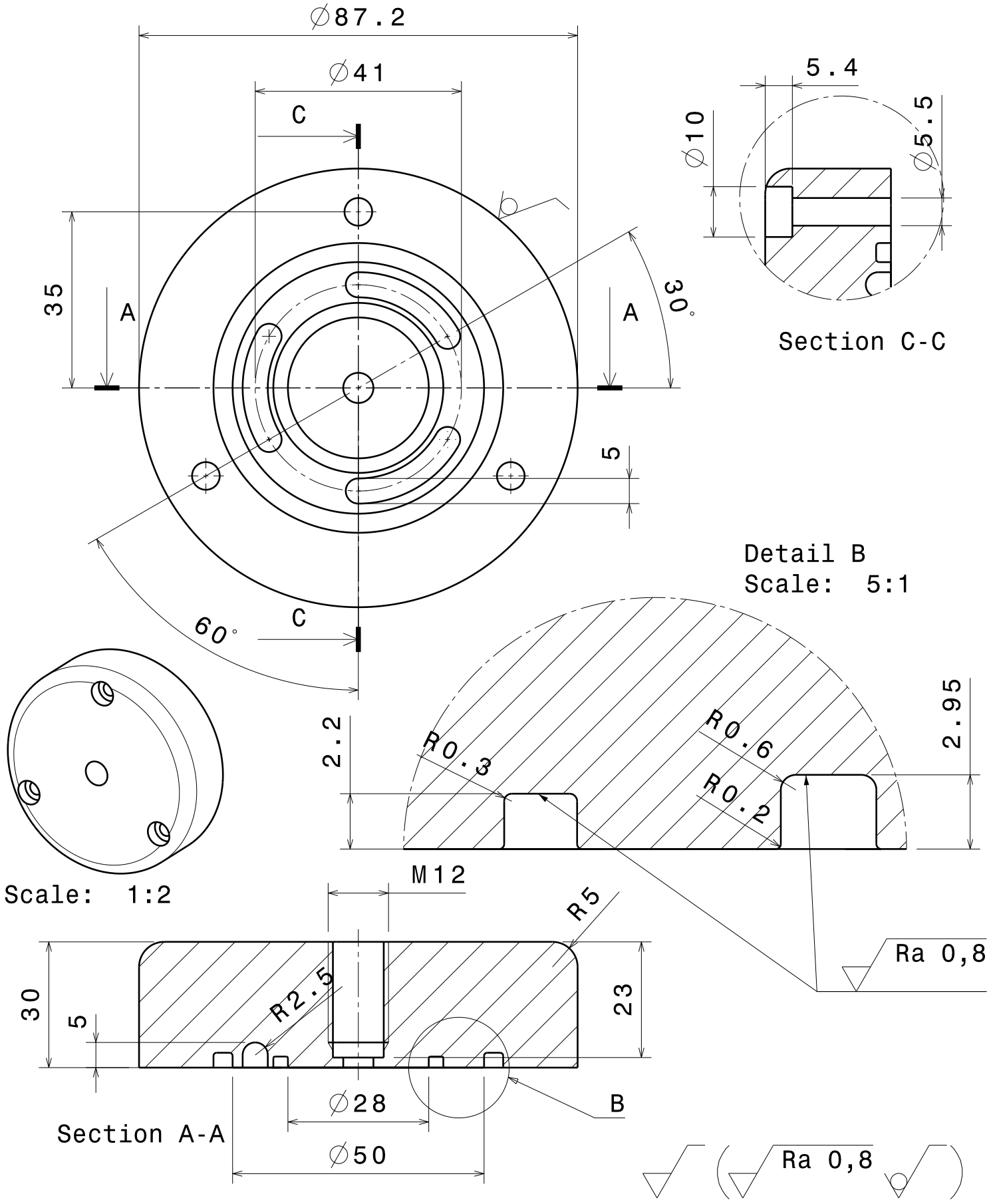

PAGE	TECHNICAL REFERENCE	MADE BY	VALIDATED BY	SCALE
		BORJA AMORES		1:1

Institut für Verbundwerkstoffe

DOCUMENT	STATUS
TITTLE: FRONT COVER	DIN ISO 2768-mK

OTHER	DATE	Spr.	SHEET
	30/04/2015		3/8

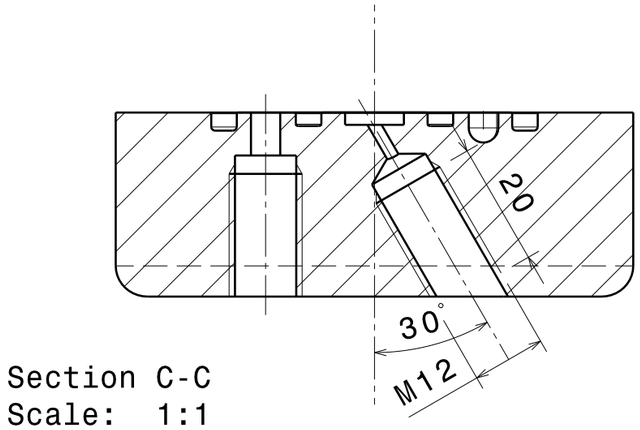

Section C-C
Scale: 1:1

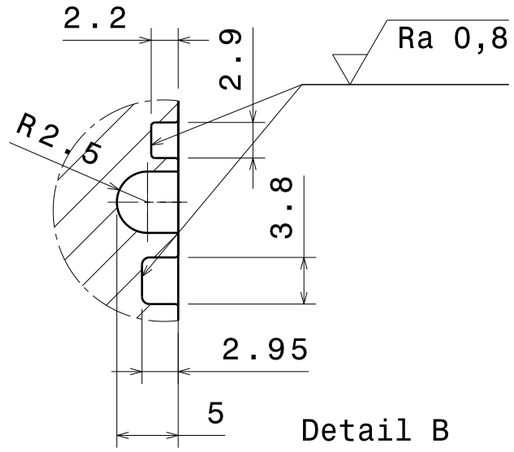

Detail B
Scale: 2:1

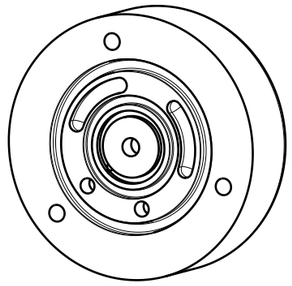

Isometric View
Scale: 1:2

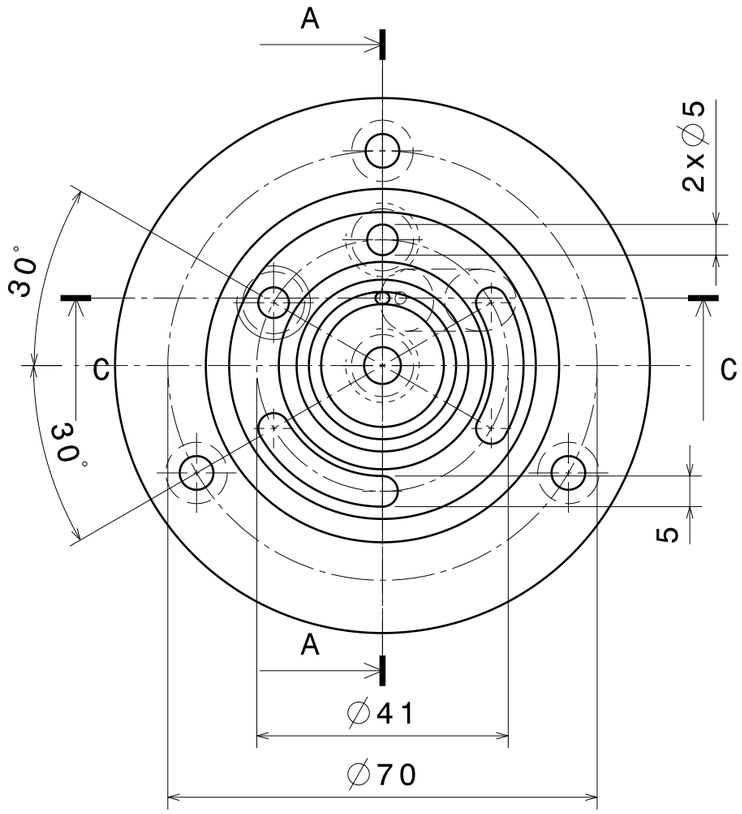

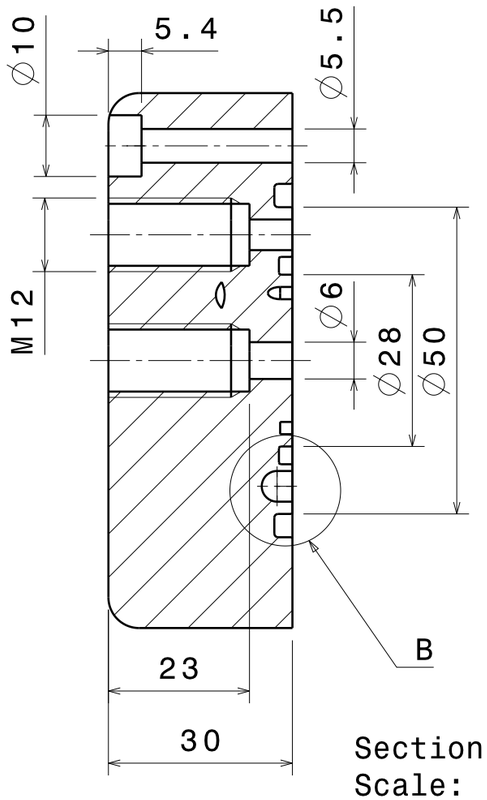

Section A-A
Scale: 1:1

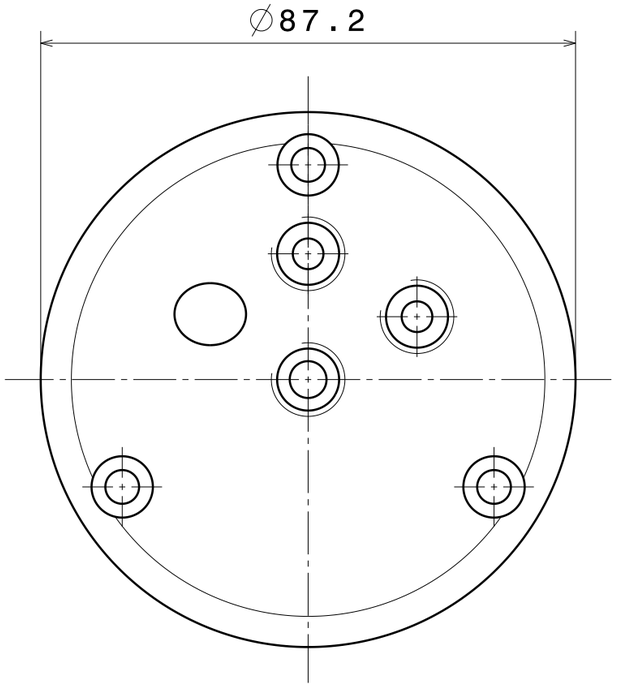

Auxiliar view D
Scale: 1:1

Ra 0,8

PAGE	TECHNICAL REFERENCE	MADE BY	VALIDATED BY	SCALE
		BORJA AMORES		1:1

Institut für Verbundwerkstoffe

DOCUMENT	STATUS
TITTLE: REAR COVER	DIN ISO 2768-mK

OTHER	DATE	Spr.	SHEET
	30/04/2015		4/8

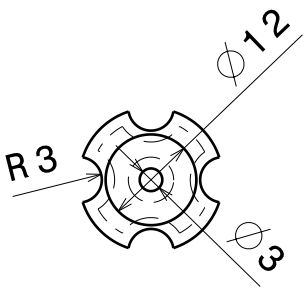

Front view
Scale: 1:1

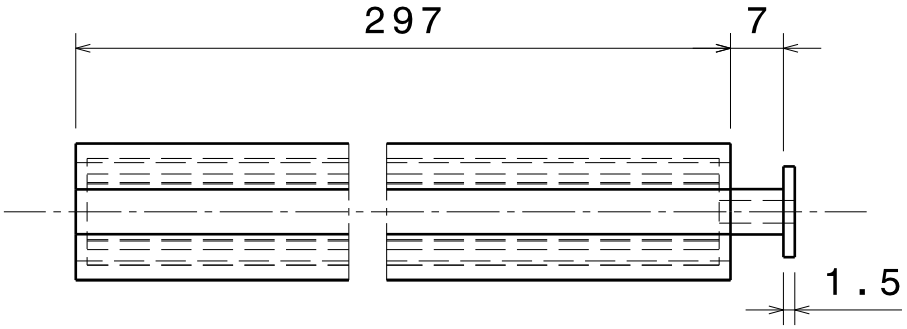

Left view
Scale: 1:1

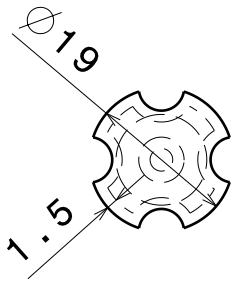

Rear view
Scale: 1:1

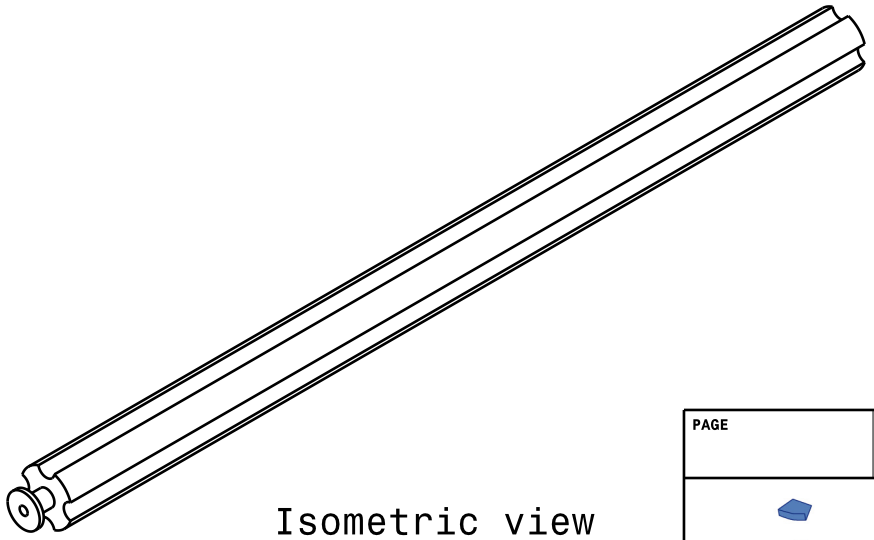

Isometric view
Scale: 1:2

PAGE	THECHNICAL REFERENCE	MADE BY	VALIDATED BY	SCALE
		BORJA AMORES		1:1

Institut für Verbundwerkstoffe

DOCUMENT	STATUS
TITTLE: INFLATABLE BLADDER	DIN ISO 2768-mK

OTHER	DATE	Spr.	SHEET
	30/04/2015		5/8

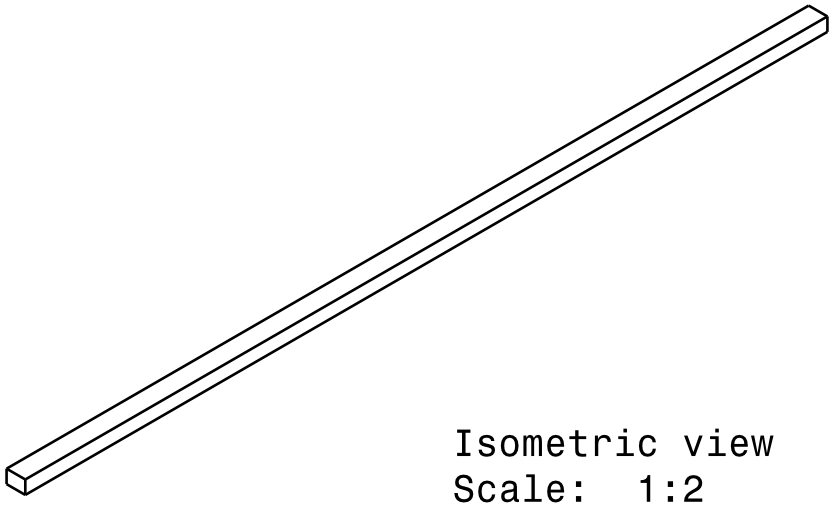

Isometric view
Scale: 1:2

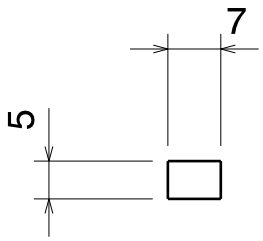

Front view
Scale: 1:1

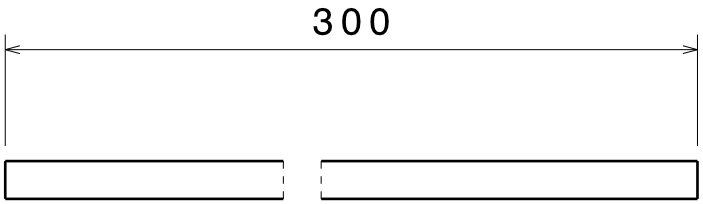

Left view
Scale: 1:1

PAGE	TECHNICAL REFERENCE	MADE BY	VALIDATED BY	SCALE
		BORJA AMORES		1:1

Institut für Verbundwerkstoffe

DOCUMENT	STATUS

TITTLE	DIN ISO 2768-mK
LONG. GASKET	

OTHER	DATE	Spr.	SHEET
	30/04/2015		6/8

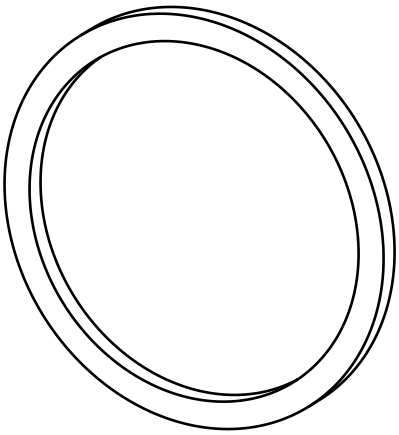

Isometric view
Scale: 1:1

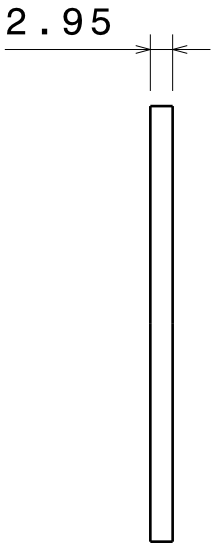

Right view
Scale: 1:1

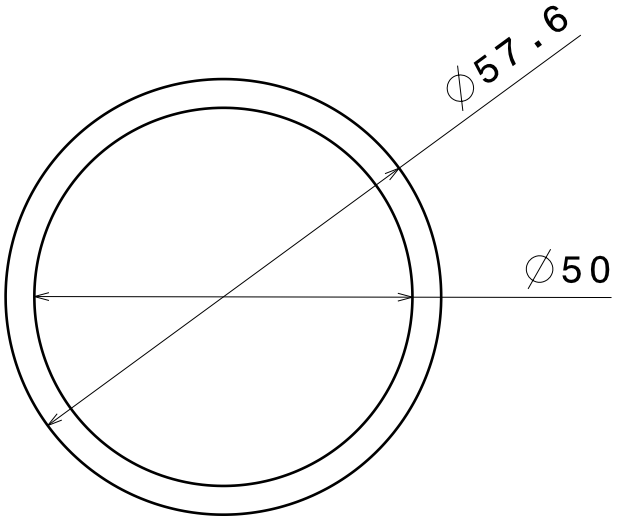

Front view
Scale: 1:1

PAGE 1	TECHNICAL REFERENCE	MADE BY BORJA AMORES	VALIDATED	SCALE 1:1
Institut für Verbundwerkstoffe		DOCUMENT	STATUS	
		TITTLE OUTER CIRC. GASKET	DIN ISO 2768-mK	
			OTHER / DATE 30/04/2015 / Spr. / SHEET 7/8	

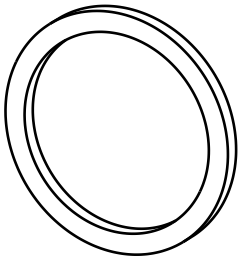

Isometric view
Scale: 1:1

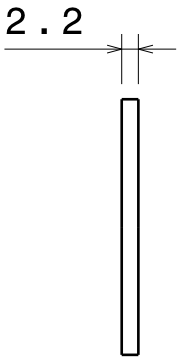

Right view
Scale: 1:1

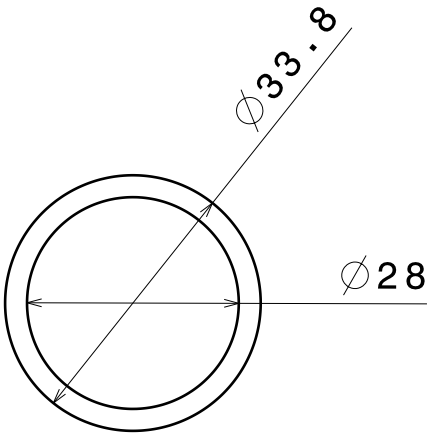

Front view
Scale: 1:1

PAGE	TECHNICAL REFERENCE	MADE BY	VALIDATED	SCALE
2		BORJA AMORES		1:1

Institut für Verbundwerkstoffe

DOCUMENT	STATUS
TITTLE: INNER CIRC. GASKET	DIN ISO 2768-mK

OTHER	DATE	Spr.	SHEET
	30/04/2015		7/8

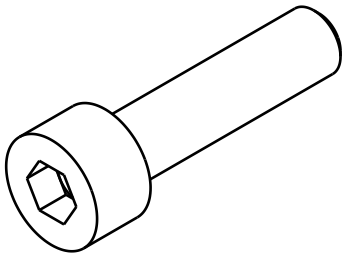

Isometric view
Scale: 2:1

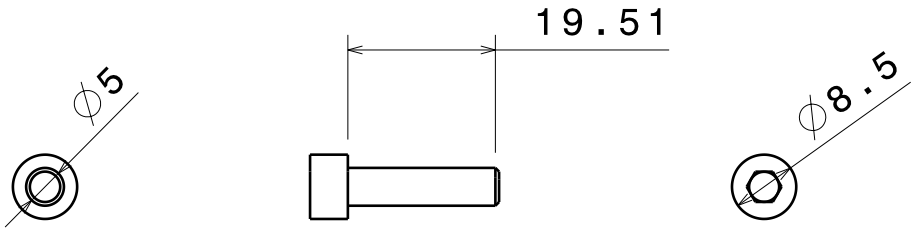

Front view
Scale: 1:1

Left view
Scale: 1:1

Rear view
Scale: 1:1

PAGE	TECHNICAL REFERENCE	MADE BY	VALIDATED	SCALE
		BORJA AMORES		1:1

Institut für Verbundwerkstoffe

DOCUMENT	STATUS
TITTLE: SCREW	DIN ISO 2768-mK

OTHER	DATE	Spr.	SHEET
	30/04/2015		8/8

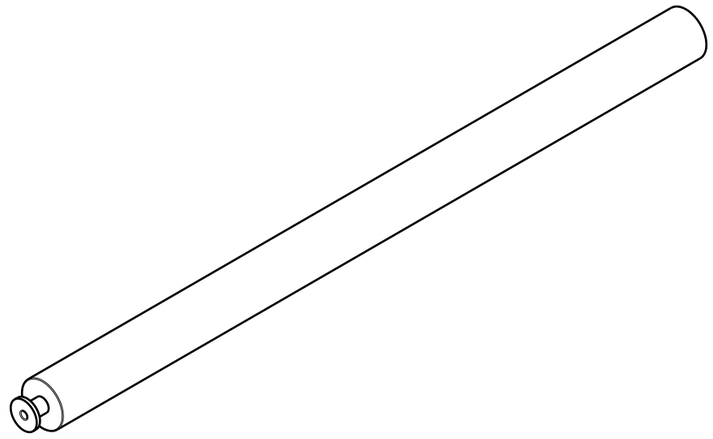

Isometric view
Scale: 1:2

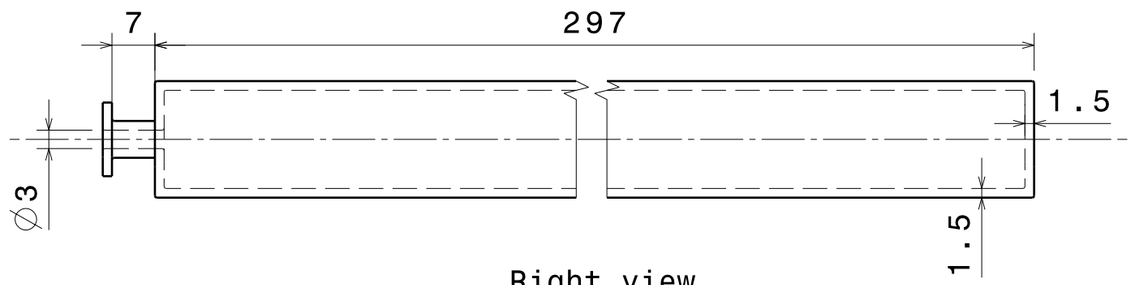

Right view
Scale: 1:1

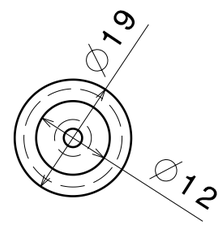

Front view
Scale: 1:1

PAGE	TECHNICAL REFERENCE	MADE BY	VALIDATED BY	SCALE
		BORJA AMORES		1:1

Institut für Verbundwerkstoffe

DOCUMENT	STATUS
TITTLE: SIMPLE BLADDER	DIN ISO 2768-mK

OTHER	DATE	Spr.	SHEET
	30/04/2015		1/1

Appendix D. Materials standards

1. **Fiber glass reinforcement**
2. **Epoxy resin**
3. **RTM tool material: PMMA**
4. **Inflatable bladder material**

FiberComposites

Material Specification

MULTI-AXIAL PRODUCT TYPE 62014-127-60

Construction: +45°/-45°
is produced of continuous E-glass under quality system conforming to ISO 9001.

Raw materials

ver 1 Minna Venalainen

Element	+45°	90°	-45°	Stitch yarn			
Nominal weight g/m²	296	19	296	10			
Tex (ISO 1889)	300 ± 10 %	160 ± 10 %	300 ± 10 %	-			
Type of yarn	EC 300	EC 160	EC 300	Synthetic			
Notice	Compatible with polyester, vinyl ester and epoxy resins.						

Product

Standard elements	Roll length	Moisture content	Thickness	Weight	Width with fringes		
Nominal value	60 m	0.01 %	0.56 mm	621 g/m²	1270 mm		
Tolerance	59 - 61	< 0.20 %	± 15 %	± 5 %	1245 - 1295		
Test method	ISO 5025	ISO 3344	ISO 4603	ISO 3374	ISO 5025		
Notice							
Custom elements	**Gauge**						
Value	28/10 cm						
Notice							

Delivery	
Customer	
Address	
Order no.	
Delivery number	
Quantity	
Batch codes	
Notice	

STORAGE: The product should be stored in its original packaging in a dry, cool environment. If the product is stored at a temperature below +15°C conditioning in the workshop is recommended for at least 24 hours. It is recommended that the product is used within 12 months of delivery.

Mikkeli
13.1.2005

SIGNATURE: Helena Kortelainen

EPIKOTE™ Resin MGS® RIM 935

EPIKURE™ Curing Agent MGS® RIM H 936 / 937

Content

Characteristics

Approval	-
Application	application that require high heat resistances, boat- and shipbuilding, automotive, tooling and moulding
Operational temperature	-60 °C up to +130 °C (-76°F up to +266 °F) after suitable heat treatment
Processing	at temperatures between 15 °C and 50 °C (59 °F-122 °F) , preferably 25 °C - 35 °C (77 °F - 95 °F), infusion, hand lay-up and others
Features	very high heat resistance, low mixed viscosity, good mechanical properties potlife approx. 2-5 h short curing times at elevated temperatures
Special modifications	on request
Storage	shelf life of 24 months in originally sealed containers

Am Ostkai 21/22
70327 Stuttgart
Germany
Phone: +49 (0) 711 - 3 89 80 00
Fax: +49 (0) 711 - 3 89 80 011
www.hexionchem.com

EPIKOTE™ Resin MGS® RIM 935

Application

Low viscous infusion resin system for processing of woven and none crimp multiaxial fabrics of low to high areal weight. Due to its very good mechanical properties, these system is suitable for the production of components featuring high static and dynamic loadability and high heat resistance.

Infusion resin RIM 935 is based on bisphenol A/F resin. Hardener RIMH 936 and RIMH 937 are a modification of aliphatic and cycloaliphatic amines. As crystallisation of both A and B component is possible, special care should be given to this issue. It appears as a clouding or solidification of the contents of the container. Before processing, the crystallization must be removed by warming up.

Potlife (100 g mixed at 30 °C/86 °F) is approximately 2 hours for RIMH 936 and 3,5 h for RIMH 937. Optimum viscosities for infusion are realized at temperatures in the range of 25 - 35 °C (77 °F - 95 °F). Pot life is then between approx. 1 h (RIMH 236 at 40°C/104 °F) to 5 h (RIMH 937 at 25°C/77 °F). Following initial curing at room temperature, the parts are still brittle and require heat treatment at a min. temperature of 50 °C/122 °F before processing or demolding. Direct curing at Selevated temperatures (60 °C-100 °C/140 °F-212 °F) is possible . The curing time can be reduced to a few minutes by this.

Non-tacky, high-gloss surfaces are obtained even with unfavorable curing conditions, such as low temperatures or high relative humidity.

The Infusion resin systems does not contain any unreactive components. All raw materials and additives feature a very low vapor pressure, therefore permitting processing of the material under vacuum even at elevated temperatures. Compatibility problems are not to be expected in combination with suitable gelcoats, various paints (e.g. PUR-based), etc. However, comprehensive tests are indispensable.

These hardeners can be stored for at least 24 months in their carefully sealed original containers. Even though it is unlikely, these hardeners may crystallize at temperatures below +15 °C. The crystallization is visible as a clouding or solidification of the contents of the container. If crystallisation of either component should be observed, it can removed by warming up. Slow warming up to approx. 50 °C-60°C (122 °F-140 °F) in a water bath or oven and stirring or shaking will clarify the contents of the container without any loss of quality. Use only completely transparent products. Before warming up, open containers slightly to permit equalization of pressure. Caution during warm-up! Do not warm up over an open flame! While stirring up use safety equipment (gloves, eyeglasses, respirator equipment).

The relevant industrial safety regulations for the handling of epoxy resins and hardeners and our instructions for safe processing are to be observed.

Am Ostkai 21/22
70327 Stuttgart
Germany
Phone: +49 (0) 711 - 3 89 80 00
Fax: +49 (0) 711 - 3 89 80 011
www.hexionchem.com

EPIKOTE™ Resin MGS® RIM 935

Specifications

		Infusion resin RIM 935
Density	[g/cm³]	1,14 - 1,2
Viscosity	[mPas]	300 - 600
Epoxy equivalent	g/equivalent	155 - 165
Epoxy value	equivalent /100g	0,61 - 0,64
Refractory index		1,5350-1,5450

Measuring conditions:
measured at 25 °C / 77 °F

		Hardener RIMH 936	Hardener RIMH 937
Density	[g/cm³]	0,92 - 0,97	0,95 - 0,96
Viscosity	[mPas]	10 - 50	30 - 100
Amine value	[mg KOH/g]	550 - 650	450 - 500
Refractory index		1,4850 - 1,4920	1,485 - 1,505

Measuring conditions:
measured at 25 °C / 77 °F

Am Ostkai 21/22
70327 Stuttgart
Germany
Phone: +49 (0) 711 - 3 89 80 00
Fax: +49 (0) 711 - 3 89 80 011
www.hexionchem.com

EPIKOTE™ Resin MGS® RIM 935

Processing details

	Injection resin RIM 935	Hardener RIMH 936	Hardener RIMH 937
Average EP - Value	0,63	-	
Average amine equivalent	-	45	59

Mixing ratios

	RIM 935 : RIMH 936	RIM 935 : RIMH 937
Parts by weight	100 : 29 ± 2	100 : 38 ± 2
Parts by volume	100 : 35 ± 2	100 : 45 ± 2

The specified mixing ratios must be observed as exactly as possible. Adding more or less hardener will not result in a faster or slower reaction - but in incomplete curing which cannot be corrected in any way.
Resin and hardener must be mixed very thoroughly. Mix until no clouding is visible in the mixing container. Pay special attention to the walls and the bottom of the mixing container.

Viscosity development

Viscosity development at 40°C in thin layer

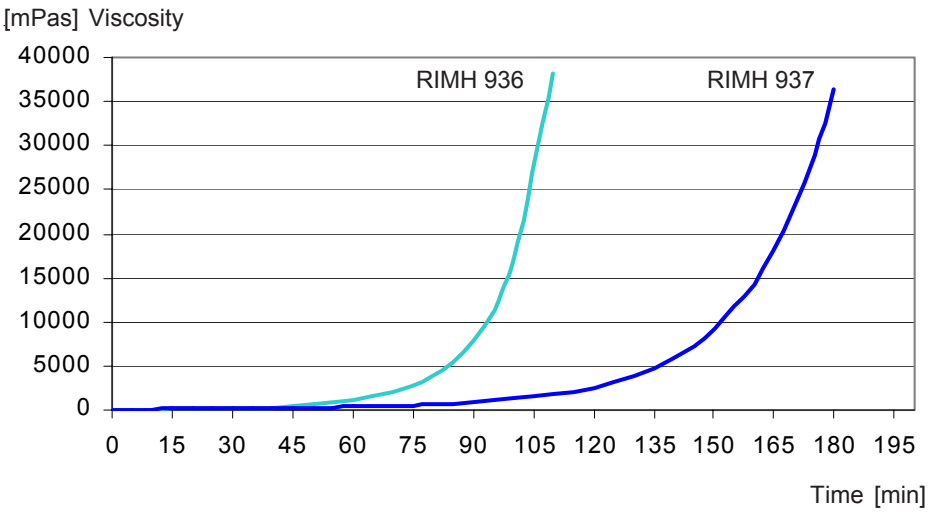

Am Ostkai 21/22
70327 Stuttgart
Germany
Phone: +49 (0) 711 - 3 89 80 00
Fax: +49 (0) 711 - 3 89 80 011
www.hexionchem.com

Temperature development

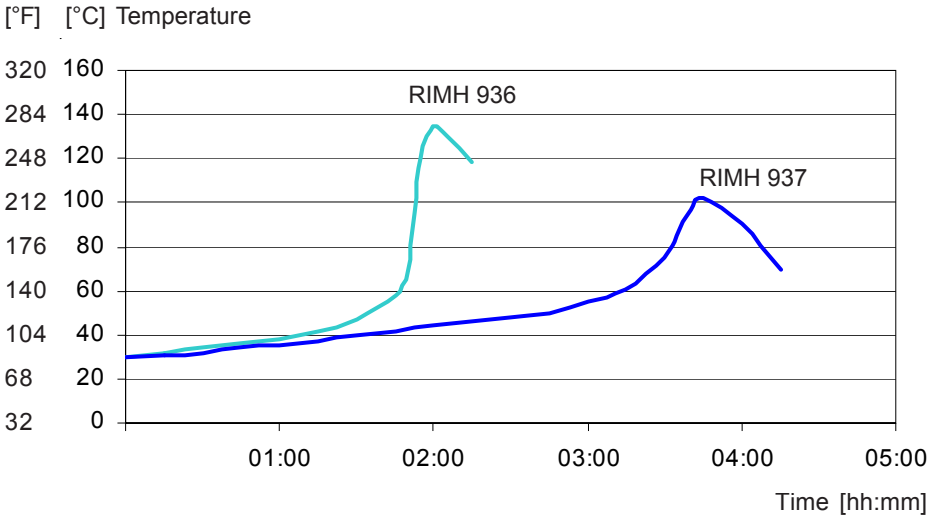

Quantity: 100g in air at 30 °C (86 °F)

The optimal processing temperature is in the range between 20 and 25°C (68 - 77°F). Higher processing temperatures are possible, but will shorten pot life. A rise in temperature of 10 °C (18°F) will halve the pot life. Water (for example very high humidity or contained in fillers) causes an acceleration of the resin/hardener reaction. Different temperatures and humidities during processing have no significant effect on the strength of the cured product.

Viscosity of mixture

Viscosity of the mixture at different temperatures

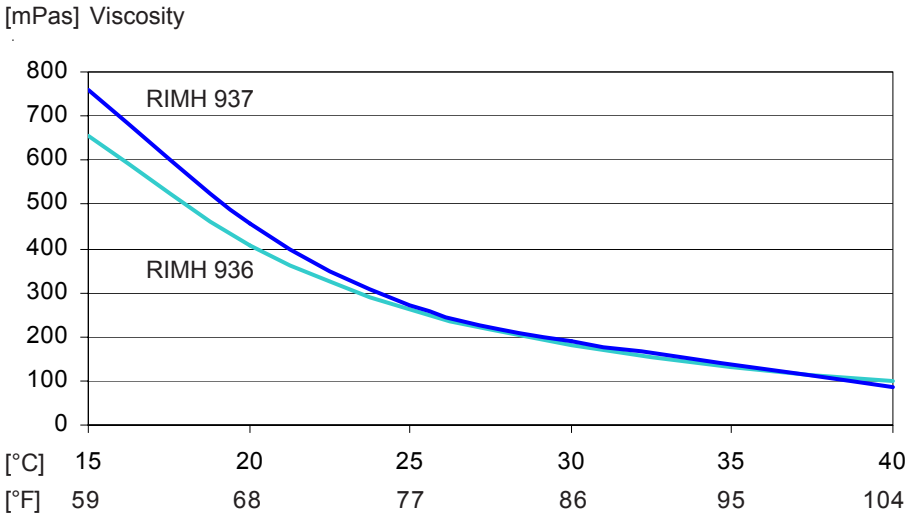

Am Ostkai 21/22
70327 Stuttgart
Germany
Phone: +49 (0) 711 - 3 89 80 00
Fax: +49 (0) 711 - 3 89 80 011
www.hexionchem.com

EPIKOTE™ Resin MGS® RIM 935

Glass transition temperature (T_G) unconditioned

Max. T_G at 80 °C (176 °F) post cure	90-100 °C (194-212 °F)
Max. T_G at 100 °C (212 °F) post cure	105-120 °C (221-248 °F)
Max. T_G at 140 °C (284 °F) post cure	135-150 °C (275-302 °F)

DMA

DMA-Measuring after heat treatment
DMA-T_G(peak) tan delta: Infusion resin RIM 935 with hardener RIMH 937

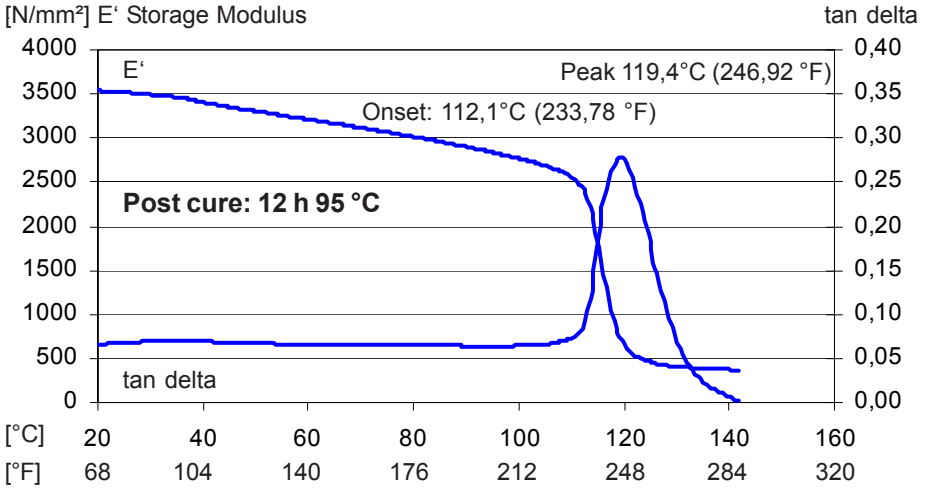

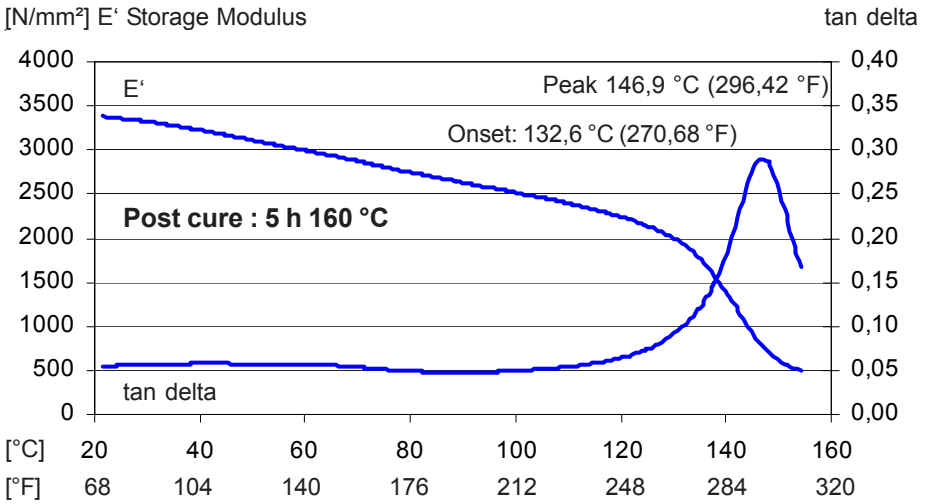

Measuring conditions:

Frequency:	1Hz
Coupon thickness:	2mm
Heating rate:	2K/min

Am Ostkai 21/22
70327 Stuttgart
Germany
Phone: +49 (0) 711 - 3 89 80 00
Fax: +49 (0) 711 - 3 89 80 011
www.hexionchem.com

Product Information

PLEXIGLAS® 8N Molding Compound

Product Profile:

PLEXIGLAS® 8N is an amorphous thermoplastic molding compound (PMMA).

Typical properties of PLEXIGLAS® molding compounds are:
- good flow
- high mechanical strength, surface hardness and abrasion resistance
- high light transmission
- very good weather resistance
- free colorability due to crystal clarity

Special properties of PLEXIGLAS® 8N are:
- optimum mechanical properties
- maximum heat deflection temperature
- good flow / melt viscosity
- AMECA listing.

Application:

Used for injection molding optical and technical items.

Examples:

optical waveguides, luminaire covers, automotive lighting, instrument cluster covers, optical lenses, displays, etc.

Processing:

PLEXIGLAS® 8N can be processed on injection molding machines with 3-zone general purpose screws for engineering thermoplastics.

Physical Form / Packaging:

PLEXIGLAS® molding compounds are supplied as pellets of uniform size, packaged in 25kg polyethylene bags or in 500kg boxes with PE lining; other packaging on request.

Properties:

	Parameter	Unit	Standard	PLEXIGLAS® 8N
Mechanical Properties				
Tensile Modulus	1 mm/min	MPa	ISO 527	3300
Stress @ Break	5 mm/min	MPa	ISO 527	77
Strain @ Break	5 mm/min	%	ISO 527	5.5
Charpy Impact Strength	23°C	kJ/m²	ISO 179/1eU	20
Thermal Properties				
Vicat Softening Temperature	B / 50	°C	ISO 306	108
Glass Transition Temperature		°C	IEC 10006	117
Temp. of Deflection under Load	0.45 MPa	°C	ISO 75	103
Temp. of Deflection under Load	1.8 MPa	°C	ISO 75	98
Coeff. of Linear Therm. Expansion	0 - 50°C	E-5 /°K	ISO 11359	8
Fire Rating			DIN 4102	B2
Flammability UL 94	1.6 mm	Class	IEC 707	HB
Rheological Properties				
Melt Volume Rate, MVR	230°C / 3.8kg	cm³/10min	ISO 1133	3
Optical Properties	d=3 mm			
Luminous transmittance	D65	%	ISO 13468-2	92
Haze			ASTM D1003	< 0.5
Refractive Index			ISO 489	1.49
Other Properties				
Density		g/cm³	ISO 1183	1.19
Recommended Processing Conditions				
Predrying Temperature		°C		max. 98
Predrying Time in Desiccant-Type Drier		h		2 - 3
Melt Temperature		°C		220 - 260
Mold Temperature (Injection Molding)		°C		60 - 90

All listed technical data are typical values intended for your guidance. They are given without obligation and do not constitute a materials specification.

Evonik Röhm GmbH Kirschenallee D-64293 Darmstadt
Telefon: +49 6151 18-4711 Telefax: +49 6151 18-3177
www.plexiglas-polymers.com

Ref. No.: MC106-E v0160 Date: 2010-01-15

ELASTOSIL® RT 607

RTV-2 Silicone Encapsulant

Characteristics

ELASTOSIL® RT 607 is a pourable, addition-curing RTV-2 silicone rubber.

Special characteristics

- Two-part, 9 : 1 mixing ratio
- Low viscosity
- Rapid heat cure
- High hardness
- Excellent heat stability
- Flame retardant

Product data (uncured)

Property	Test method	Unit	Value	
Component			**A**	**B**
Color			Reddish brown	Transparent
Viscosity at 23 °C	ISO 3219	[mPa s]	12,000	200
Density at 23 °C		[g/cm³]	1.5	0.97

These figures are only intended as a guide and should not be used in preparing specifications.

Product data (catalyzed A+B)

Property	Test method	Unit	Value
Platinum-catalyst in component			A
Mixing ratio (by weight)		A : B	9 : 1
Viscosity of mix	ISO 3219	[mPa s]	10,000
Pot life at 23 °C (up to 100,000 mPa s)		[min]	80

These figures are only intended as a guide and should not be used in preparing specifications.

Product data (cured)

Property	Test method	Unit	Value
Color			Reddish brown
Density at 23 °C	ISO 2781	[g/cm³]	1.43
Hardness Shore A	ISO 868		55
Tensile strength	ISO 37	[N/mm²]	3.5
Elongation at break	ISO 37	[%]	100
Dielectric strength	IEC 243	[kV/mm]	23
Volume resistivity	IEC 93	[Ω cm]	10^{15}
Dielectric constant	VDE 0303 T4 / 50 Hz	[ε_r]	3.7
Dissipation factor	VDE 0303 T4 / 50 Hz	[tan δ]	370×10^{-4}
Tracking resistance	IEC 112	[CTI]	> 600
Flame retardancy	ASTM D 2863	LOI [%]	28

Cured for 30 min at 150 °C in a circulating air oven.

These figures are only intended as a guide and should not be used in preparing specifications.

Application

- General purpose encapsulant

Processing

Caution
Only components A and B with the **same lot number** may be processed together!

To ensure homogeneity of the material, the components must be stirred thoroughly before they are removed or processed in their containers, in order to uniformly disperse any filler that might have settled during storage.

Surface preparation
All surfaces must be clean and free of contaminants that will inhibit the cure of ELASTOSIL® RT 607. Examples of inhibiting contaminants are sulfur containing materials, plasticizers, urethanes, amine containing materials and organometallic compounds – especially organotin compounds.
If a substrate's ability to inhibit cure is unknown, a small scale test should be run to determine compatibility.

Mixing
Component A of ELASTOSIL® RT 607 contains the platinum catalyst, component B the crosslinker. Even traces of the platinum catalyst may cause gelling of the component containing the crosslinker. Therefore tools (spatula, stirrers, etc.) used for handling the platinum-containing component or the catalyzed compound must not come into contact with this component.
The two components should be thoroughly mixed at a 9 : 1 ratio by weight.
To eliminate any air introduced during dispensing or trapped under components or devices a vacuum encapsulation is recommended.

Curing
Curing time of addition-curing silicone rubber is highly dependent on temperature, size and heat sink properties of the component being potted.

Temperature	Curing time, thickness 1 cm
23 °C	24 h
100 °C	10 min
150 °C	5 min

The reactivity can be adjusted within wide limits by adding Catalyst EP or Inhibitor PT 88 to suit the processing requirements of the particular application.
Catalyst EP increases the reactivity, i.e., pot life and curing time are reduced.
Inhibitor PT 88 is a pot life extender and prolongs pot life and curing time.
Further information is given in our leaflet "Catalyst EP/Inhibitor PT88".

We recommend running preliminary tests to optimize conditions for the particular application. Comprehensive processing instructions are given in our leaflet "Wacker RTV-2 Silicone Rubber - Processing".

Storage

ELASTOSIL® RT 607 has a shelf life of at least 12 months when stored between 5 °C and 30 °C in the originally sealed container. The 'Best use before end' date of each batch appears on the product label.

Storage beyond the date specified on the label does not necessarily mean that the product is no longer usable. In this case however, the properties required for the intended use must be checked for quality assurance reasons.

Safety information

According to the latest findingsaddition-curing silicone rubber ELASTOSIL® RT 607 contains neither toxic nor aggressive substances which would require special handling precautions. General industrial hygiene regulations should be observed.

Detailed safety information is contained in each Material Safety Data Sheet, which can be obtained from our sales offices.

The management system has been certified according to DIN EN ISO 9001 and DIN EN ISO 14001
The Business Unit Elastomers of the Division Silicones is ISO/TS 16949 certified.

Version 3.00 from 09-02-04 replaces Version 2.00 from 30-07-03

For technical, quality, or product safety questions, please contact:

Wacker-Chemie GmbH
WACKER-SILICONES
Hanns-Seidel-Platz 4
D-81737 Munich, Germany

Silicone-Info Service
Germany:
Tel.: 0-800-6279-800
International:
Phone: +800-6279-8000

www.wacker.com
silicones@wacker.com